Universitat Autònoma de Barcelona

Functional studies on the circadian regulation of mitochondrial activity in Arabidopsis thaliana

Luis Manuel Cervela Cardona

Universitat Autònoma de Barcelona

CENTRE FOR RESEARCH IN AGRICULTURAL GENOMICS

Functional studies on the circadian regulation of mitochondrial activity in *Arabidopsis thaliana*

PhD Thesis

Luis Manuel Cervela Cardona

Barcelona 2019

Universidad Autónoma de Barcelona

Facultad de Biociencias

Departamento de Biología Animal, Biología Vegetal y Ecología

Programa de Doctorado en Biología y Biotecnología Vegetal

Functional studies on the circadian regulation of mitochondrial activity in *Arabidopsis thaliana*

Memoria presentada por Luis Manuel Cervela Cardona para optar por el título de doctor por la Universidad Autónoma de Barcelona

Directora

Dra. Paloma Mas Martínez

Doctorando

Luis Manuel Cervela cardona

PhD Thesis

Luis Manuel Cervela Cardona

Barcelona 2019

A Silvia, Maku, Tati y Xoel.

Y a Pablo Carollo Ramos (PC), porque siempre será nuestro alcaldable.

TABLE OF CONTENTS

INTRODUCTION

1. Circadian clocks: an overview

The diurnal changes in environmental conditions have influenced life on earth ever since its origin. These periodic environmental fluctuations, mostly light and temperature, have a major effect on the physiology, behavior, and metabolism in all organisms. To predict and anticipate these changes, selective pressure has imposed the development of a molecular timekeeper mechanism that allows organisms to adapt to the changing environment by generating a wide range of biological rhythms such as sleep-wake patterns, feeding, or reproductive behavior (Bell-Pedersen et al., 2005).

From Jean-Jacques d´Ortous de Mairan, a French astronomer who in 1729 studied the rhythmic leaf movement of *Mimosa* plants, to Prof. Jeffrey Hall, Prof. Michael Rosbash and Prof. Michael Young, scientists awarded with the 2017 Nobel Prize in Physiology or Medicine for their work on the circadian clock in *Drosophila*, biological rhythms have been fascinating scientists over almost 300 years. There are many scientific contributions through history that have helped to increase our knowledge about the circadian clock (Bell-Pedersen et al., 2005). Initial research mostly focused on the description of observable biological rhythms such as leaf movement, pigment rhythms of arthropods or rat activity. Under constant environmental conditions (i.e. in the absence of environmental changes), the rhythms persisted and the time to complete one cycle was not exactly 24 hours. These observations suggested that rhythms were endogenous and not just responses to external cues. However, it wasn't until the 80's when the first clock gene *PERIOD* (*PER)* was cloned from *Drosophila,* providing for the first time, a genetic bases for circadian rhythms (Ni et al., 2014), a term coined by Franz Halberg in 1959 from the Latin words "*circa"* (about) and "*dies"* (day).

From a classical point of view, and despite diverse phylogenetic origins and differences among species, circadian systems can be described in a simplified way as cellular mechanisms composed of three main functional modules: (1) the *input pathways* or components and mechanisms responsible for perceiving and transmitting the environmental information to the (2) *central oscillator* that is responsible for the generation of rhythms that are translated to (3) biological processes or *output pathways* (**Figure 1**) (Kumar and Sharma, 2018). The core of the clock is a cell-autonomous oscillator with a basic structure composed of a transcription- and translation-based negative feedback loops (Masri and Sassone-Corsi, 2010; Hirano et al., 2016). This classical view of the clock

with the three components arranged in a linear pathway is an over-simplification. The circadian system is a much complex intricate network, with oscillatory inputs controlled by the clock, oscillators regulating their own sensitivity to the external synchronizing signals and outputs feeding back to the clock (**Figure 1**).

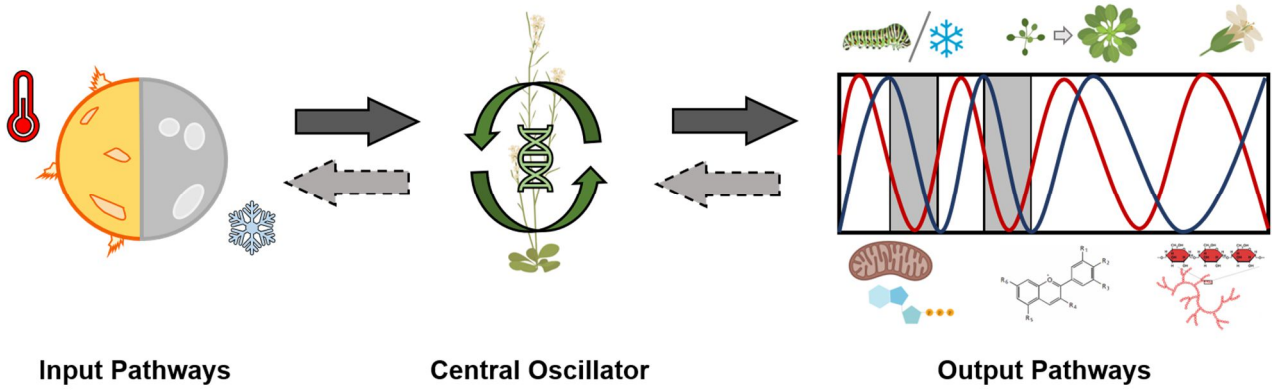

Figure 1. Schematic representation of the circadian clock in *Arabidopsis thaliana.* The input pathways responsible for perceiving the daily environmental changes (light, temperature) and transmit them to the central oscillator that is responsible for the generation of biological rhythms in biotic/abiotic stress, growth, flowering, energetic metabolism, hormone signaling and starch turnover, among others (Black arrows). In turn, processes controlled by the clock can control the oscillator pace, which influence and adjust the input pathways (Dashed gray arrows).

1.1. Mathematical analyses of circadian rhythms

Circadian rhythms are sinusoidal waveforms that can be mathematically analyzed. There are few parameters frequently used to define the properties of the circadian waves (**Figure 2**). The time required to complete one cycle is defined as *period*. It is commonly measured from peak to peak but could be also measured from trough to trough or any other recurrent point on the waveforms. The circadian period is about 24 hours. The *amplitude* is the distance from a peak or a through to the midpoint of the waveform (McClung, 2006; Bell-Pedersen et al., 2005). The *phase* is the state of a rhythm (usually the peak) relative to a reference rhythm (e.g. the day–night cycle). For example, if the peak of a circadian waveform occurs at dawn, the peak-phase is 0 (the time of lights-on). If a waveform peaks at dusk, its peak-phase would be 12 (the time of lights-off in a 12h light: 12h dark cycle). Any signal detected by the clock with the ability to entrain it with the local time is known as a *Zeitgeber* (from the German word “time giver”). Therefore, the phase is often defined in *Zeitgeber Time* (ZT). One of the most relevant Zeitgebers is the light/dark cycle. The term “*free-running”* refers

to the rhythms occurring under constant conditions (e.g. constant light or temperature). Under free-running conditions, the phase of the organism's subjective time is notated as circadian time (CT). For an organism entrained under 12h light/12h dark cycles and then transferred to constant light conditions, the CT0 indicates the beginning of a subjective day while CT12 indicates the start of subjective night (Nakamichi et al., 2004; McClung, 2006) (**Figure 2**).

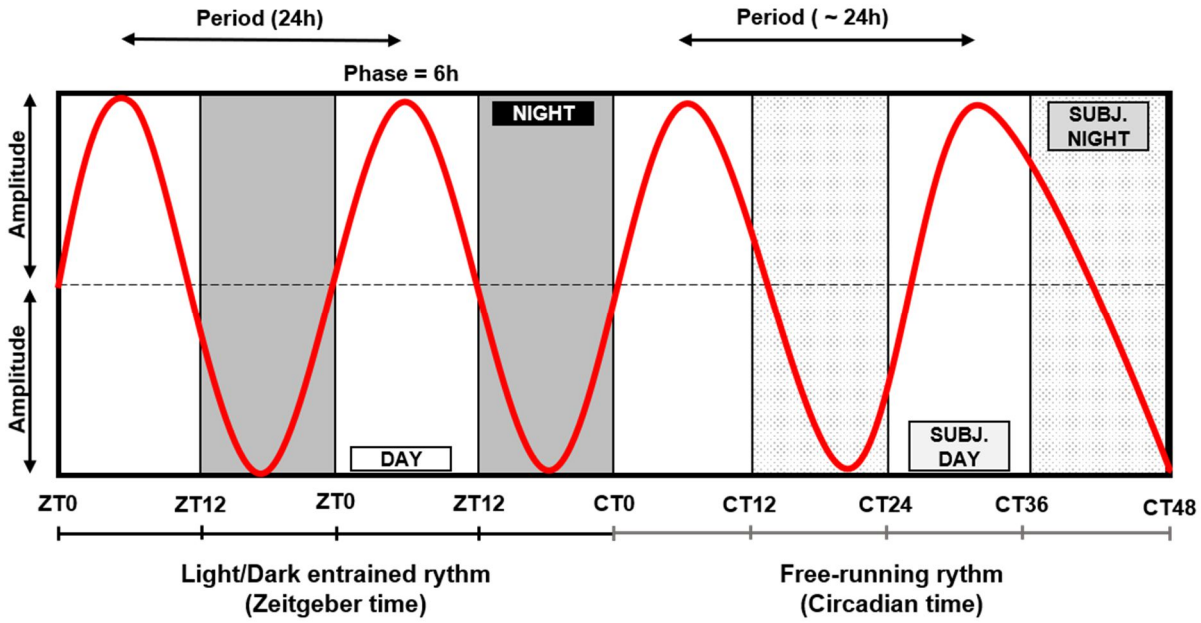

Figure 2. Circadian clock mathematical terminology. Period as the amount of time required to complete one cycle. The phase is particular time point of a physiological event relative to an external cue (e.g. day/night cycle). The amplitude defines half of the difference between a peak and a trough of an oscillatory wave. Under entrained cycles time is given in Zeitgeber time (ZT) whereas under free-running cycles is given in Circadian time (CT). Under constant conditions day and night are defined as subjective day (Subj. day) and subjective night (Subj. night).

2. The Plant Circadian clock

Plants have been fundamental for the history of circadian research from the times of de Marian observations to nowadays. Specifically, the use of the model system *Arabidopsis thaliana* have provided detailed information about the molecular networks at the core of the clock, the importance of environmental changes resetting the oscillator and the myriad of processes controlled by the clock (Greenham and McClung, 2015; Millar, 2016). In the next sections, we briefly describe the main three components of the plant circadian system.

2.1 The *Arabidopsis* central oscillator

The first *Arabidopsis thaliana* mutant of TIMING OF CAB EXPRESSION (TOC1), also known as PSEUDO RESPONSE REGULATOR1 (PRR1), was isolated almost 25 years ago (Millar et al., 1995). The two first clock components CIRCADIAN CLOCK ASSOCIATED 1 (CCA1) and LATE ELONGATED HYPOCOTYL (LHY), two partially redundant proteins that heterodimerize (Lu et al., 2009) were described three years later (Wang and Tobin, 1998; Schaffer et al., 1998). The first feedback loop of the *Arabidopsis* circadian clock was proposed to be composed of *CCA1*, *LHY* (morning-expressed genes) and *TOC1* (evening-expressed gene) (Strayer et al., 2000; Alabadí et al., 2001). In this first loop, the MYB-domain transcription factors CCA1 and LHY repressed the expression of *TOC1* by direct binding to the evening element (EE) motif, a cis-element found in the promoter of *TOC1*. In turn, TOC1 was thought at that time to activate the expression of both *CCA1* and *LHY.* Research over the last years has contributed to extend the knowledge on the molecular circadian network, adding numerous new components and regulatory mechanisms (Nohales and Kay, 2016). For instance, TOC1 was reported to be a repressor rather than an activator of *CCA1* and *LHY* (Pokhilko et al., 2012; Gendron et al., 2012; Huang et al., 2012). Notably, TOC1 is a repressor of nearly all the oscillator genes (Huang et al., 2012). The initially conceived activating function of TOC1 was based on correct experimental evidence that was later on override by the additional regulatory components discovered at the core of the clock.

The other members of the PRR gene family *PRR3*, *PRR5*, *PRR7* and *PRR9* (Matsushika et al., 2000; Makino et al., 2000) are also clock-associated components (Nakamichi et al., 2005; Adams et al., 2015). CCA1 and LHY repress the *PRR*s, which in turn suppress *CCA1* and *LHY* transcription (Kamioka et al., 2016). The PRRs are sequentially expressed, starting with PRR9 with a peak-phase closed to dawn to be followed by *PRR7* and *PRR5* at midday and by *TOC1* that displays a peak-phase of expression at dusk (Nakamichi et al., 2010).

Other evening-expressed components include the *EARLY FLOWERING 3* (*ELF3*) and *ELF4* genes coding for two plant-specific proteins without recognizable domains (Hicks et al., 2001; Doyle et al., 2002) and *LUX ARRHYTMO* (*LUX*) gene coding for a single MYB-like GARP transcription factor (Hazen et al., 2005). These three additional evening-expressed clock proteins were first identified

by genetic screens for photoperiodism (ELF3 and 4) and long hypocotyl mutants (LUX). These proteins were later found to be interacting in a multiprotein complex called the EVENING COMPLEX (EC) (Nusinow et al., 2011). The EC components are repressed by CCA1 and LHY in the morning (Portolés and Más, 2010; Li et al., 2011; Lu et al., 2012) and by TOC1 in the evening (Huang et al., 2012). In turn, EC acts as a transcriptional repressor directly binding to the *GI*, *PRR9*, *PRR7 and LUX* promoters and repressing their expression (Dixon et al., 2011; Chow et al., 2012; Mizuno et al., 2014). By repressing the repressors of *CCA1* and *LHY*, the EC indirectly promotes *CCA1* and *LHY* expression. Moreover, *GIGANTEA* (*GI*), a plant-specific protein that was initially shown to be important for sustaining proper circadian clock amplitude and period length (Park et al., 1999; Gould et al., 2006; Martin-Tryon et al., 2007). *GI* is repressed by *CCA1* and *LHY* in the morning and by *TOC1* and the EC in the evening (Lu et al., 2012; Huang et al., 2012; Mizuno et al., 2014) (**Figure 3**).

The complexity of the central oscillator further increased over the recent years as a result of the discovery of new components that act as activators of clock gene expression. For instance, the *LIGHT-REGULATED WD1* (*LWD1*) and *LWD2*, both of which encoded WD (for Trp and Asp)-containing proteins, were described as clock proteins involved in photoperiodic control (Wu et al., 2008). The LWDs directly bind to the promoters of *CCA1*, *PRR9*, *PRR5* and *TOC1* to activate their expression (Wang et al., 2011b; Wu et al., 2016) (**Figure 3**) Moreover, REVEILLE 8 (*RVE8* also known as LHY-CCA1-LIKE5 or LCL5), a CCA1 and LHY homolog that belongs to the same single MYC protein family, promotes the expression of *TOC1* and *PRR5*, opposing to the CCA1 and LHY repressing function (Farinas and Mas, 2011; Rawat et al., 2011). RVE8 also directly promotes the expression of *PRR9*, *GI*, *ELF4* and *LUX* (Hsu et al., 2013) (**Figure 3**). Additionally, the *RVE8* homologs *RVE4* and *6*, appear to be functionally redundant as the *rv4rve6rve8* triple mutant accentuate the long period phenotype of *rve8* single mutant (Hsu et al., 2013).

Far from being completely untangled, the wiring inside the central oscillator is still growing. The LNK1 and LNK2 (NIGHT LIGHT-INDUCIBLE AND CLOCK-REGULATED 1 and 2) plant-specific proteins were proposed to be essential for co-activation of *PRR5*, *TOC1* and *ELF4* along with *RVE8* (Rugnone et al., 2013; Xie et al., 2014; Pérez-García et al., 2015) (**Figure 3**). The RVE8/LNKs direct protein interaction allowed the recruitment of the transcriptional machinery at the clock gene

promoters to trigger the transcription initiation and elongation of the *PRR5* and *TOC1* nascent RNAs (Ma et al., 2018). In contrast, *PRR*s bind to the *LNK*s to repress their expression adding another negative feedback loop to the central oscillator (Nakamichi et al., 2012; Rugnone et al., 2013).

A remarkable fact of clock regulation is that every cell in the plant has its own self-autonomous oscillatory mechanism (Yakir et al., 2011). These cell-autonomous clocks operate differently in distinct tissues and organs, displaying varied degrees of coupling (Endo et al., 2014). Nevertheless, as the SCN (Suprachiasmatic Nucleus) in mammals (Mohawk et al., 2012), the shoot apex *Arabidopsis* clocks are closely coupled and function in synchrony as a master clock with the capacity to harmonize distant clocks like those in roots (Takahashi et al., 2015).

2.2 Regulatory networks ensuring a proper oscillation of TOC1 expression and function

The results in this Doctoral Thesis show a direct role for TOC1 controlling mitochondrial activity. TOC1 has been previously found to control a vast array of clock outputs. For instance, TOC1 and ABAR/CHLH/GUN5 (ABAR-RELATED/H SUBUNIT OF THE MAGNESIUM-PROTOPORPHYRIN IX CHELATASE/GENOMES UNCOUPLED 5) comprise a reciprocal feedback loop to regulate abscisic acid (ABA) signaling pathway and stomata opening, which are important for plant responses to drought (Legnaioli et al., 2009). TOC1 can also physically interact with the transcription factors PHYTOCHROME INTERACTING FACTOR 3 (PIF3) and PIF4 after dusk (Soy et al., 2016; Zhu et al., 2016; Martín et al., 2018) to control hypocotyl growth (Leivar and Quail, 2011) (Nozue et al., 2007). The decreasing accumulation of TOC1 from the middle of the night relieves the repression on *PIF3* and thereby, assisting in the control of PIF-related growth just before dawn (Soy et al., 2016). Furthermore, TOC1 is also involved in the regulation of cold responses through interaction with PIF7 to regulate the expression of *DREB1/CBF* (*DEHYDRATION-RESPONSIVE ELEMENT BINDING B1/C-REPEAT-BINDING FACTOR*) (Kidokoro et al., 2009). It has been also reported that TOC1 sets the time of the DNA pre-replicative machinery to control plant growth in synchrony with the environment by direct binding of TOC1 to the promotor of the DNA replication licensing gene (*CELL DIVISION CONTROL 6*) *CDC6.* TOC1 represses *CDC6* expression safeguarding the G1-to-S transition and controlling the timing of the mitotic cycle and the endocycle throughout leaf development (Fung-Uceda et al., 2018).

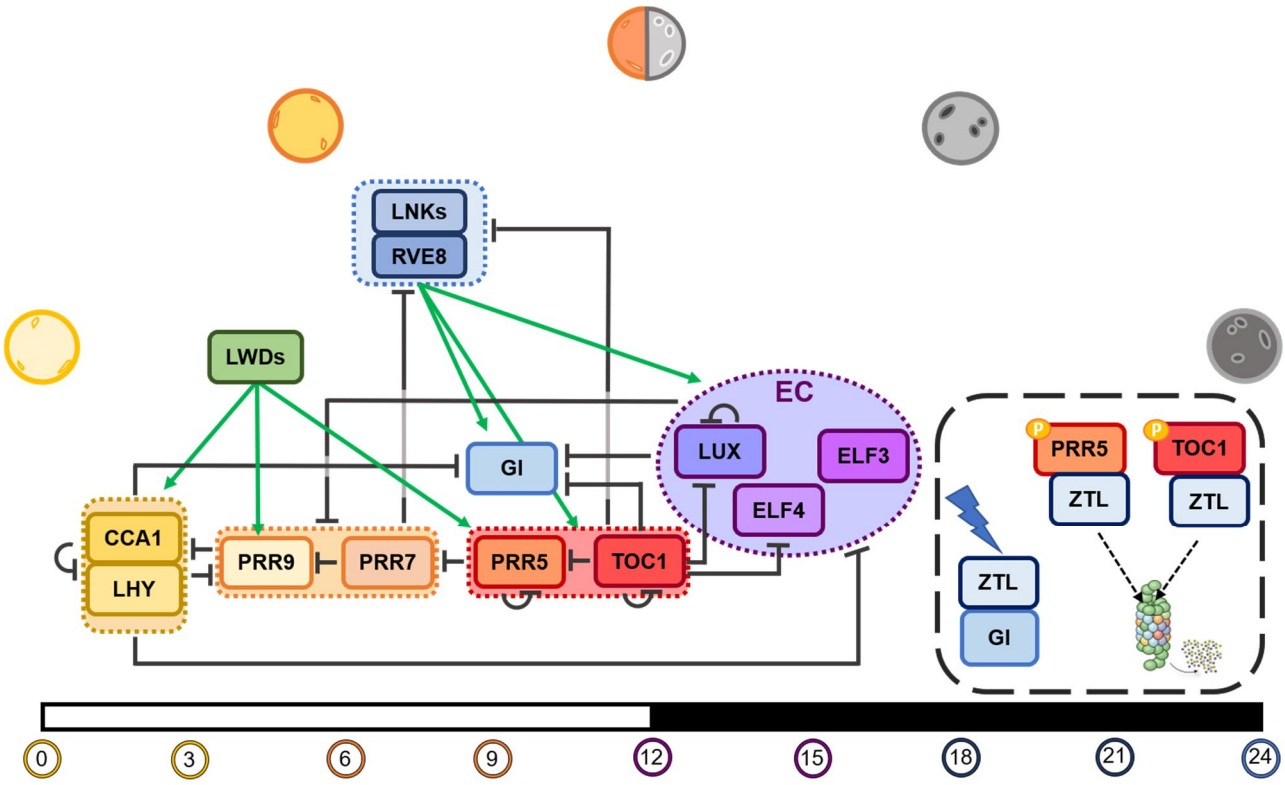

Figure 3. Schematic representation of the transcriptomic and post-translational interactions at the central oscillator. The sequential expression of each component during a day/night cycle is shown from left to right, and the time of activity is expressed in hours after dawn below the withe (day) black (night) bar on the bottom. Black bars indicate repression, and green arrows indicate activation of transcription. Components within a colored dashed box belong to the same functional group. Within the black dashed box, schematic representation of the blue-light (blue lighting) GI-mediated ZTL stabilization and the phosphorylation of PRR5 and TOC1 what enhance their binding to ZTL promoting their degradation later in the evening by 26S proteasome. EC; Evening Complex.

Post-translational regulatory mechanisms are also important at the core of the clock. The direct interaction of the F-box protein ZEITUPLE (ZTL) with TOC1 promotes TOC1 protein degradation by the proteasome 26S through ubiquitination (Más et al., 2003b). PRR3 and PRR5 interact with TOC1 and prevent its ZTL-directed proteasomal degradation (Para et al., 2007; Fujiwara et al., 2008; Wang et al., 2010) (**Figure 3.Black doted box**). Furthermore, GI stabilize ZTL in a blue-light dependent manner enhancing the stability of TOC1 and PRR5, which in turn are degraded by direct interaction with the other ZTL homologs, FLAVING-BINDING, KELCH REPEAT AND F-BOX (FKF1) AND LOV KELCH PROTEIN 2 (LKP2) (Kim et al., 2007; Wang et al., 2010). The PRR5 and TOC1 degradation by ZTL is enhanced by increased phosphorylation while TOC1 and PRR3 phosphorylation is essential for their interaction (Fujiwara et al., 2008). Hence, direct protein-protein interaction as well

as post-translational modifications, such are ubiquitination or phosphorylation, are essential for proper clock regulation and timing.

As described above, TOC1 plays a central role at the core of the clock as it is a general repressor of nearly all the circadian oscillator components (Huang et al., 2012). The regulation of *TOC1* diurnal and circadian oscillatory expression relies on the concomitant and antagonistic function of various clock components. On one hand, the morning expressed genes *CCA1* and *LHY* repress the expression of *TOC1* during the day by direct binding to a motif known as Evening Element (EE) present in the *TOC1* promoter (Alabadí et al., 2001). On the other hand, the activation of *TOC1* expression relies on the RVE8 function. CCA1 and RVE8 differentially regulate *TOC1* gene expression by antagonistically regulating the pattern of Histone 3 acetylation at the *TOC1* promoter. Recruitment of Histone acetylases and deacetylases alters the chromatin compactness at the *TOC1* loci impeding (CCA1) or facilitating (RVE8) *TOC1* transcription (Perales and Más, 2007; Farinas and Mas, 2011). Rhythmic accumulation of Histone acetylation and other histone marks was also observed at the promoters of *CCA1*, *LHY*, *LUX* and *PRR*s (Malapeira et al., 2012; Hemmes et al., 2012). As mentioned above, the direct interaction of RVE8 with LNKs activate the transcriptional initiation and elongation of *TOC1* and *PRR5* expression by recruiting the transcriptional machinery to *TOC1* and *PRR5* promoters (Hsu et al., 2013; Xie et al., 2014; Pérez-García et al., 2015; Ma et al., 2018). Additionally, the PRR9, 7, 5 and TOC1 bind to the LNKs' promoters to negatively regulate their expression from the midday to the early evening, establishing a negative feedback look with CCA1/LHY and LNKs as activators and PRRs as repressors (Nakamichi et al., 2012; Rugnone et al., 2013). Altogether, these loops shape the rhythmic oscillation pattern of *TOC1* expression with a peak around dusk and a progressive transcript decline during the night (Matsushika et al., 2000; Strayer et al., 2000).

The complexity of the regulation of TOC1 by different clock components and mechanisms is reciprocated in turn by the intricate control of clock components by TOC1. Indeed, the repressing function of TOC1 is not just limited to *CCA1* and *LHY* (Gendron et al., 2012; Pokhilko et al., 2012) but is extended to *PRR9*, *PRR7*, *GI*, *LUX*, *ELF4* and *TOC1* itself. Repression relies on the rhythmic binding of TOC1 to it target promoters enriched in G-BOX-related and EE motifs. The highest

enrichments observed through ChIP-Seq experiments were observed after dusk, the peak of TOC1 protein (Huang et al., 2012). TOC1 protein also interacts directly with other clock components such as ELF3 (Huang et al., 2016a) and CCA1 HIKING EXPEDITION (CHE), which was proposed to be important for *CCA1* regulation (Pruneda-Paz et al., 2009).

Miss-expression of TOC1 affects circadian clock period, phase and amplitude (Nagel and Kay, 2012). A constitutively over-expressed *TOC1* lead to arrhythmic phenotypes under free-running conditions (Más et al., 2003a) while additional copies of rhythmically expressed *TOC1* showed longer periods and delayed phase (Más et al., 2003b). Loss-of-function of *TOC1* and *PRR5* advanced the phase and shortened the period (Millar et al., 1995; Somers et al., 1998b; Strayer et al., 2000; Yamamoto et al., 2003) while *prr7* and *prr9* single mutants showed a slightly longer period phenotype (Farré et al., 2005). *CCA1* and *LHY* are constitutively expressed in the *prr9prr7prr5* triple mutant at a high level while *TOC1* is expressed low (Nakamichi et al., 2005)

Overall, proper oscillator pace relies on an utterly complex machinery, which is integrated by transcriptional feedback loops, epigenetic alterations, protein-protein interactions and post-translational regulation. Furthermore, this machinery works perfectly synchronized at a cell, tissue and organismal level to anticipate and respond to environmental changes. The next section briefly describes the major environmental signals perceived by the clock and the molecular mechanism behind this perception.

2.3 Environmental information to the oscillator: Input pathways

Proper sensing and integration of the environmental signals by organisms are crucial for the daily synchronization of the circadian clock with the surrounding environment. Light and temperature are the two most studied environmental signals for clock entrainment (Harmer, 2009). Recent studies are also beginning to uncover a role for metabolic signals as important input cues for clock synchronization (Haydon et al., 2013b; Frank et al., 2018).

2.2.1 Light

Light has major effects dictating the pace of the clock. As stated by the Aschoff's rule (Aschoff, 1979), in diurnal organisms, high-light intensities speed up the pace of the clock, leading to short circadian periods whereas low intensities of light make the clock to run slower, resulting in long circadian periods. Oscillations of circadian reporters are absent or very low in continuous dark when sucrose is not present in the growth medium (Dalchau et al., 2011; Haydon et al., 2013b). Light input to the clock is tightly related to the action of different types of photoreceptors, which perceive light and transmit the light quality and quantity information to the central oscillator (Oakenfull and Davis, 2017). Different families of photoreceptors have been described to be involved in the regulation of the *Arabidopsis thaliana* circadian clock. For instance, the PHYTOCHROME family (PHYA to E) responsible for the red/far-red light perception (Quail, 1996) and the CRYPTOCHROME family (CRY1 and 2) (Cashmore et al., 1999) implicated in the blue light sensing. Other photoreceptors include the ULTRAVIOLET RESISTANT LOCUS 8 (UVR8) that drives the signaling for the majority of ultraviolet B light (UVB) responses (Rizzini et al., 2011) and the ZTL family, blue light receptors that are required for the integration of multiple wavelengths of light into the oscillator (Jarillo et al., 2001; Kim et al., 2007).

While the ZTL-TOC1 interaction is a well understood mechanism of light-mediated regulation of circadian period by the clock (Más et al., 2003b), there is a lack of complete understanding of how the phytochromes, cryptochromes and UVB8 influence clock progression. Although none of the phytochromes or cryptochromes are fully required to maintain the oscillation, mutant or over-expressing lines have a clear effect on proper clock function (Somers et al., 1998a; Devlin and Kay, 2000; Yanovsky et al., 2000). Many studies have indeed verified the implication of these components in the light entrainment of the clock (Oakenfull and Davis, 2017). For instance, PHYB interacts with ELF3 (Xing Liang Liu et al., 2001) and some other clock components in a light dependent-manner (Yeom et al., 2014). Moreover, PHYB is important for the LDW1-TOC1 interaction as well as for the ELF3 interaction with other components for the regulation of various processes (Huang et al., 2016a).

2.2.2 Temperature

Temperature is another fundamental environmental signal that influences the circadian clock in two different ways. On one hand, temperature can act as a resetting cue for the clock. Indeed, temperature fluctuations as small as ±4°C within a day can reset the plant circadian (Somers et al., 1998b; Thines and Harmon, 2010). The core clock components PRR9 and PRR7 seem to be crucial for temperature entrainment as the *prr7-3 prr9-1* double mutant fails both to maintain an oscillation after entrainment to thermocycles and to reset the clock in response to cold pulses (Salomé and McClung, 2005). The EC has also been related to clock temperature responsiveness. Transcriptional levels of *PRR7*, *PRR9*, *GI* and *LUX* are induced after temperature increases. This response is abolished in the *elf4*, *elf3* or *lux* (EC components) single mutants (Mizuno et al., 2014) and the EC repressive activity decreases at high temperatures (Ezer et al., 2017). The circadian clock function is also important for cold-sensing pathways. Furthermore, cold signaling is also integrated into the clock by the C-REPEAT BINDING FACTOR, CBF-mediated regulation of *LUX* expression (Chow et al., 2014).

The oscillator also presents a remarkable property known as temperature compensation by which it can buffer the changes in ambient temperature so that the circadian period remains relatively constant within a physiological range of temperatures (Gould et al., 2006). This process safeguards the precision of the clock regardless the environmental temperature variations. The core clock components such as PRR7, PRR9, CCA1 and LHY have a critical role maintaining a functional temperature compensation mechanism (Salomé et al., 2010). Furthermore, high temperatures increase the CCA1 promoter-binding activity stimulating clock gene repression. In contrast, the CASEINE KINASE 2 (CK2)-mediated CCA1 phosphorylation is induced by high temperatures, and reduces the affinity of CCA1 for the promoters of clock genes. Consequently, these two antagonistic activities similarly regulated by temperature are precisely balanced to control temperature compensation in plants (Portolés and Más, 2010).

Temperature can also modulate circadian clock gene expression through alternative splicing events. Splicing variants of the *CCA1*, *LHY*, *PRR9*, *PRR7*, *TOC1* and *ELF3* clock genes can accumulate in a heat- or cold-dependent manner (James et al., 2012; Seo et al., 2012; Kwon et al., 2014). This

process is fundamental for both temperature compensation and entrainment, which require the involvement of multiple mechanisms (Wang et al., 2012b; Schlaen et al., 2015; Marshall et al., 2016).

2.2.3 Metabolism

Changes in metabolism have been shown to be important for clock entrainment (Haydon et al., 2013a). Sugar availability varies across the day and night. Under diurnal cycles, sugar oscillation and the circadian clock function control a significant fraction of the daily fluctuations in gene expression (Bläsing et al., 2005). Exogenous sucrose increases the expression of the core central oscillator genes *CCA1*, *GI*, and *TOC1* and shortened the circadian clock period under constant light conditions (Knight et al., 2008; Philippou et al., 2019). Conversely, low energy availability lengthened circadian period (Haydon et al., 2013b). Moreover, under constant dark conditions, sucrose addition is sufficient to maintain circadian rhythms by a GI-dependent mechanism (Dalchau et al., 2011). The endogenous sugar accumulation as a result of photosynthesis (photoassimilates) also has an influence on the clock pace. The accumulation of photoassimilates represses the *PRR7* promoter activity, leading to the activation of *CCA1* (Haydon et al., 2013b). Under low sugar conditions, the transcription factor BASIC LEUCINE ZIPPER63 (bZIP63) activates the promoter of *PRR7* (Frank et al., 2018). Sucrose and other soluble sugars have also been reported as fundamental for the GI protein stabilization by a process that requires ZTL (Haydon et al., 2017). The clock in *gi* single mutant is insensitive to sugars addition in the dark which is a unique feature among single mutants of the oscillator genes (Haydon et al., 2017). These results suggest that sugars might regulate circadian period and phase through a signaling pathway involving direct regulation of oscillator gene expression (Frank et al., 2018). Accumulation of other metabolites, such as the 3′-phosphoadenosine 5′-phosphate (PAP) and nicotinamide also increases the circadian period (Dodd et al., 2007; Litthauer et al., 2018).

Hormonal metabolic pathways have been also related to the circadian function. Transcript levels of hormone-responsive genes are circadian regulated (Covington et al., 2008; Mizuno and Yamashino, 2008) and the circadian regulation of several hormone signaling pathways was confirmed by a subset of studies for ethylene (Thain et al., 2004), brassinosteroids (Bancos et al., 2006), auxin

(Covington and Harmer, 2007), cytokinin (Ishida et al., 2008), gibberellin (Arana et al., 2011), salicylic acid (Zhou et al., 2015) and jasmonic acid (Zhang et al., 2018). The regulatory mechanism underlying the clock-hormone regulatory network were recently reviewed (Singh and Mas, 2018). A good example of circadian control of hormone metabolism is the phytohormone abscisic acid (ABA). ABA is known as an stress hormone and is involved in the regulation of seed germination, stomatal opening, osmotic stress tolerance, and pathogen attack responses (Seung et al., 2012). The studies showed that ABA acutely activates the expression of *TOC1* just in the morning in a gated mechanism that requires the function of the putative receptor ABA-RELATED (ABAR) and the transcription factor MYB96. Subsequently, TOC1 directly represses *ABAR* expression to establish a negative feedback mechanism that ensures a rapid ABA response during the day (Legnaioli et al., 2009; Lee et al., 2016).

Altogether, the results clearly indicate that environmental and metabolic signals are key resetting every day the circadian function to keep it in synchrony with the external conditions and adjusting its phase to favor proper responses to the cellular conditions.

2.4 Rhythmic biological processes: Output pathways

As mention above, the components of the central oscillator generate rhythms in their own expression and activity that are transduced into rhythms in biological processes essential for proper plant fitness and survival (Dodd et al., 2005; Webb et al., 2019). A myriad of processes including the photoperiodic regulation of flowering time (Andrés and Coupland, 2012; Shim et al., 2017), leaf senescence (Kim et al., 2018), stomatal opening (Somers et al., 1998b; Hassidim et al., 2017), hormonal signaling (Singh and Mas, 2018), hypocotyl, stem and root lengthening (Nozue et al., 2007; Ruts et al., 2012; Martín et al., 2018), cell growth and cell cycle (Gray et al., 2017; Jones et al., 2017; Fung-Uceda et al., 2018), abiotic and biotic stress responses (Wang et al., 2011a; Zhang et al., 2013; Korneli et al., 2014) and metabolism (Dodd et al., 2005; Sulpice et al., 2014; Flis et al., 2019) are under the influence of the circadian clock. In the following sections, we focus on the role of the circadian clock controlling metabolic pathways.

2.4.1 Diurnal and circadian control of starch and sugar metabolism

Growth relies on the photosynthetic carbon assimilation during the day but requires the reserves accumulated during the light period to grow during the night. One of the major carbon storage resource in plants is starch, which follows a diurnal accumulation (Smith et al., 2004). Another important carbon sink is fumarate (please check section 3.1.2). Starch accumulates during the day and is used during the night in a near-linear manner. Starch is not fully depleted during the night as approximately 5% of starch still remains before the onset of light (Gibon et al., 2004a; Smith et al., 2004). This pattern is highly robust and it is maintained across a wide range of photoperiods and growth light conditions (Smith and Stitt, 2007; Gibon et al., 2009; Sulpice et al., 2014; Mengin et al., 2017). Furthermore, it can be rapidly adjusted despite abrupt changes in irradiance, timing of dusk, temperature and even light pulses at night (Pokhilko et al., 2014; Pilkington et al., 2015). The robustness and plasticity maximize growth under carbon limiting conditions by effectively utilizing the fixed carbon for growth within the 24h cycle (Pyl et al., 2012; Pilkington et al., 2015). This precise regulation allows the plant to avoid premature exhaustion of starch before the end of the night, which would trigger transient carbon starvation, protein catabolism and growth inhibition (Gibon et al., 2004c, 2009; Ishihara et al., 2015, 2017).

The circadian clock is implicated in the control of both starch turnover and of its major degradation product, maltose (Lu et al., 2005;Yazdanbakhsh et al., 2011). Starch degradation was faster in *cca1/lhy* double mutant than in WT plants resulting in a growth inhibition at dawn. While WT plants growing under 28h cycles showed a similar starvation phenotype than the *cca1/lhy* mutant plants under 24h cycles, the double mutant showed a similar WT behavior when grown under 17h cycles (Graf et al., 2010). In contrast, the clock mutant *elf3* and double mutant *prr7prr9*, degraded starch slower than the WT, resulting in starch accumulation at dawn (Flis et al., 2019) (**Figure 4**).

Two models have been proposed to explain how starch turnover happens. Both models consider clock signaling and carbon status measurement as key variables. However, they differ in how temporal and metabolic information is integrated. The A Model suggests that the plant calculates the nocturnal starch degradation rate based on the amount of starch at dusk (measured by unknown S components) and the time remaining to dawn, which is estimated by the circadian clock (by unknown

T components) (Scialdone et al., 2013). The A model has been validated by experimental observations (Moraes et al., 2019). Nevertheless, the molecular mechanism (S and T) controlling the process remains still unknown. The B Model considers a retrograde metabolic signaling that modifies clock gene expression and clock phase, which in turn affect starch turnover (Feugier and Satake, 2013; Seki et al., 2017) (**Figure 4**).

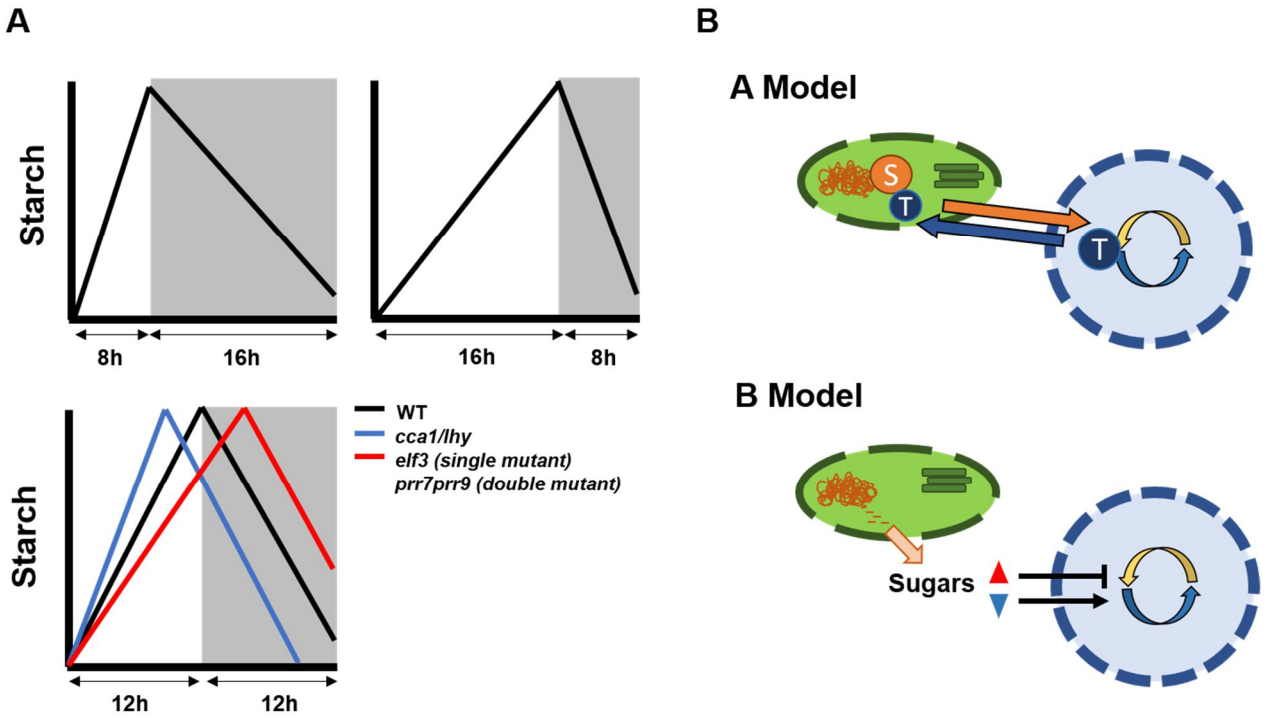

Figure 4. Schematic representation of the linear starch turnover and the theoretical models of its regulation. (A) Starch turnover pattern its adjusted to the photoperiod and disrupted in circadian clock mutants. The *elf3* single mutant and *prr7prr9* double mutant (red line) displayed a slower rate of starch degradation resulting in a starch overaccumulation. The *cca1/lhy* double mutant (blue) displayed a high rate of degradation resulting in a carbon starvation phenotype at the end of the night period. (B) Theoretical model of starch turnover diurnal control. A model is based in 2 unidentified molecular components. One measures the starch abundance (S; yellow) and the other measures time till dawn (T; blue). Model B is based in a retrograde mechanism that control the pace of the clock by sugar-mediated signaling. Circular yellow and blue arrows represent the circadian clock in the nucleus.

One of the proposed inputs in the B model would be the above described sucrose-dependent bZIP63-PRR7 interaction (see section 2.2.3) (Frank et al., 2018). Furthermore, the α-subunit (AKIN10) of the metabolic sensor SUCROSE NON-FERMENTING 1 (SNF1)-RELATED KINASE 1 (SNRK1) complex that is involved in the bZIP63-PRR7 interaction has also been reported to modulate *GI* expression (Shin et al., 2017). Other proposed input would be the GI protein stabilization by ZTL in a sucrose-dependent manner (Dalchau et al., 2011; Haydon et al., 2017). The B Model

does not completely explain the rapid adjustment of starch degradation to abrupt perturbations but it provides a potential mechanism of adjustment to light intensity and environmental changes.

Regardless which model is correct (Webb et al., 2019), it is clear that optimal growth and biomass accumulation by mobilization of starch reserves requires the complex integration of photoperiodic information and circadian clock function (Graf et al., 2010; Flis et al., 2019).

2.4.2 Amino acids

In addition to starch, other primary metabolites also accumulate following a diurnal pattern (Gibon et al., 2006; Ishihara et al., 2015; Annunziata et al., 2018). For instance, nitrogen reserves increase during the light period in the form of amino acids (AA) to later support protein synthesis at night (Urbanczyk-Wochniak et al., 2005; Fritz et al., 2006). The nitrate and ammonium assimilation are the primary steps in the AA biosynthetic process (Coruzzi, 2003) and accounts for 50% of the total cost for protein synthesis (Amthor, 2000). Therefore, pacing the accumulation of AA in the light reduces growth energetic cost during the night (Amthor, 2000; Pal et al., 2013). Various studies have implied the involvement of the circadian clock on AA turnover. For instance, the accumulation of a number of AA displayed a peak during the subjective night (Espinoza et al., 2010). Furthermore, a fluctuating pattern was reported for the expression of genes encoding enzymes related to the AA catabolism, especially the branched chain amino acid (BCAA) catabolism (Peng et al., 2015). The expression of *nitrate reductases* (*NR*), genes encoding key enzymes in nitrogen metabolism, is under circadian regulation exerted by CCA1 (Pilgrim et al., 1993; Teng et al., 2017). These results are in agreement with the key role of CCA1 as a central regulator of nitrogen metabolism (Gutiérrez et al., 2008)

2.4.3 ROS homeostasis

The photosynthetic and respiratory activities result in the generation of toxic by-products of oxygen (O_2) known as Reactive Oxygen Species (ROS). Plants have evolved enzymatic and non-enzymatic scavenging machineries to maintain physiologically tolerable levels of ROS and minimize their damage (Ahmad et al., 2010). Some of these ROS-related enzymatic components include among

many others, the SUPEROXIDE DISMUTASE (SOD), ASCORBATE PEROXIDASE (APX), CATALASE (CAT) while examples of non-enzymatic components include ascorbate, glutathione, carotenoids, tocopherols and phenolic compound (including flavonoids and anthocyanins). ROS production and scavenging follow a diurnal pattern. Furthermore, CCA1 mutant plants showed an alteration not only in the transcription of ROS-related genes but also in tolerance to oxidative stress (Lai et al., 2012). The mechanism might involve CCA1 binding to the promoters of ROS-related genes to regulate the proper timing of plant responses to oxidative stress (Lai et al., 2012). Consistently, proper expression and function of other clock components including TOC1, LUX and ELF3 are also important for ROS production, suggesting a key role of the circadian clock controlling ROS signaling and response. The study also reported the function of ROS as a possible clock input cue (Lai et al., 2012). Furthermore, the MYB-like transcriptional regulator KUODA1 (KUA1) directly represses the expression of seven apoplast *peroxidases* (*PRX*s) by direct binding to their promoters (Lu et al., 2014). The repression of the PRXs lead to decreased H_2O_2 levels, which promoted leaf cell size. The *KUA1* expression showed a diurnal expression that was controlled by CCA1 and LHY (Lu et al., 2014). Additionally, the evidences supporting a clock-controlled ROS homeostasis are not just relying on the enzymatic ROS scavenging machineries. For instance, one the most important protectants against ROS over-production are anthocyanins, water-soluble pigments, which have antioxidant activities. It has been reported that the complex formed by the clock components LNKs and RVE8 shapes the diurnal oscillation of the anthocyanin pathway. The clock component RVE8 binds to the promoter of a subset of anthocyanin biosynthetic genes enhancing their expression at dawn. At midday, LNKs interact with RVE8 impedes this activation (Pérez-García et al., 2015). Altogether, the evidences support the notion that the circadian clock is a key mechanism controlling ROS homeostasis.

Many of the metabolic processes controlled by the clock converge on the main energy-related organelles in plants: chloroplasts and mitochondria. The connection of the clock and chloroplasts has been firmly established (Noordally et al., 2013; Haydon et al., 2013b; Atkins and Dodd, 2014). The molecular mechanistic insights linking the circadian clock with mitochondria function are less well understood. In the following sections, we briefly describe the main aspects of mitochondria function and its possible connection with the circadian clock in plants.

3. Mitochondria as a central energetic hub

3.1 Mitochondrial function in mammals and plants

Mammals rely on the mitochondrial function for the production of ATP (Mitchell, 1961) through oxidative phosphorylation, fatty acid oxidation, the tricarboxylic acid cycle (TCA, also known as Krebs cycle), urea cycle, gluconeogenesis and keto-genesis (Spinelli and Haigis, 2018). Mitochondria function is not isolated but entangles with other cellular compartments in the regulation of a vast array of processes including non-shivering thermogenesis, amino acid metabolism, lipid metabolism, biosynthesis of heme and iron–sulfur clusters, calcium homeostasis, apoptosis, ROS signaling and cell dead (Nunnari and Suomalainen, 2012). Approximately 1,500 different nuclear genes encode mitochondrial proteins while about thirteen proteins are encoded by mitochondrial DNA (mtDNA). The mitochondrial proteins encoded by nuclear DNA are translated in the cytoplasm and then imported across the mitochondrial membrane with the aid of a complex import machinery (Calvo and Mootha, 2010; Schmidt et al., 2010).

The generation of ATP relies on an intricate network initiated in the mitochondrial matrix, where the TCA cycle enzymes generate electron carriers (nicotinamide adenine dinucleotide [NADH] and flavin adenine dinucleotide [$FADH_2$]). These carriers provide reductant power by donating electrons to the electron transport chain (ETC) located in the inner mitochondrial membrane (Baldwin and Krebs, 1981; Osellame et al., 2012). The ETC consist of four multi-subunit complexes (I-IV), which interact with each other through the small lipid ubiquinone (UQ10; I/II to III) and the small protein cytochrome c (CYTC; III to IV). By sequential redox reactions, the ETC components undergo conformational changes that favor proton pumping from the matrix to the intermembrane space (Guo et al., 2017). There are two electron transport pathways in the ETC: (1) the complexes I, III, IV with NADH as substrate, and (2) the complexes II, III, IV with succinic acid as substrate. Complex II (Succinate dehydrogenase) is a shared component of the TCA and the ETC (Cecchini, 2003). The proton gradient generated by complex I, II, III and IV is released through the rotatory turbine-like ATP synthase complex (complex V), which drives phosphorylation of ADP to ATP (Stock et al., 1999) (**Figure 5A**).

Due to its relevant function, it is not surprising that mitochondrial dysfunction in mammals is linked to serious diseases including myopathies, neuropathies, cardiovascular disorders and metabolic syndrome (Calvo and Mootha, 2010; Nunnari and Suomalainen, 2012; Radelfahr and Klopstock, 2019). Mitochondrial diseases can affect any organ at any age and can result in fatality. Therefore, tight control of the mitochondrial development and function by the cell is essential to prevent any disturbance of this fundamental organelle.

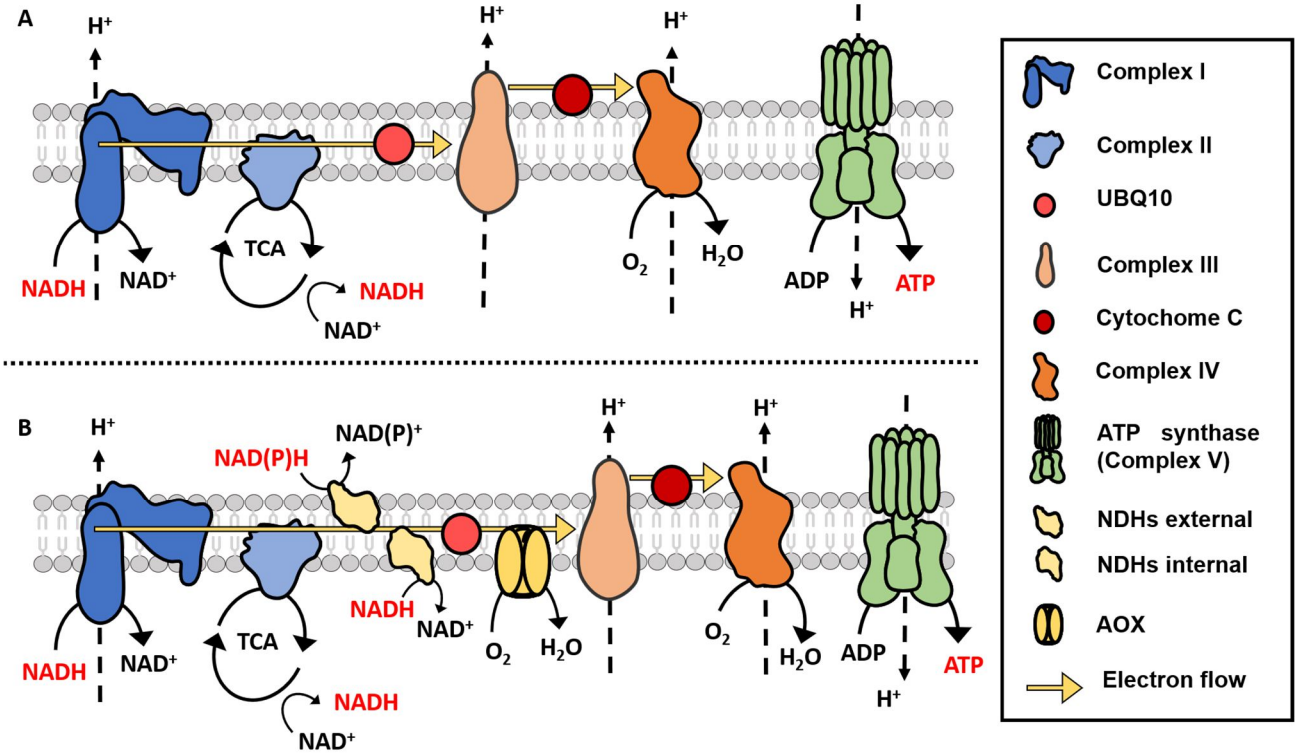

Figure 5. Schematic representation of the ETC components in (A) mammals and in (B) plants. From left to right (A) Complex I, complex II, ubiquinone (UBQ10), complex III, cytochrome c, complex IV, ATP synthase. Also from left to right (B) Complex I, complex II, NDHs external, NDHs internal, ubiquinone (UBQ10), AOX, complex III, cytochrome c, complex IV, ATP synthase. In red NAD(P)H and ATP. Dashed arrows represent proton pumping direction. Yellow arrow represents the electron flow. In (A) and (B) Upper part represent the internal mitochondrial space and lower part represents the mitochondrial matrix were TCA cycle takes place.

In plants, the generation of energy relies not only in mitochondria but also in chloroplasts, which synthetize ATP and respiratory substrates through light-dependent photosynthetic reactions. The coexistence of two energetic organelles requires a meticulous coordination in order to precisely meet the cellular energetic demands without unnecessary waste of resources.

Under illumination, the photosystems transform light energy into ATP and NADPH, which in turn are used to fix CO_2 by the Calvin–Benson cycle. Carbon fixed during the daytime is stored as starch or

exported to the cytosol for sucrose synthesis. During the night, when photosynthesis is inactive, key catabolic processes like glycolysis in the cytosol and the plastid, and the TCA cycle and OXPHOS in mitochondria, break down carbohydrates to generate ATP. In heterotrophic plant tissues as well as all plant tissues in the dark, mitochondria are the main producers of ATP for the cell (Millar et al., 2011; Gardeström and Igamberdiev, 2016).

Although mitochondria in plants resemble in essence the mammalian mitochondrion, plant mitochondria also display some particularities like the presence of additional subunits in complex I, II and IV (Millar et al., 2004; Klodmann et al., 2010; Huang and Millar, 2013) and the presence of an entire subset of non-phosphorylating (non-energy conserving) oxidoreductases, which constitute an alternative respiratory pathway (AOXP) of electron transport from NAD(P)H to oxygen (**Figure 5B**).

The AOXP is shaped by the seven type-II NAD(P)H dehydrogenases (NDH) (NDA1–NDA2, NDB1–NDB4 and NDC1) and five alternative oxidases (AOX) (four AOX1 A-D and one AOX2) (Michalecka et al., 2003; Polidoros et al., 2009). The AOXP introduces a divergent pathway at the ETC where the electrons in the ubiquinol pool can flow through the cytochrome pathway (III-CYTC-IV) or to the AOXP. This branching reduces the energy yield of respiration since AOXP proteins are not proton pumping and the electron flow through AOXP bypass the proton pumping complexes III and IV (Schertl and Braun, 2014) (**Figure 5B**). The function of the AOXP seems to be important for the prevention of excessive reduction of the mitochondrial ETC, which could result in a disruption of glycolysis and TCA under high substrate availability. Furthermore, AOX reduces the effect of oxidative stress by preventing accumulation of ROS, which is a required to sustain high photosynthetic rates (Dinakar et al., 2010). The AOX is also involved in the regulation of reactive nitrogen species (RNS) production (Gupta et al., 2012). NDHs are located in the inner mitochondrial membrane either on its external (NDBs) or on its internal (NDAs and NDC1) surface (Elhafez et al., 2006; Yoshida and Noguchi, 2009). NDHs were proposed to function as cooperative functional units with the AOX (van Dongen et al., 2011). Their enzymatic function is believed to be important in the context of an overflow protection mechanism for the ETC, which is especially relevant during high-light conditions.

3.1.1 Key processes regulated by plant mitochondria

Mitochondria in plants are also related to numerous light-associated processes such as photosynthesis, photorespiration, nitrogen metabolism and the maintenance of redox balance (Rasmusson and Escobar, 2007). One important example is glycine metabolism, which is a fundamental step in the photorespiratory cycle (also known as C2 metabolism) and occurs within the mitochondrial matrix. Organic acids synthetized during the night in mitochondria also provide the carbon skeletons that support amino acids synthesis in the chloroplast during the light (Gauthier et al., 2010).

In non-photosynthetic plant tissue or photosynthetic tissue in the night period, the plant TCA cycle resembles the basic situation in animal cells. However, in illuminated plant photosynthetic tissues, NADH generation in the TCA is reduced due to the utilization of some TCA cycle intermediates in anabolic reactions (Sweetlove et al., 2010; Maurice Cheung et al., 2014; Shameer et al., 2019). In illuminated photosynthetic tissues, the TCA cycle appears to operate predominantly in a non-cyclic manner, consisting of two weakly connected branches operating in opposite directions (Sweetlove et al., 2010). In one branch, citrate accumulated during the previous night is converted to 2-OG (Gauthier et al., 2010; Tcherkez et al., 2012) to re-assimilate ammonium released by photorespiration, while in a separate branch, oxaloacetate (OAA) is reduced to malate and fumarate, enabling excess reducing equivalents from glycine decarboxylation to be exported out of the mitochondria. Furthermore, most of the reactions in the TCA cycle can be bypassed by reactions in the cytosol, with only those catalyzed by citrate synthase and SDH being unique to the mitochondrion (Millar et al., 2011).

Mitochondria also plays a key role for carbon-nitrogen metabolic balance (Szal and Podgórska, 2012), biotic stress response (Amirsadeghi et al., 2007), photosynthetic optimization (Meyer et al., 2009; Yoshida et al., 2011) and plant cell redox homeostasis and signaling (Rhoads et al., 2006; Schwarzländer and Finkemeier, 2013; Aon and Camara, 2015). Mitochondria are also intimately involved in the production of ROS and the processes of programmed cell death (Huang et al., 2016b; Van Aken and Van Breusegem, 2015), flower development (Carlsson et al., 2008), seed germination (Glen Uhrig et al., 2017; Ratajczak et al., 2019) and senescence (Chrobok et al., 2016; Zhang et al., 2017).

Besides organic acids and ATP, mitochondria produces various metabolites, which are used in many fundamental metabolic processes during growth and maintenance of the cell such as fatty acid (Gueguen et al., 2000; Shinde et al., 2016), vitamins and their cofactors such as the antioxidant ascorbate (vitamin C) (Bartoli et al., 2000; Chew et al., 2003; Szarka et al., 2013) and iron-sulphur clusters (Braymer and Lill, 2017). Furthermore, mitochondria are the site of AA catabolism such as glycine (Gly) (Engel et al., 2007), glutamate (Glu) (Miyashita and Good, 2008; Fontaine et al., 2012), γ-aminobutyrate (GABA) (Michaeli et al., 2011), proline (Pro) (Schertl et al., 2014; Launay et al., 2019), lysine (Lys) (Araújo et al., 2010) and branched chain amino acids (BCAA) (valine (Val), leucine (Leu) and isoleucine (Ile)) (Ishizaki et al., 2005a; Peng et al., 2015; Pedrotti et al., 2018).

Under carbon starvation conditions, Pro, Lys and BCAAs can act as substrates for ATP generation. For instance, Pro is oxidized in the mitochondria to Glu by the sequential action of Pro dehydrogenase (ProDH) and Δ^1-pyrroline-5-carboxylate dehydrogenase (P5CDH). ProDH is bound to the inner mitochondrial membrane with its active site facing the matrix, whereas P5CDH is located inside the mitochondrial matrix (Cabassa-Hourton et al., 2016). Lys and BCAAs are metabolized by specialized dehydrogenases in the mitochondria and the electrons derived from dehydrogenation are delivered directly to the ETC through electron transfer flavoprotein/electron transfer flavoprotein:ubiquinone oxidoreductase (ETF/ ETFQO) system (Araújo et al., 2010; Peng et al., 2015). (**Figure 6**).

As in mammals, mitochondria display a prevalent role in plant cells. Hence, disruption of mitochondria importantly affects normal plant activity. For instance, knock-out of the mitochondria TCA fumarase (Pracharoenwattana et al., 2010), ATP synthetase core subunits (Robison et al., 2009), the succinate dehydrogenase 1 (SDH1 subunit of Complex II) (León et al., 2007) or SDHAF2, an assembly factor of SDH (Huang et al., 2013) and the mitochondrial specific RNA polymerase (Kühn et al., 2009) resulted in embryo lethality. Analyses of plants lacking other mitochondrial components such as the mitochondrial malate dehydrogenases (MDH1 and MDH2) (Tomaz et al., 2010), aconitase 1 (ACO1) (Carrari et al., 2003), the complex I subunit 18-kD (NDUFS4) (Meyer et al., 2009), the NADH:ubiquinone oxidoreductase flavoprotein 1 (NDUFV1) (Kühn et al., 2015) or the gamma carbonic anhydrase 1 and 2 (Fromm et al., 2016) resulted in a range of mild to severe growth phenotypes. All these studies indeed reinforce the idea that mitochondria are essential for plant cell activity.

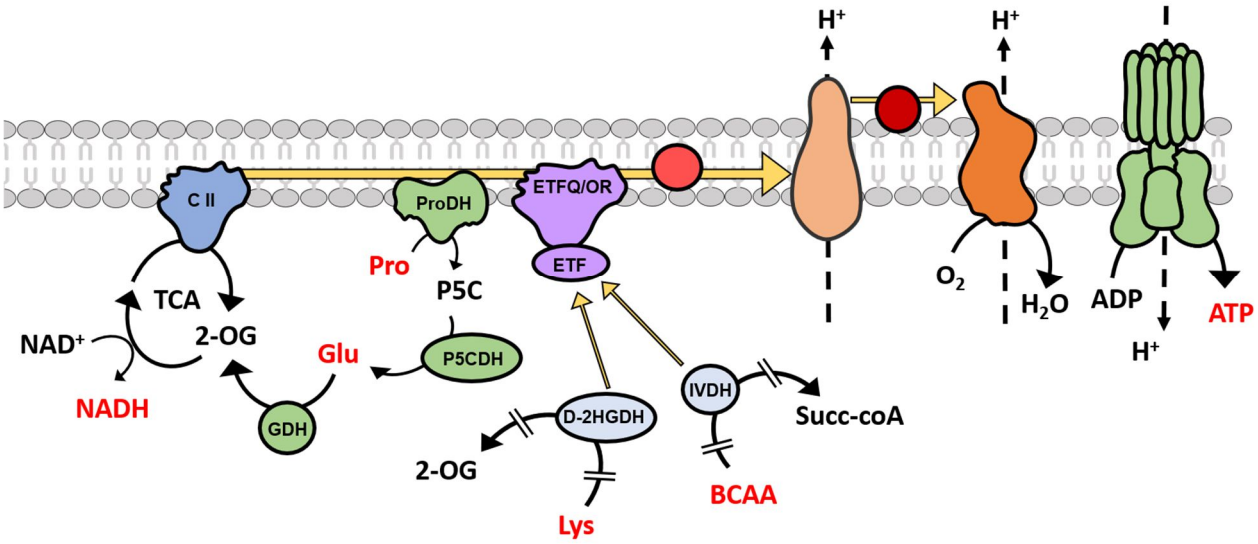

Figure 6. Schematic representation of several amino acid pathways fueling the ETC under carbon limitation. ProDH oxidize Pro and the subsequent reactions lead to 2-OG to the TCA. The electron generated by Lys and BCAAs oxidation are transfer to the ETC by the ETFQ/OR system. From left to right complex II (CII), GDH (glutamate dehydrogenase), P5CDH (pyrroline-5-carboxylate dehydrogenase), ProDH (proline dehydrogenase), ETFQ/OR (electron transfer flavoprotein ubiquinone oxidoreductase), ETF (electron transfer flavoprotein), D-2HGDH (D-2-hydroxyglutarate dehydrogenase), IVDH (isovaleryl-coenzyme A dehydrogenase). Glu (glutamate), Pro (proline), 2-OG (2-oxoglutarato), Lys (lysine), BCAA (branched chain amino acids). Other components as in Figure 5. Broken lines represent intermediary reactions.

3.1.2 Fumarase activity: a key metabolic function in plants

The results of this Doctoral Thesis have uncovered the direct regulation of *Fumarase 2* (*FUM2*) expression by TOC1. Fumarate, is a TCA cycle intermediate with a multiplicity of functions in both plants and non-plant systems. Several studies have clearly identified fumarate as a counter anion for pH regulation and nitrate assimilation during the day (Tschoep et al., 2009). When *Arabidopsis* plants were grown under low nitrate and/or ammonium, fumarate accumulated in small amount. However, when grown under sufficient nitrogen, the carbon accumulated in the form of fumarate reached similar levels as the carbon accumulated as starch (Chia et al., 2000a). Additionally, in the starch-deficient *pgm1* mutant much more carbon was accumulated in the form of fumarate (Chia et al., 2000a; Pracharoenwattana et al., 2010). Hence, fumarate is a temporary carbon sink for photosynthate similar to starch (Gibon et al., 2009).

Fumarate is generated by the oxidation of succinate and the subsequent reduction of ubiquinone to ubiquinol by complex II (succinate dehydrogenase). Fumarate diurnally accumulate, rising until the end of the light period and decreasing during night, in a trend comparable to starch (Chia et al.,

2000b; Gibon et al., 2006). Fumarate has been proposed as a regulator of other TCA cycle enzymes activity such as NAD-malic enzyme 1 (ME1) and ME2 by allosteric competition with malate (Tronconi et al., 2012, 2015). In the light, high ME1 activity is reached when malate levels are elevated in mitochondria. At the end of the night, when fumarate levels increase in *Arabidopsis* leaves, ME1 becomes a high substrate-affinity enzyme by the displacement of malate from the allosteric site. Under this circumstances, ME2 activity would be very low, as this isoform is competitively inhibited by fumarate (Tronconi et al., 2012).

Fumarate accumulates to high amounts in *Arabidopsis* leaves due to the activity of the Fumarase (or Fumarate hydratase) (FUM) enzyme. In fungi and animal cells, FUM is encoded by a single gene and presents a dual localization: mitochondrial and cytosolic (Friedberg et al., 1995; Yogev et al., 2011). The distinctive regulation and function of the two echoforms still remain unclear. In *Arabidopsis thaliana*, FUM activity is encoded by two genes, the mitochondrial *FUM1* and the cytosolic *FUM2* (Heazlewood and Millar, 2005; Pracharoenwattana et al., 2010). FUM1 and FUM2 enzymes can act as fumarate hydratases (FH) (fumarate mobilization) or malate dehydratases (MD) (fumarate generation) (Zubimendi et al., 2018). The MD activity is stimulated by the amino acids Gln, Asn and organic acids such oxaloacetate (OAA), i.e. under organic acid and amino acid accumulation, fumarate synthesis by FUM is favored (Zubimendi et al., 2018). The study also showed that FUM1 and FUM2 could act coordinately during the day, when nitrogen assimilation in leaves is more relevant. At night, FUM2 would be responsible for fumarate accumulation and its mobilization (Zubimendi et al., 2018). The results are consistent with other studies showing that FUM2 activity accounts for the majority of the fumarate accumulation in leaves, as total FUM activity was reduced by 85% in *fum2* mutants while fumarate accumulation was reduced by 90% compared to Wild-Type (WT) plants (Pracharoenwattana et al., 2010). In agreement with the diurnal fluctuations of fumarate, *FUM2* expression also follows a diurnal pattern, reaching a peak in the middle of the day period (Gibon et al., 2004c; Bläsing et al., 2005).

A recent study has shown that the *FUM2* loci displays 2 different alleles, one corresponding to the COL-0 accession and the other to C24 *Arabidopsis* accession (Riewe et al., 2016). The COL-0 accession allele led to greater fumarate levels in rosette leaves than the C24 allele. This reduction

was linked to a reduced *FUM2* transcript accumulation in C24 compared with COL-0 (Brotman et al., 2011). Later studies confirmed that in the C24 allele, there was an insertion of 2kb length fragment at the promoter that was absent in COL-0. This promoter polymorphism was reported as the causal genetic factor of altered fumarate accumulation and plant growth (Riewe et al., 2016).

The correlation between *FUM2* expression levels with fumarate accumulation and biomass was also confirmed under stress conditions in a study using *Arabidopsis* mutant lines displaying low or high salicylic acid levels grown under chilling (5ºC) conditions (Scott et al., 2014). The correlation was established by analyzing the metabolic profiles of salicylic acid (SA)-deficient mutants (*sid2*, *eds5* and *NahG*) and the SA over-producer mutant *cpr1*, which accumulate more and less biomass, respectively. While *sid2*, *eds5* and *NahG* displayed increased biomass and fumarate relative to WT, the opposite phenotypes were found for the *cpr1* mutant (Scott et al., 2014).

FUM2 also plays a key role for the photosynthetic acclimation to low temperatures. At 4ºC, the accumulation of fumarate increased 200% relative to 20ºC without losing its diurnal pattern (Dyson et al., 2016). In *fum2* knock-out plants, the accumulation at 4ºC was lost. The photosynthetic rate in WT plants at 4ºC was lower than at 20ºC, but after 7 days, the photosynthetic rate of WT at 4ºC was similar than at 20ºC. However, the *fum2* never recovered its 20ºC photosynthetic rates. The non-cold-acclimation phenotype of *fum2* plants was consistent with the differential expression observed in WT and *fum2* of genes encoding components of the photosynthetic apparatus (Dyson et al., 2016).

Further studies have also focused on the metabolic profile of the ABA insensitive *srk2dsrk2esrk2i* triple mutant and ABA-biosynthesis *aba2-1* mutant displaying an anomalous growth phenotype (Yoshida et al., 2019). In these mutants, fumarate accumulated at a lowest level compared to WT. *FUM2* expression was significantly reduced in consonance with the reduced fumarate level. The authors attributed the growth defects observed in the ABA mutants to an effect on the TCA cycle, directly resulting from the alteration of *FUM2* expression (Yoshida et al., 2019).

Altogether, FUM2 appears to be a key enzyme for carbon turnover management as well as for nitrogen metabolism, photosynthetic efficiency and cold acclimation. A precise regulation of FUM2 expression and activity is essential for proper plant growth.

3.1.3 A connection between mitochondrial function and the circadian clock in mammals

As in plants, the circadian clock is also responsible for the control of vital aspects of mammal's physiology such as rhythmical food intake, neurotransmitter secretion and cellular metabolism among others (Sahar and Sassone-Corsi, 2009). The core of the circadian oscillator in mammals is also composed by a quite complex regulatory network. Briefly, two basic helix-loop-helix (bHLH) transcription factors, CIRCADIAN LOCOMOTOR OUTPUT CYCLES KAPUT (CLOCK) and BRAIN AND MUSCLE ARNT-LIKE1 (BMAL1) heterodimerize and bind to conserved E-box sequences in promoters driving the rhythmic expression of the key clock genes *PERIOD* (*PER1*, *PER2*, and *PER3*) and *CRYPTOCHROME* (*CRY1* and *CRY2*). PER and CRY proteins form a complex that translocate back to the nucleus to inhibit *CLOCK-BMAL1* mediated gene expression (Dibner et al., 2010).

Important aspects of the circadian metabolic regulation have been extensively studied in mammals. However, the connection between the circadian clock and mitochondrial function is only starting to emerge. Recent evidence supports the existence of daily rhythms in mitochondrial content and function, thereby indicating a widespread interplay between the circadian clock and organellar metabolism (Bass, 2012; Asher and Sassone-Corsi, 2015). For instance, ATP production (Neufeld-Cohen et al., 2016), oxygen consumption rate (OCR) (Peek et al., 2013) and reactive oxygen species levels (Wang et al., 2012a; Magnone et al., 2015) have been shown to oscillate. Furthermore, mitochondrial fission–fusion cycles, which regulate various aspects of mitochondrial biology, show circadian rhythmicity (Andrews et al., 2010; Kohsaka et al., 2014; Jacobi et al., 2015). Rhythmic fission–fusion dynamics are due to circadian regulation of phosphorylation and activity by BMAL1 of DYNAMIN- RELATED PROTEIN 1 (DRP1), which is a key mediator of fission. This process is also regulated by the circadian regulation in the expression of key regulators of mitochondrial dynamics (Schmitt et al., 2018).

Utilization of nutrients by mitochondria also follows a circadian pattern, which is due to the circadian control of the NAD-dependent deacetylase SIRTUIN 3 (SIRT3) (Peek et al., 2013) and rate limiting enzymes such as CARNITINE PALMITOYLTRANSFERASE 1 (CPT1) for lipids and PYRUVATE DEHYDROGENASE (PDH) for carbohydrates (Neufeld-Cohen et al., 2016). Moreover, the mitochondrial lipidome and proteome showed circadian oscillations (Mauvoisin et al., 2014; Loizides-

Mangold et al., 2017). The patterns of specific mitochondrial protein post- translational modifications such as acetylation (but likely also others) also showed circadian oscillations. This rhythmic acetylation could be directly regulated by CLOCK, which has acetyltransferase activity (Masri et al., 2013; Cela et al., 2016). The PEROXISOME PROLIFERATOR-ACTIVATED RECEPTOR-γ CO-ACTIVATOR 1A (PGC1α), a master metabolic regulator fundamental for mitochondrial regulation (Villena, 2015) has been shown to directly regulate metabolism through the interaction with clock genes PER2, CRY1 and CRY2 (Liu et al., 2007; Grimaldi et al., 2010; Kriebs et al., 2017). Altogether, the research developed in the last decade unarguably proves the close relationship between mitochondria homeostasis and the circadian clock function in mammals (Reinke and Asher, 2019).

3.1.4 A connection between mitochondrial function and the circadian clock in plants

The circadian clock regulates many metabolic processes such as nitrogen metabolism, organic acid metabolism, amino acid catabolism or ROS homeostasis (please check section 2.4). These processes are directly related to the mitochondrial function. However, evidences for a direct connection between the circadian clock and mitochondrial components are scarce.

The diurnal regulation of mitochondrial-related intermediates has been already reported. For instance, organic acids accumulate during the light period, providing a substrate for respiration at night. Some of the tricarboxylic acid (TCA) cycle intermediates such as fumarate, malate, citrate and succinic acid, display diurnal and circadian oscillation (Sulpice et al., 2014; Annunziata et al., 2018). Consistently, the expression and activity of a number of enzymes involved in the TCA cycle show oscillations under diurnal cycles (Lee et al., 2010). The function of the clock components PRR9, 7 and 5 was shown to be important for chloroplast and mitochondrial metabolism, as chlorophyll biosynthesis, carotenoid and ABA pathways as well ascorbate, α-tocopherol synthesis and the accumulation of TCA intermediates were affected in triple *prr9prr7prr5*mutant plants (Fukushima et al., 2009).

The organic acids and AA metabolism are interlinked due to the role of organic acids as counter anions for nitrate and nitrogen acceptors during AA synthesis (Nunes-Nesi et al., 2010). For instance, citrate synthesis during the night by the TCA cycle is stored in the vacuole and then exported during

the day to be metabolized into 2-oxoglutarate (2-OG) and sustain the AA glutamate (Glu) synthesis (Gauthier et al., 2010; Maurice Cheung et al., 2014). Moreover, inhibition of the major citrate metabolic enzyme, the ACONITASE (ACO), by nitric oxide (NO) lead to an increase of AA biosynthesis due to an outflow of citrate from the TCA cycle (Gupta et al., 2012). Consistent with the intricate connection between organic acid, AA and circadian function, analyses of the *prr9prr7prr5* triple mutant plants showed that not only the TCA intermediates but also AA accumulation were impaired in the mutant (Fukushima et al., 2009). Signaling of both pathways converges in the mitochondrion, where AA catabolism can fuel organic acid oxidation to satisfy the energetic demands under carbon starvation conditions (Pedrotti et al., 2018). Recent extensive metabolic studies with different clock mutants has confirmed the close link between amino- and organic acids homeostasis and the circadian clock (Pokhilko et al., 2014; Flis et al., 2019). Some metabolite levels were analyzed through diurnal and circadian cycles in a subset of clock mutants. Malate, fumarate, and total amino acid levels were shown to oscillated in continuous light and the period of this oscillations were dependent of the clock period, being shorter in the *cca1/lhy* and in *prr7prr9* double mutants (Flis et al., 2019). Furthermore, there was opposed responses of metabolite accumulation in *lhy/cca1* and *prr7prr9.* While *lhy/cca1* presented low levels of many organic acids (malate, fumarate, citrate, isocitrate, and aconitate), *prr7prr9* presented high levels of these metabolites (Flis et al., 2019). Carbon and Nitrogen metabolism has been reported to be synergically regulated by the interactions between carbon and nitrogen signaling and transcriptional and posttranslational regulation of the enzymes in the central metabolism (Nunes-Nesi et al., 2010; Figueroa et al., 2016). Nevertheless, considering the recent studies, circadian clock seems to play a major role regulating organic acid and N metabolism which is important for establishing and maintaining pools or organic acids, as well as amino acid reserves to support protein synthesis in the night.

Mitochondrial RNA levels remain constant during the day (Okada and Brennicke, 2006). Hence, the mitochondrially-encoded proteins are readily provided by the available organellar RNA in quantities sufficient throughout the day (Okada and Brennicke, 2006). However, the nuclear genes that account for 95% of the mitochondrial proteome (Braun and Schmitz, 1999) show diurnal accumulation of RNA and protein levels (Lee et al., 2010). Several nuclear genes coding for mitochondrial proteins such as cytochrome oxidase 6b-2 (Cyt6b-2), Cyt5b-2, cytochrome c1, cytochrome c2, alternative

oxidase 1c have been shown to be enriched in GGGCC/T (site II) motifs at their promoters. The presence of these motifs was related to their diurnal transcript oscillation (Welchen and Gonzalez, 2006; Giraud et al., 2010). The site II motif is the binding site of the TEOSINTE BRANCHED1, CYCLOIDEA and PCF (TCP) family, a plant-specific family of transcription factors. The TCP family has been shown to be connected with the circadian clock through the interaction of TCP21 (CHE) with TOC1 (Pruneda-Paz et al., 2009). In a later study, members of the TCP protein family were reported to interact with a number of clock proteins. For instance, TCP3 with TOC1, TCP15 with PRR5 and TCP11 with TOC1, LHY, CCA1 and PRR3 (although no interaction of TOC1 with TCP21 was observed (Giraud et al., 2010). The TCP11 was the member interacting with many different clock components. Surprisingly, TCP11 is the only *Arabidopsis* TCP that is not diurnally regulated at a transcript level (Giraud et al., 2010).

OBJECTIVES

The main goal of this Thesis is to understand the molecular basis underlying the circadian control of mitochondrial activity and energy homeostasis in *Arabidopsis thaliana*. This general goal was studied through the following specific objectives:

1. **To analyze the influence of the circadian clock regulating the expression of mitochondrial-related genes.** We will perform bioinformatic and transcriptomic analyses to unravel diurnal and circadian regulation of mitochondrial-related gene expression.

2. **To determine the diurnal and circadian oscillation of ATP production**. We will analyze the oscillation of cytosolic ATP content by fluorometric analysis in WT plants grown under different photoperiodic conditions.

3. **To examine the role of TOC1 in the regulation of mitochondrial-related gene expression.** We will examine diurnal and circadian transcriptional profiles of mitochondrial-related genes in WT and TOC1 miss-expressing plants.

4. **To examine the role of TOC1 in the regulation of metabolite accumulation.** We will compare metabolite profiles of WT and TOC1 miss-expressing plants grown.

5. **To characterize physiological phenotypes related to mitochondrial dysfunction in TOC1 over-expressing plants.** We will analyze biomass, size and starvation-like marker genes in WT and TOC1 miss-expressing plants.

6. **To elucidate the molecular mechanism coupling the circadian clock with mitochondrial function.** We will perform chromatin immunoprecipitation assays in order to identify the possible direct binding of TOC1 to mitochondrial-related gene loci.

7. **To verify the molecular mechanism of TOC1 regulation of mitochondrial activity by performing genetic interaction studies.** We will examine molecular and physiological phenotypes in double over-expressing plants (TOC1 and the direct mitochondrial-related gene).

RESULTS

1. Pervasive diurnal and circadian oscillation of mitochondrial-related gene expression

To examine the connection between the circadian clock and the mitochondrial function in *Arabidopsis thaliana*, we first performed bioinformatic analyses using the DIURNAL database, which contains the rhythmic patterns of gene expression based on multiple microarray experiments (Mockler et al., 2007). By using a previously published list of genes encoding proteins targeted (or putatively targeted) to the mitochondrion (Chrobok et al., 2016), we found a significant number of mitochondrial-related genes (MRG) rhythmically expressed under diurnal and/or circadian conditions (**Figure 7.**).

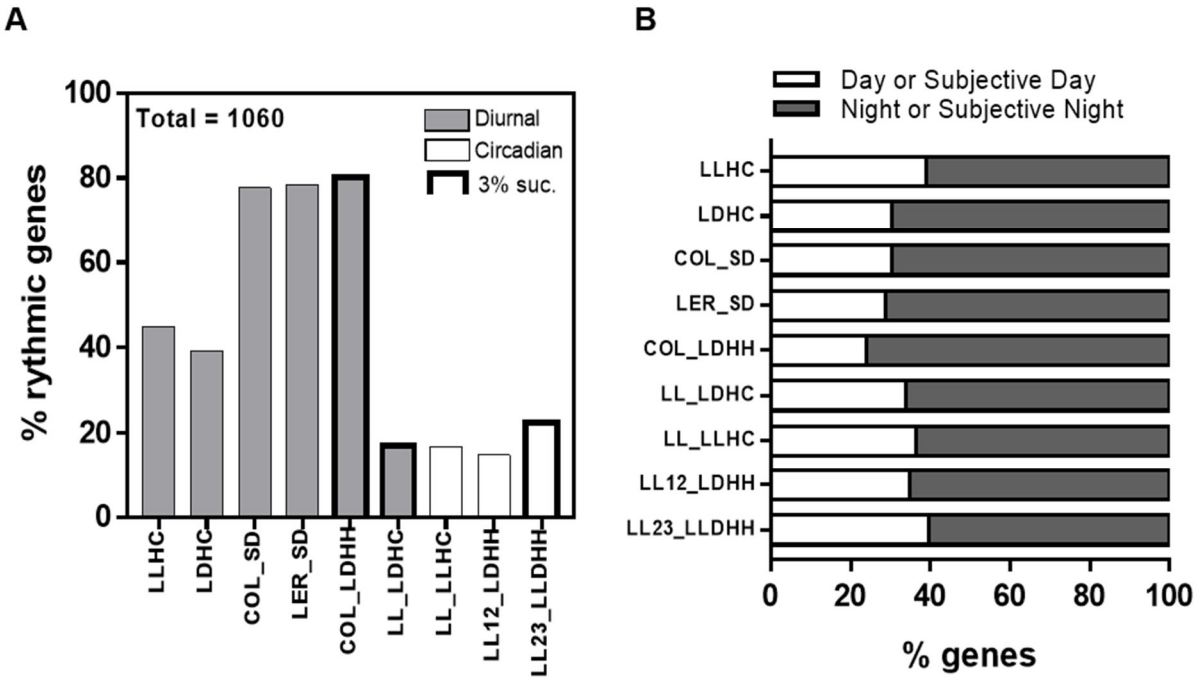

Figure 7. Percentage of mitochondrial-related genes showing a robust oscillation. (A) Proportion of rhythmic MRG present in the Diurnal database in the specified conditions (LLHC, LDHC, COL_SD, LER_SD, COL_LDHH, LL_LDHC, LL_LLHC, LL12_LDHH, LL23_LLHH) with a cut-off value above 0.8. (B) Peak time of the rhythmic MRG during the day or subjective day (ZT0-11) or during the night or subjective night (ZT12-23) for the LLHC, LDHC, COL_LDHH, LL_LDHC, LL_LLHC, LL12_LDHH, LL23_LLHH datasets or during the day or subjective day (ZT0-7) or during the night or subjective night (ZT8-23) for for datasets under ShD. 1060 refers to the number of mitochondrial-related genes analyzed.

Out of the 1060 genes present on the mitochondrial gene list, and using datasets of 7-9-day-old seedlings, we clustered two main groups of rhythmic genes corresponding to entraining conditions (diurnal) or constant conditions (circadian). Overall, we found that the percentage of rhythmic genes

amply varied depending on the condition examined. As expected, the percentage of rhythmic genes was higher for the diurnal than for the circadian datasets. Within the circadian cluster, the percentage of rhythmic genes (14%-22%) was similar for all the circadian datasets examined, independently of the previous entraining growth condition. Among the diurnal datasets, about 80% of the genes were rhythmic when plants were grown under light:dark entraining cues (e.g. COL_SD, LER_SD with 8h light/16h dark; no sucrose; 22ºC and COL_LDHH with 12h light/12 dark; 3% sucrose; 22ºC) (**Figure 7A**). Under temperature-dependent entraining conditions [e.g. LLHC (constant light; 12h 22ºC/ 12h 12ºC; no sucrose)] we found that only 40% of the genes were rhythmic (**Figure 7A**). Despite the variability in the percentage of rhythmic genes, analyses of the peak phases for each condition revealed that about 33% of the genes had a peak phase of expression during the day while aproximately 66% of the genes display a peak during the night (**Figure 7B**).

To obtain a better view of the distribution of the peak phases of expression, we used polar plots to represent the number of genes peaking at each time point over the 24h cycle. Under light and/or temperature entraining conditions, the majority of genes displayed a peak-phase of expression from ZT17 to ZT22 (Zeitgeber Time: number of hours after lights-on) (**Figure 8A-C**). Under constant conditions, the distribution of peaks was wider, even though the majority of genes still showed a peak of expression during the subjective night (**Figure 8D-F**). Comparative analyses of genes that were rhythmic under both circadian and their corresponding entraining condition showed that a high proportion of diurnally regulated genes was also circadianly regulated (**Figure 8G-I**). Moreover, the timing of the peak phase of the overlapped genes followed a similar trend (**Figure 8G-I**).

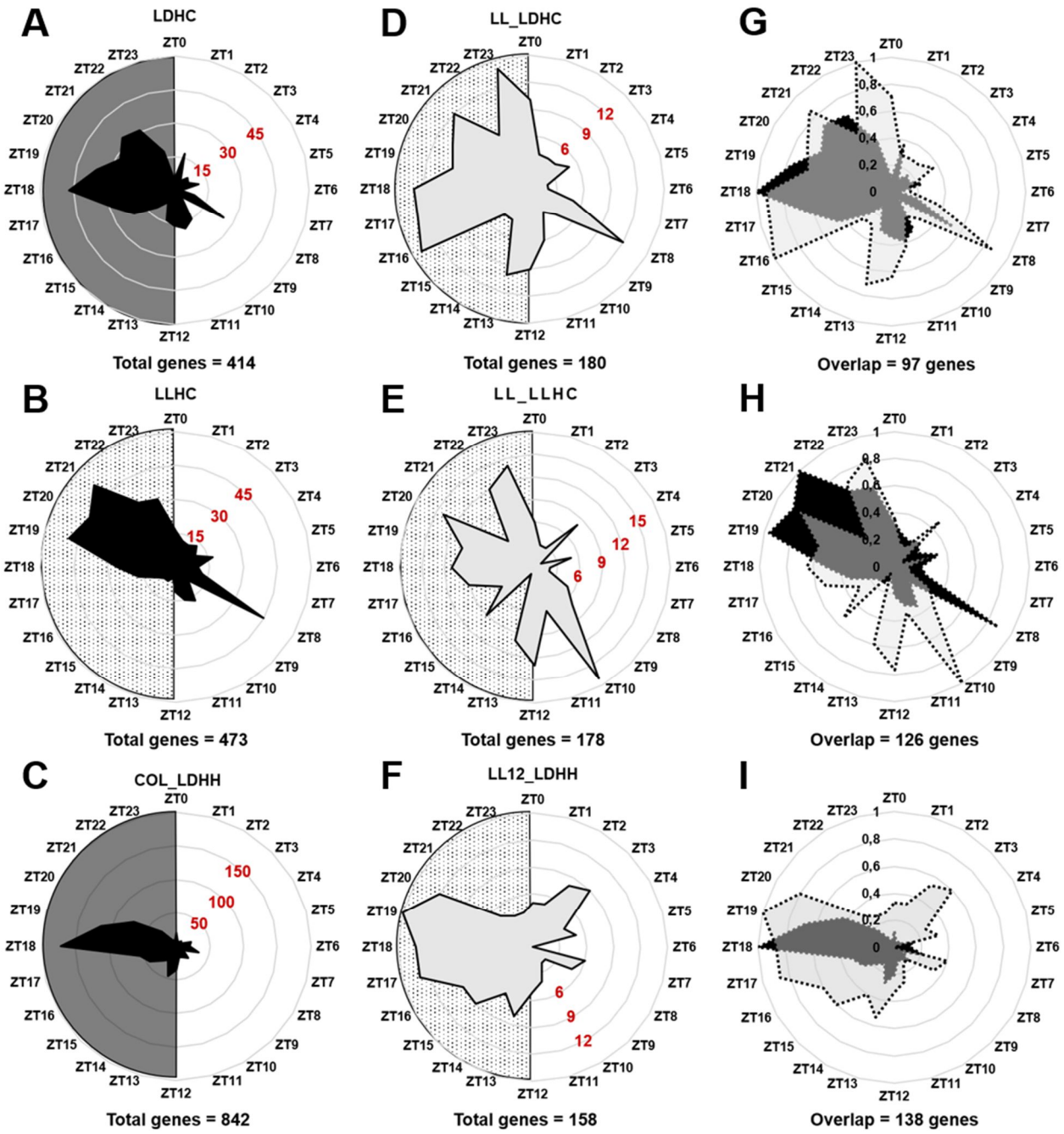

Figure 8. Conserved peak distribution of oscillatory mitochondrial-related genes in the different datasets. Radar plots representing the number of the genes peaking at a certain time point (ZT). (A-C) Diurnal datasets of (A) light and temperature, (B) temperature or (C) light entraining conditions. (D-F) Circadian conditions of (D-E) constant light and (F) constant temperature. (G-I) Overlap of the circadian datasets and their respective entraining condition. The number of total genes analyzed is specified under each radar plot. Red number over the grid lines = gene number. (G-H) Relative gene number to peak is represented in the axis. Black shadows (diurnal datasets) and gray shadows (circadian datasets).

Further comparative analyses of the different growing conditions showed 126 common rhythmic genes, with about 50% of them displaying similar peaks of expression (± 4h) (**Figure 9A**). The

proportion of genes with similar peaks of expression (± 4h) increased up to ~90% when comparing datasets with fluctuating temperature under diurnal light:dark cycles or constant light conditions (LLHC and LL_LDHC, respectively) (**Figure 9B**). Analyses of datasets from samples grown in medium with 3% sucrose and under constant temperature (22ºC) rendered similar peak-phases of expression and with similar percentages of overlapping genes between the entraining and circadian conditions (**Figure 9C**). Altogether, our analyses indicate that the expression of a relevant fraction of the MRG diurnally and circadianly oscillates and show preferential peak-phases of expression during the night or subjective night.

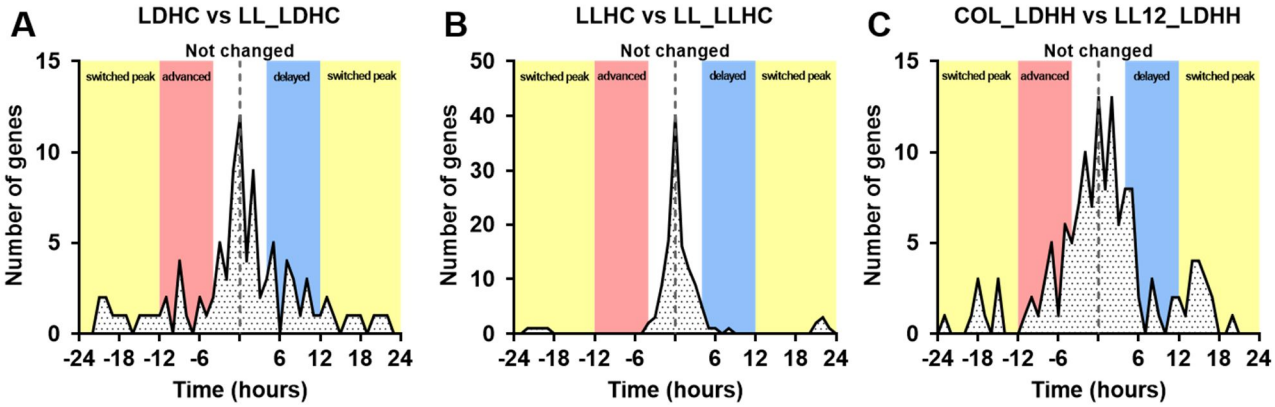

Figure 9. Oscillating mitochondrial-related gene expression sustains similar peak phases between diurnal and circadian conditions. Time of the peak of every gene under circadian conditions was subtracted to the time of the peak under diurnal conditions (A) Phase difference of LL_LDHH relative to LDHC (B) LL_LLHC relative to LLHC and (C) LL12_LDHH relative to COL_LDHH. Total genes with a differential phase change of 0 to 4 in absolute value were considered unchanged (white background). Changes in +6 hours are considered to have a delayed phase (blue background) and with -6 hours considered to be have advanced phase (red background). Differential changes above 12 in absolute value were considered to have shifted phases (yellow background).

2. Functional categorization of the rhythmic mitochondrial-related genes

To examine whether the peak-phases of the mitochondrial-related rhythmic genes could be ascribed to specific mitochondrial functional sub-pathways, we performed Gene Ontology (GO) analyses exploiting the web-based tool PANTHER (Mi et al., 2019). By using the Reactome Pathway annotation dataset with our rhythmic MRG lists, we found that the “metabolism of amino acids and derivatives” was enriched in all of the conditions examined, with peak phases of MRG expression during the day and night (**Figure 10A**) as well as during the subjective day and subjective night (**Figure 10B**).

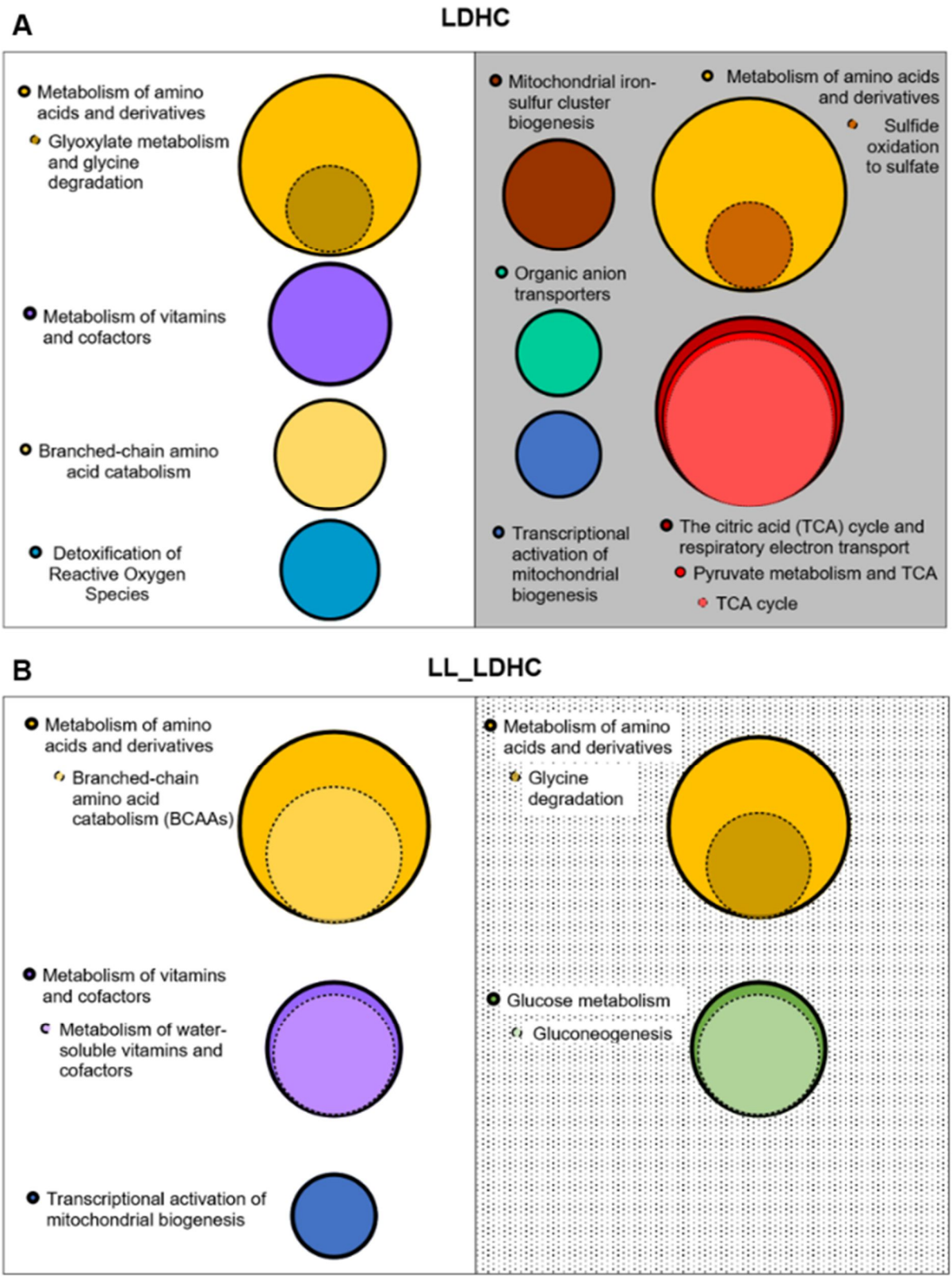

Figure 10. Reactome Pathways represented among the rhythmic mitochondrial-related genes. (A) MRG represented in the LDHC dataset split by day peaking genes (ZT0-11) (left) or night peaking genes (ZT12-23) (right) (B) MRG represented in the LL_LDHC dataset split by subjective day peaking genes (ZT0-11) (left) or subjective night peaking genes (ZT12-23) (right). Bubble size represent the number of genes belonging to any category of the annotation dataset "reactome pathway". Analyzed by Panther Overrepresentation test performing a Fisher's Exact test corrected by False Discovery Rate (FDR). Reactome pathway categories and subcategories with a fold enrichment > 10, raw P-value < 10^{-4} and FDR < 0,05 were selected to be represented.

The “metabolism of vitamins and cofactors” and the “branched chain amino acid catabolism (BCAAs)” pathways were exclusively present during the day or subjective day while the “tricarboxylic acid (TCA) cycle” and the “respiratory electron transport” processes were enriched during the night (**Figure 10A**) and “gluconeogenesis” during the subjective night (**Figure 10B**). Other enriched categories included the “detoxification of reactive oxygen species” during the day, the “mitochondrial iron-sulfur cluster biogenesis” during the night or “transcriptional activation of mitochondrial biogenesis” during the night or subjective day (**Figure 10A**). Overall, and despite the variability of conditions examined, our analysis uncovered a common functional categorization that ascribed the mitochondrial-related rhythmic genes to the TCA cycle (and the TCA-related terms) and the amino acid metabolism.

3. Analysis of mitochondrial-related rhythmic gene expression

Our bioinformatics analyses have provided an overall view of the connection between the circadian clock and its possible role fine-tuning the mitochondrial function. As the disparity of the growing conditions included in the different datasets might confound the actual circadian function on mitochondrial activity, we performed a detailed transcriptomic analysis using Wild-Type (WT) plants homogenously grown under 12h light:12h dark (LD) cycles in medium without sucrose i.e. in the absence of external sources of metabolic energy. Time course assays by RT-QPCR (Reverse Transcription-Quantitative Polymerase Chain Reaction) confirmed the rhythmic oscillation and robust amplitudes for genes encoding proteins belonging to the mitochondrial electron transport chain (ETC) or oxidative phosphorylation (OXPHOS), the tricarboxylic acid (TCA) cycle, NADH dehydrogenases, alternative oxidases (AOXP) as well as mitochondrial transporters (TRAN.) (**Figure 11A** and representative examples in **Figure 11B**). To examine the possible role of the circadian clock regulating these rhythms, we performed analyses under constant light (LL) conditions. Time course analyses by RT-QPCR of plants synchronized under LD cycles followed by LL conditions for two days revealed the circadian rhythms of MRG (**Figure 12A-B**) displaying in some instances reduced amplitudes compared to the ones observed under LD cycles. Representative examples of genes encoding the enzymes of every step of the TCA cycle and the ETC (**Figure 13 and Figure 14**) provided a general glimpse of the influence of diel cycles and the circadian clock orchestrating the rhythms of mitochondrial gene expression.

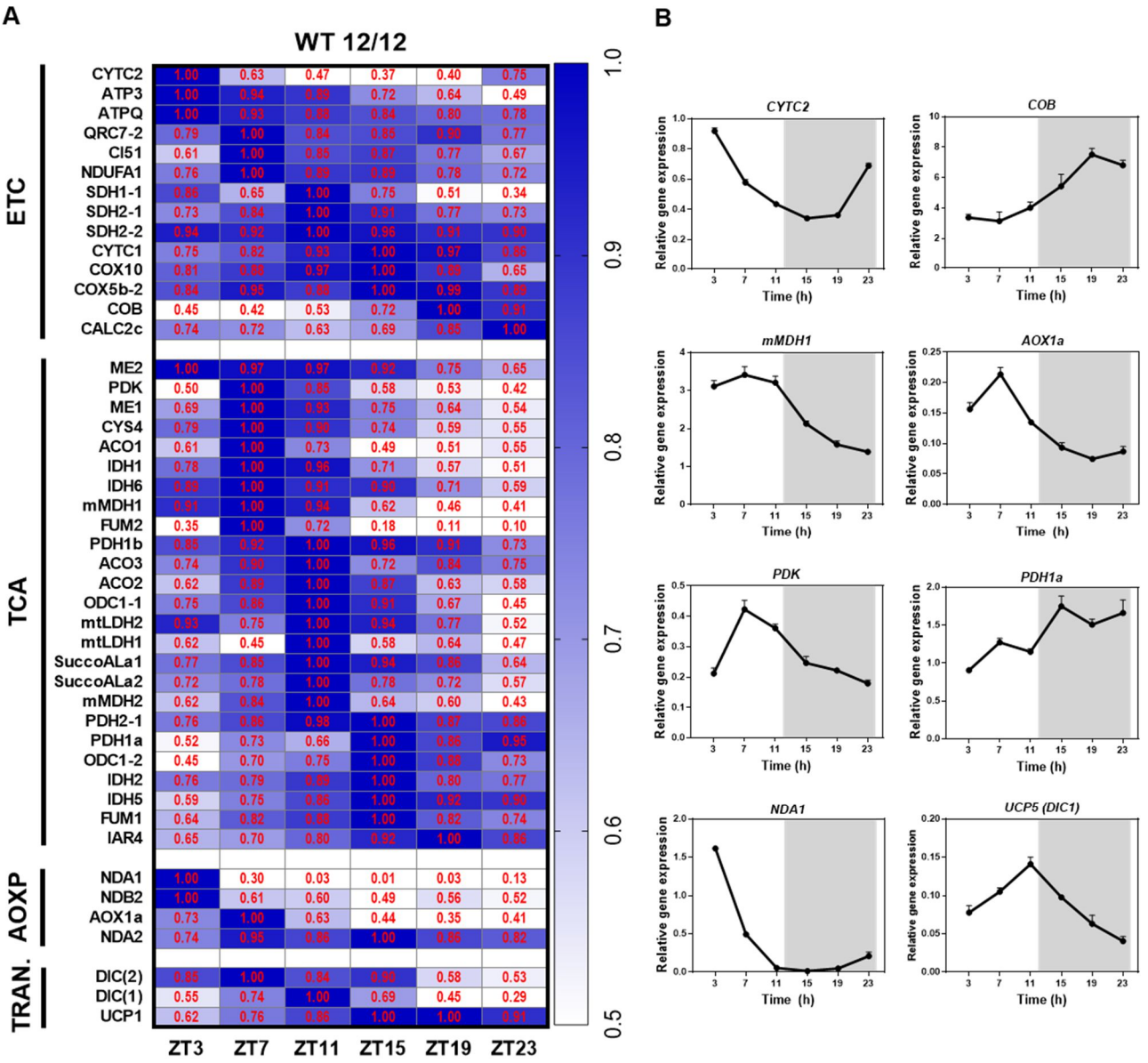

Figure 11. Mitochondrial-related mRNA expression displays robust oscillation over a 12/12 diurnal cycle. (A) Heat map showing time course analysis of MRG over a diurnal cycle under LD (12/12) at 14 days after stratification (das). Gene expression values were normalized to the peak value of each gene. *Zeitgeber time* (ZT) at when samples were collected. Gene identifier is displayed next to left side of the heat map. Red number within the square shows the normalize expression value. Dark blue represents highest value (1.00) and white represent values ≤ 0.50 (B) Representative examples of genes in panel A displaying the gene expression. Relative expression was obtained by Q-PCR analyses. Data are represented as the mean + SEM of technical triplicates. Experiments were repeated at least twice. ***ATPQ*** (ATP SYNTHASE D CHAIN); ***QRC7-2*** (CYTOCHROME BD UBIQUINOL OXIDASE); ***CI51*** (51 KDA SUBUNIT OF COMPLEX I); ***NDUFA1*** (NADH DEHYDROGENASE UBIQUINONE 1 ALPHA SUBCOMPLEX SUBUNIT); ***SDH1-1*** (SUCCINATE DEHYDROGENASE 1-1); ***SDH2-1*** (SUCCINATE DEHYDROGENASE 2-1); ***SDH2-2*** (SUCCINATE DEHYDROGENASE 2-2); ***CYTC1*** (CYTOCHROME C-1); ***COX10*** (CYTOCHROME C OXIDASE 10); ***COX5B-2*** (CYTOCHROME C OXIDASE SUBUNIT 5B-2); ***COB*** (CYTOCHROME B). ***ME2*** (NAD-DEPENDENT MALIC ENZYME 2); ***PDK*** (PYRUVATE DEHYDROGENASE KINASE); ***ACO1*** (ACONITASE 1); ***IDH6*** (ISOCITRATE DEHYDROGENASE 6); ***FUM2*** (FUMARASE 2); ***PDH1b*** (PYRUVATE DEHYDROGENASE E1

COMPONENT BETA SUBUNIT); ***ACO3*** (ACONITASE 3); ***ODC1-1*** (2-OXOGLUTARATE DEHYDROGENASE E1-1); ***mtLDH2*** (LIPOAMIDE DEHYDROGENASE 2); ***mtLDH1*** (LIPOAMIDE DEHYDROGENASE 1); ***SUCCOALA-1*** (SUCCINYL-COA LIGASE ALPHA SUBUNIT 1); ***PDH1a*** (PYRUVATE DEHYDROGENASE COMPLEX E1 ALPHA SUBUNIT or IAR4L); ***IDH2*** (ISOCITRATE DEHYDROGENASE 2); ***IDH5*** (ISOCITRATE DEHYDROGENASE 5); ***IAR4*** (IAA-CONJUGATE-RESISTANT 4); ***NDB2*** (NAD(P)H DEHYDROGENASE B2); ***DIC2*** (DICARBOXYLATE CARRIER 2); ***DIC1*** (DICARBOXYLATE CARRIER 1 or UCP5); ***UCP1*** (UNCOUPLING PROTEIN 1).

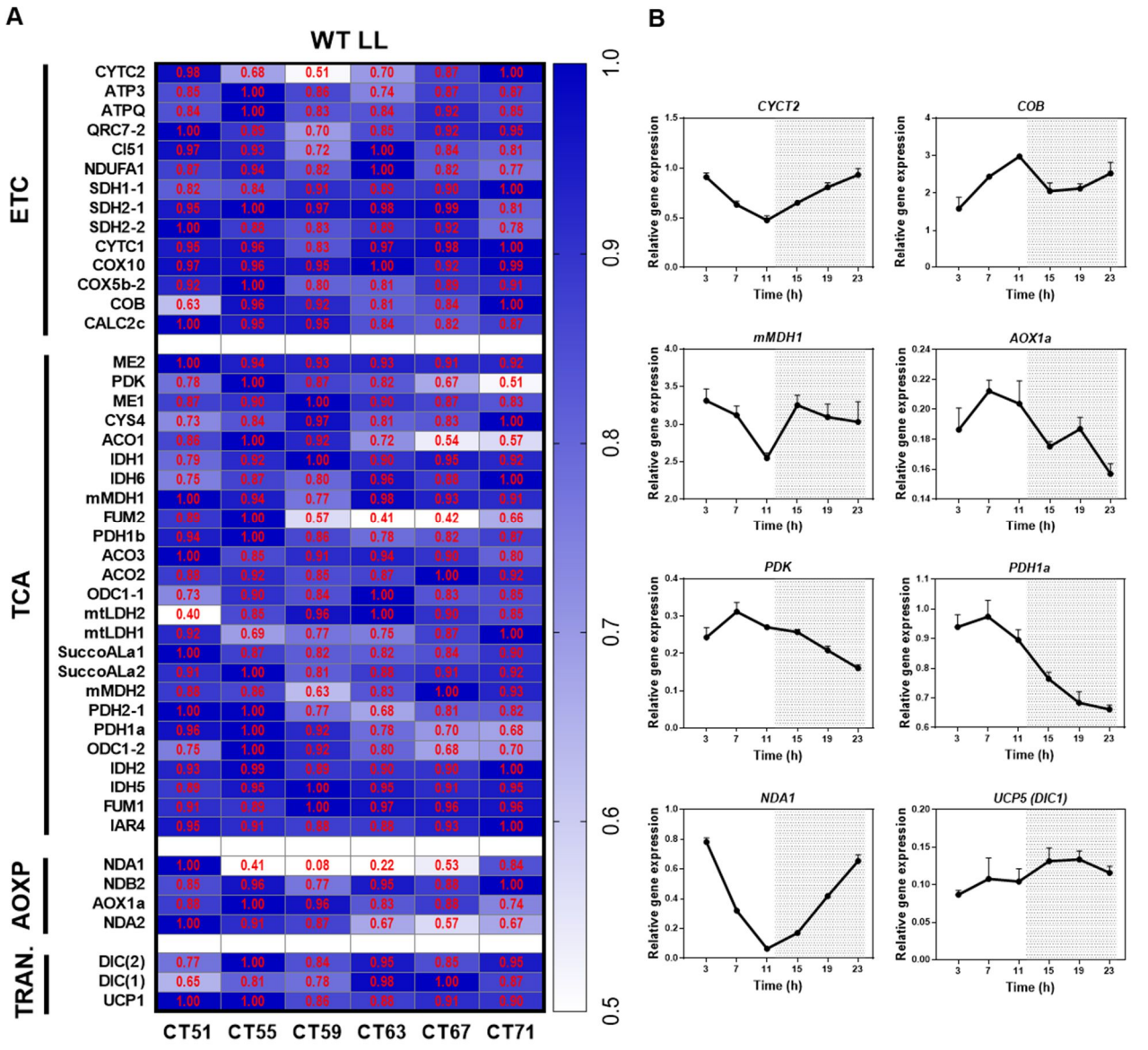

Figure 12. Expression of MRG shows robust oscillation over a 24h constant light cycle. (A) Heat map showing time course analysis of MRG over a circadian cycle under constant light (LL). Plants were entrained under 12/12 cycles over 11 days and then transfer for 2 days to constant light before sampling at 14 das. Gene expression values were normalized to the peak value of each gene. Circadian time (CT) at when sample was collected. Gene identifier is displayed next to left side of the heat map. Red number within the square shows the normalize expression value. Dark blue represents highest value (1.00) and white represent values ≤ 0.50 (B) Representative examples of genes in panel A displaying the gene expression. Relative expression was obtained by Q-PCR analyses. Data are represented as the mean + SEM of technical triplicates. Experiments were repeated at least twice.

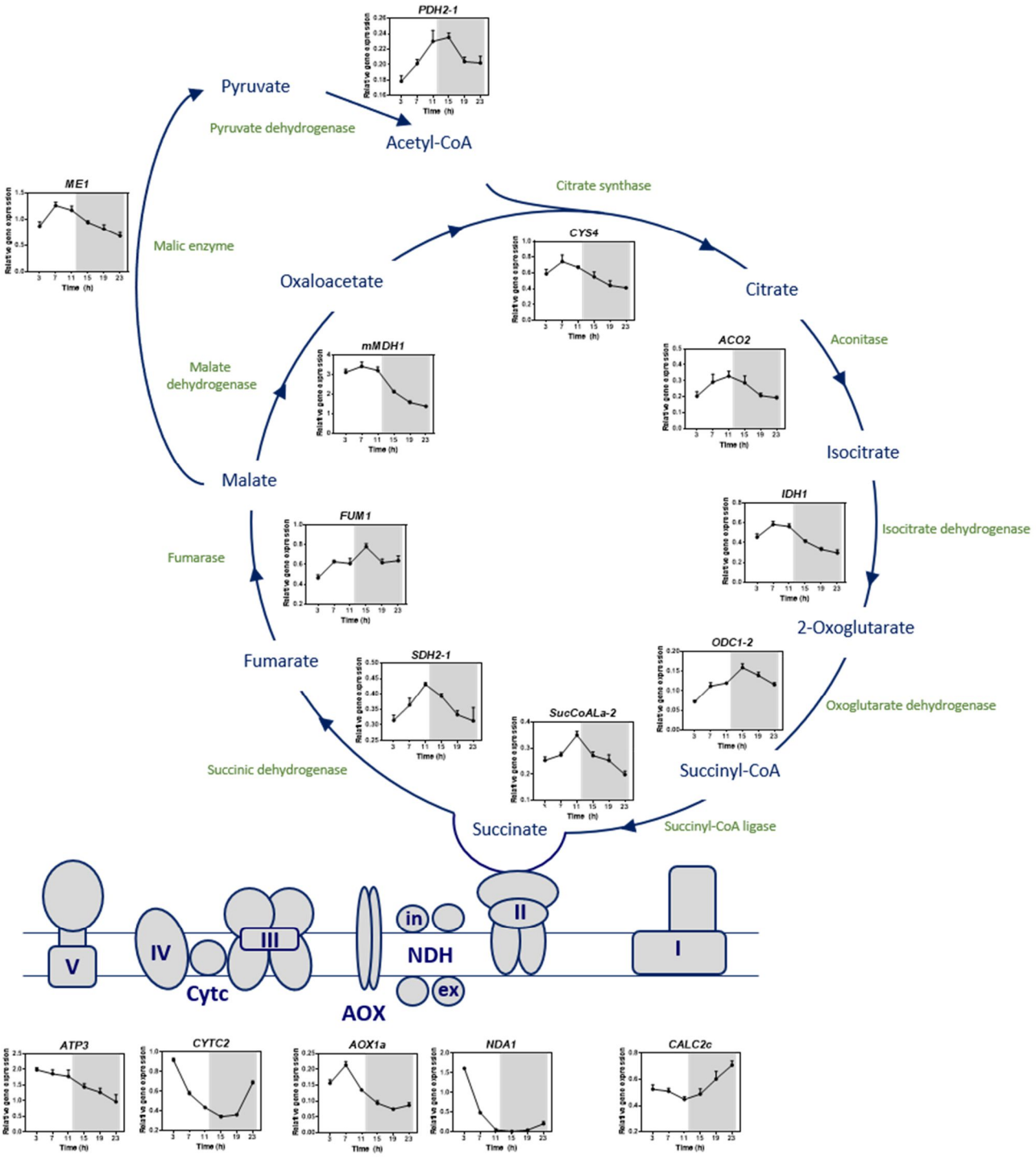

Figure 13. Mitochondrial TCA, ETC related genes shows rhythmical expression in a number of genes. Time course analyses of circadian clock genes over a diurnal cycle. Plants were grown under LD (12/12) and samples were collected at 14 das. Enzymatic metabolite products are blue colored. Enzymatic complexes are green colored. Expression graphs of representative genes of every step are represented. Relative expression was obtained by Q-PCR analyses. Data are represented as the mean + SEM of technical triplicates. The experiments were repeated at least twice. ***PDH2-1*** (MITOCHONDRIAL PYRUVATE DEHYDROGENASE SUBUNIT 2-1); ***CYS4*** (CITRATE SYNTHASE 4); ***ACO2*** (ACONITASE 2); ***IDH1*** (ISOCITRATE DEHYDROGENASE 1); ***ODC1-2*** (2-OXOGLUTARATE DEHYDROGENASE E1-2); ***SUCOALA-2*** (SUCCINYL-COA LIGASE ALPHA SUBUNIT 2); ***SDH2-1*** (SUCCINATE DEHYDROGENASE 2); ***FUM1*** (FUMARASE 1); ***mMDH1*** (MITOCHONDRIAL MALATE DEHYDROGENASE 1); ***ME1*** (NAD-DEPENDENT MALIC ENZYME 1); ***CALC2c*** (GAMMA CARBONIC ANHYDRASE-LIKE 2).

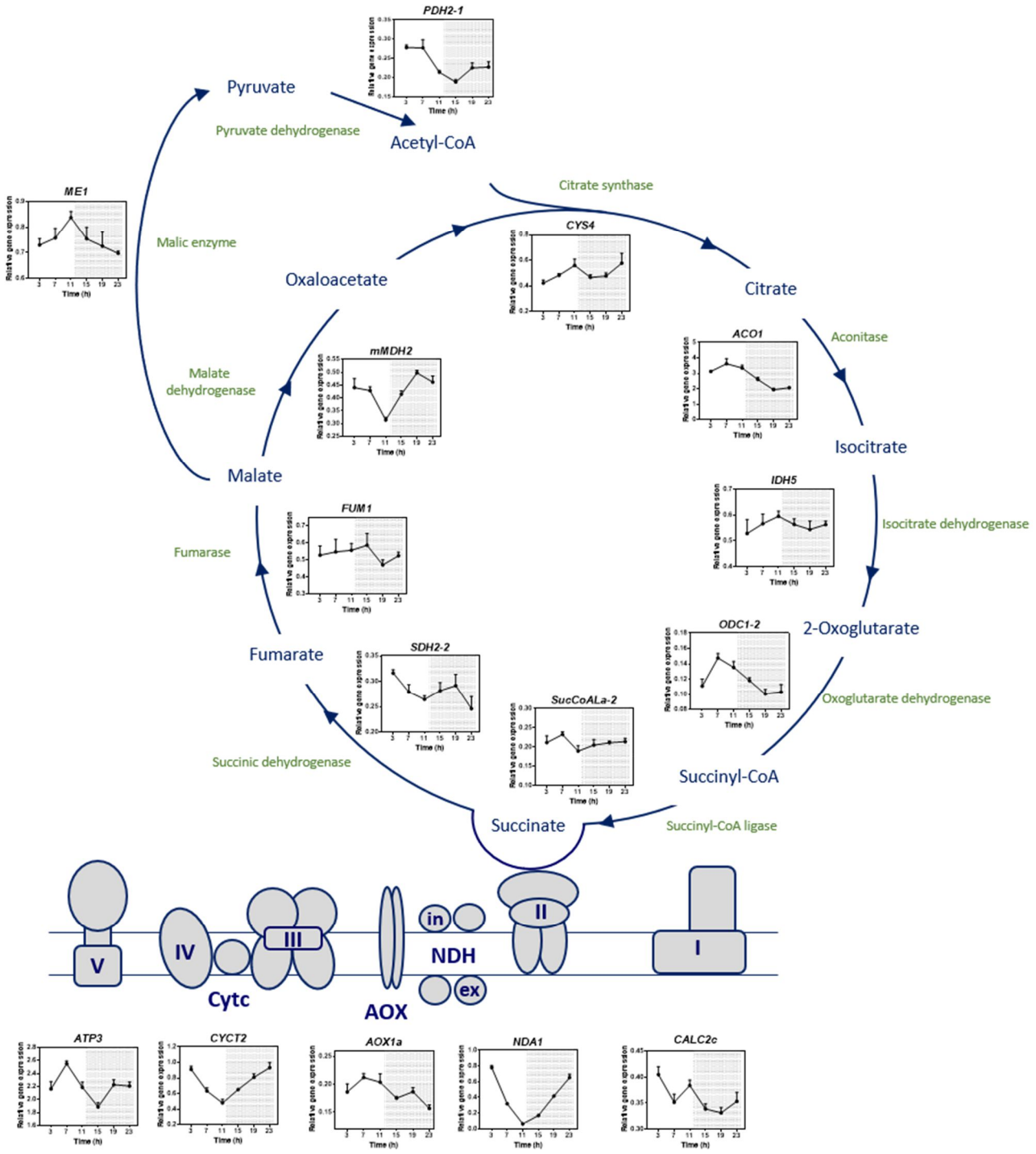

Figure 14. Mitochondrial TCA, ETC related genes shows rhythmical expression in a number of genes. Time course analyses of circadian clock genes over a circadian cycle. Plants were grown under LD (12/12) for 11 days and under constant light for 2 days. Samples were collected at 14 das. Enzymatic metabolite products are blue colored. Enzymatic complexes are green colored. Expression graphs of representative genes of every step are represented. Relative expression was obtained by Q-PCR analyses. Data are represented as the mean + SEM of technical triplicates. The experiments were repeated at least twice. ***NDA1*** (ALTERNATIVE NAD(P)H DEHYDROGENASE 1); ***AOX1a*** (ALTERNATIVE OXIDASE 1A); ***CYCT2*** (CYTOCHROME C-2). ***ATP3*** (GAMMA SUBUNIT OF MITOCHONDRIAL ATP SYNTHASE). **I, II, III, IV, V** (Complex I, II, III, IV and ATP synthase respectively). **NDH** (ALTERNATIVE NAD(P)HDEHYDROGENASES) internal (**in**) and external (**ex**). **Cytc** (Cytochrome c).

4. Cytosolic ATP dynamics controlled by the circadian clock

A central function of mitochondria is energy production. Most of the cytosolic pool of ATP mainly derives from mitochondrial activity (Voon et al., 2018). To examine whether the circadian regulation of mitochondrial-related genes correlates with actual changes in mitochondrial activity, we measured the *in vivo* dynamics of ATP concentration by using a FRET-based ATP biosensor (ATeam 1.03-nD/nA), which relies on the conformational change of the ε-subunit fragment of ATP synthase upon ATP binding (Imamura et al., 2009). The change in the protein structure brings in proximity the fused donor (CFP, cyan fluorescent protein) and acceptor (Venus) fluorophores, increasing FRET efficiency. The feasibility of the biosensor providing a map of cytosolic ATP concentrations in living seedlings have been previously demonstrated (De Col et al., 2017). Our fluorimetric analyses of the fluorescent emission ratio (539/483 nm) following excitation at 435 nm indeed confirmed the decreased ratio of the fluorescent signals following treatment with inhibitors of mitochondrial ATP production (**Figure 15C-D**) Diel time course analyses of plants grown under light:dark cycles revealed an oscillatory pattern of cytosolic ATP accumulation with an overt peak around dawn that declines during the day and reaches a trough during the night (**Figure 15E**). The amplitude of the waveforms appeared to be higher under short than under long photoperiods (**Figure 15F-G**). Rhythms were also sustained under free-running conditions (LL) albeit with decreased amplitude (**Figure 15H**). Overall, the amplitude was higher when seedlings were grown in medium without sucrose (**Figure 15F-H**). Notably, under LL, the rhythms dampened low when seedlings were grown in medium supplemented with 3% sucrose (MS3) (**Figure 15H**) suggesting that ATP rhythms are abolished when sufficient exogenous energy resources are supplied.

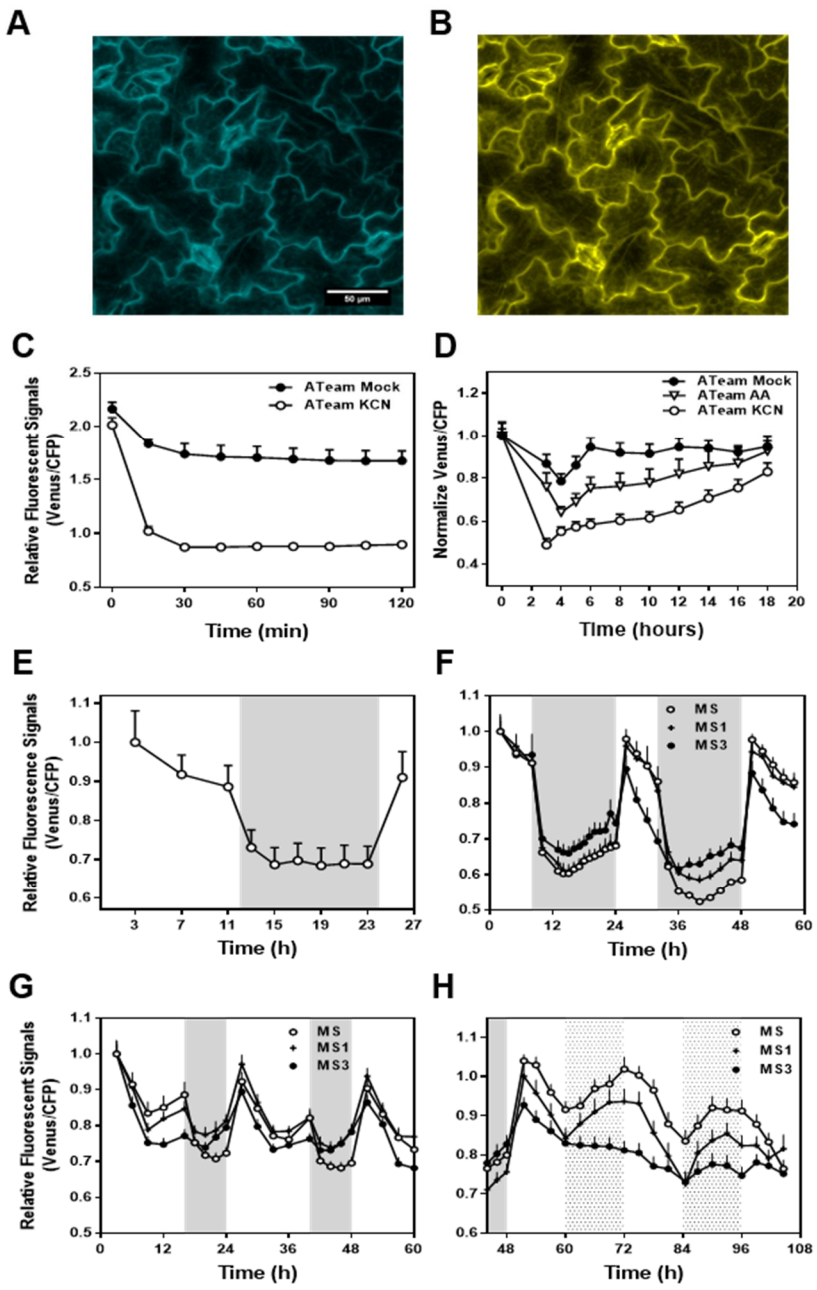

Figure 15. Cytosolic ATP levels fluctuate through diurnal and circadian cycles. Confocal image of cotyledon mesophyll cells excited at 435 nm and emission (A) 483 nm and (B) 539 nm. Scale bar 50um. 10-day old seedlings were grown vertically on 96-well microtiter plates on 200ul of half-strength MS0%,1% or 3% sucrose. Per well, three seedlings expressing no sensor (Col-0) or cytosolic ATeam were excited at 435 ± 10 nm, and the emission at 483 ± 9 nm (CFP) and 539 ± 6 nm (Venus) was recorded (C) KCN (100 µM) or (D) Antimycin A (100µM) was added after first time point while control plants were left untreated (black datapoints). (E) Time course fluorometric analysis over 24h under a LD cycle, (F) 60h under ShortD cycles (G) LongD cycles and (H) 24h under LL entrainment. Emission in wells with Col-0 plants was averaged and subtracted from that of ATeam-expressing plants to correct for background fluorescence. Data shown and used for background subtraction is the average of 12 wells and error bars are SEM.

5. The circadian expression of mitochondrial-related genes is altered in TOC1 miss-expressing plants

In order to identify clock components important for MRG circadian regulation, we analyzed gene expression in clock mutant and over-expressing plants. Previous transcriptomic profiles have shown that PRR9, 7 and 5 are important in the control of chloroplast and mitochondria function (Fukushima et al., 2009) although the analyses were performed with plants growing in medium containing sucrose (2%), which might preclude a clear conclusion about the use of metabolic energy provided by the mitochondria. Circadian time course of plants grown under LL in the absence of sucrose

revealed that the rhythmic pattern of MRG expression in WT plants was clearly affected by over-expression and mutation of TOC1 (**Figure 16**). Peak accumulation appeared to be delayed in TOC1-ox (**Figure 16B**) and advanced in *toc1-2* (**Figure 16C**), which is consistent with the previously reported circadian phenotypes (Somers et al., 1998b; Strayer et al., 2000; Más et al., 2003a, 2003b).

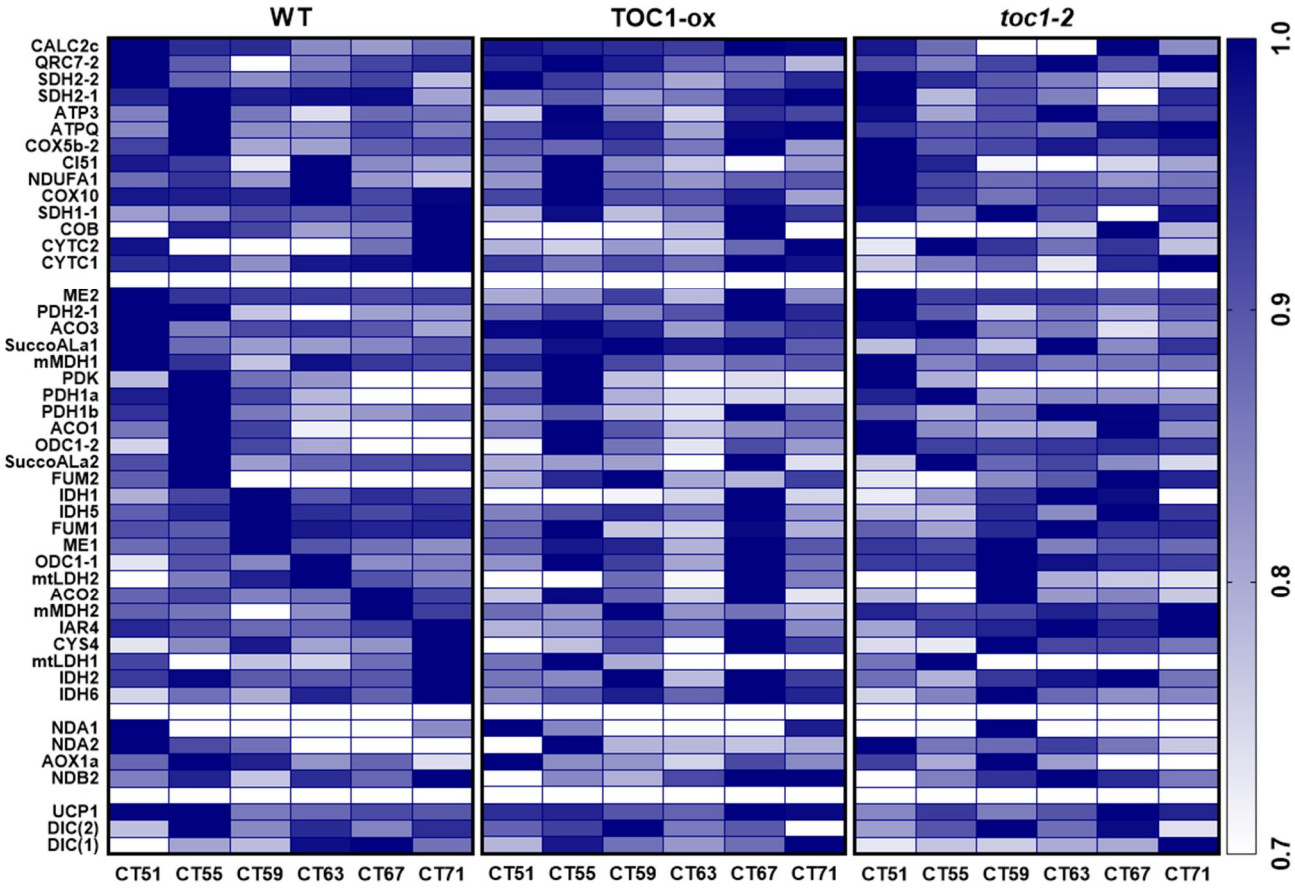

Figure 16. TOC1 miss-expression plants have a disrupted MRG expression profile. Heat map showing time course analysis of MRG over a circadian cycle under constant light (LL). WT (left), TOC1-ox (middle) and *toc1-2* (right) plants were entrained under 12/12 cycles for 11 days and then transfer for 2 days to constant light before sampling at 14 das. Circadian time (CT) at when sample was collected. Gene identifier is displayed next to left side of the heat map. The average value of gene expression at every time point was normalized to the peak value of each gene. Red number within the square shows the normalize expression value. Dark blue represents highest value (1.00) and white represent values ≤ 0.50. Relative expression was obtained by Q-PCR analyses using technical triplicates. The experiments were repeated at least twice.

Comparison of values relative to WT showed that expression of some genes was down-regulated in TOC1-ox and conversely, up-regulated in *toc1-2* (**Figure 17A-E**). The down- and up-regulation was also observed in genes with not very evident oscillation or with reduced amplitude (e.g. **Figure 17F-H**). Less frequently, the amplitude of some genes was increased in TOC1-ox (**Figure 17I**). As TOC1

functions as a general repressor (Huang et al., 2012; Gendron et al., 2012), the up-regulation might reflect an indirect regulation through other clock components.

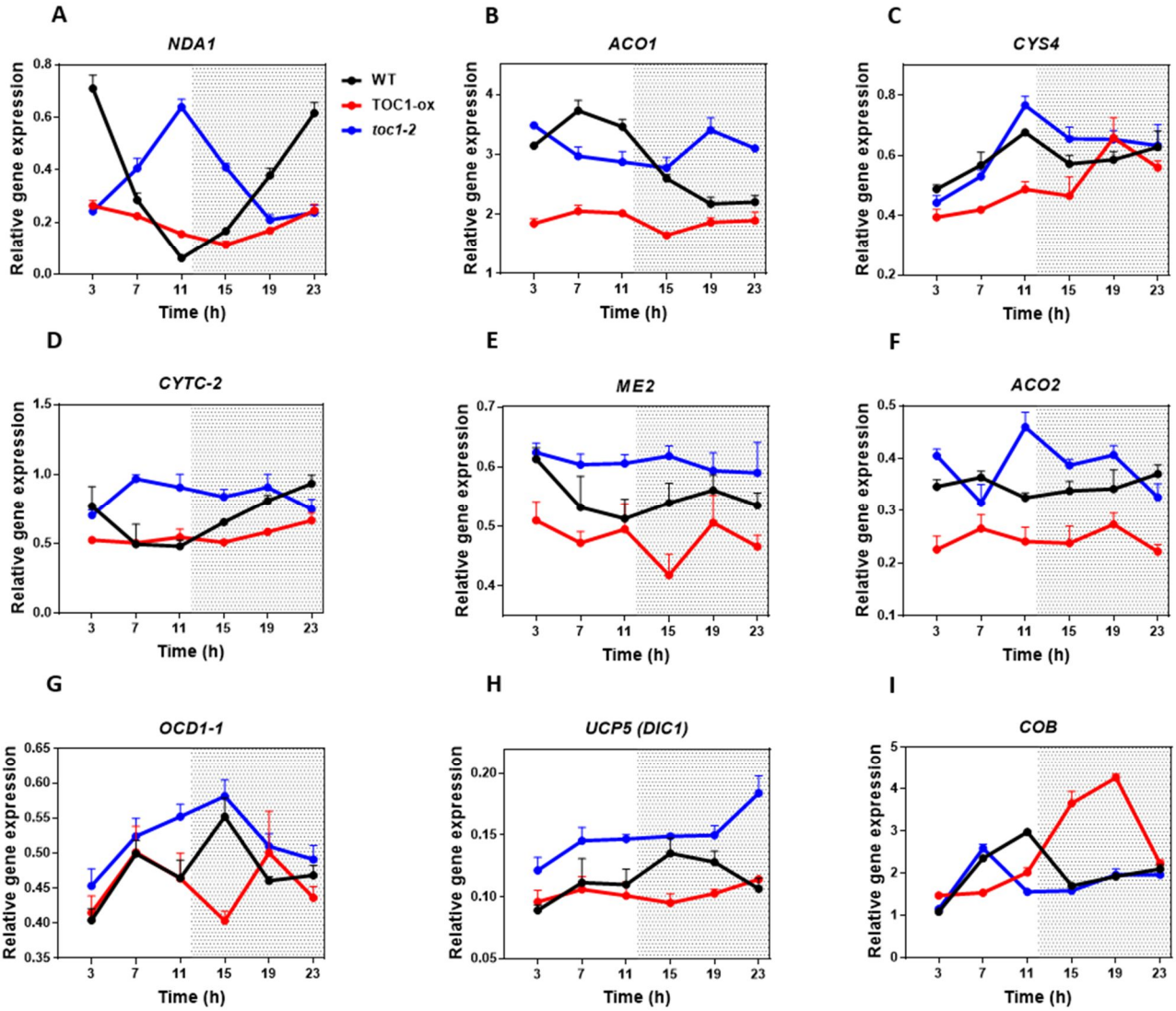

Figure 17. Miss-expression of MRG in TOC1 miss-expressing plants. Time course analyses of MRG in WT (black dataset), TOC1-ox (red dataset) and *toc1-2* (blue dataset) over constant light (LL). Plants were entrained under 12/12 cycles for 11 days and then transfer for 2 days to constant light before sampling at 14 das. Expression of (A) *NDA1*, (B) *ACO1*, (C) *CYS4*, (D) *CYTC-2*, (E) *ME2*, (F) *ACO2*, (G) *OCD1-1*, (H) *DIC1* and (I) *COB*. Relative expression was obtained by Q-PCR analyses. Data are represented as the mean + SEM of technical triplicates. The experiments were repeated at least twice.

6. Miss-expression of TOC1 alters the diurnal and circadian metabolic profiles

We next investigated whether the transcriptional changes correlated with actual alterations in metabolite accumulation. To that end, we performed Gas Chromatography/Mass Spectrometry

(GC/MS) analyses in WT, TOC1-ox and *toc1-2* plants grown in medium without sucrose. Samples were taken at ZT7 and 19 under LD cycles as well as at CT7 and CT19 following two days under LL conditions. In WT plants, a number of metabolites displayed diurnal fluctuations with higher accumulation at ZT7 during the day than at ZT19 at night. Examples include sugars such as glucose, amino acids such as serine, or TCA intermediates such as succinic acid (**Figure 18A**). Overall, metabolites with high amplitude fluctuations in WT showed decreased accumulation in TOC1-ox and were slightly increased in *toc1-2* (**Figure 18B**). Under LL conditions, a subset of the metabolites assayed also fluctuated with increased accumulation during the subjective day (e.g. glycine) or night (e.g. phenylalanine) (**Figure 18C**). The rhythmic fluctuations were altered in TOC1-ox and *toc1-2* mutant plants (**Figure 18D**). Compared to WT, amino acids accumulated either during the day or night in TOC1-ox whereas sugars and fumaric acid displayed a clear reduction. Conversely, fructose, fumaric acid or the amino acid glycine were increased in *toc1-2* (**Figure 18D**). These patterns followed a similar trend under both LD and LL conditions (**Figure 18B,D**). Together, the results indicate that proper expression and function of TOC1 is important for the diel and circadian oscillations of sugars, amino acids and TCA intermediates.

As TOC1 functions as a general repressor (Huang et al., 2012; Gendron et al., 2012), we compared metabolites miss-regulated in TOC1-ox and *toc1-2* relative to WT and focused on those down-regulated in TOC1-ox and up-regulated in *toc1-2*. We reasoned that metabolites in this cluster might provide an indication of the possible direct regulation by TOC1 of a metabolic-related gene. Our analyses uncovered the amino acid glycine, the sugar fructose and the TCA intermediate fumaric acid as down-regulated in TOC1-ox and up-regulated in *toc1-2* under both LD (**Figure 19A**) and LL (**Figure 19B**) conditions.

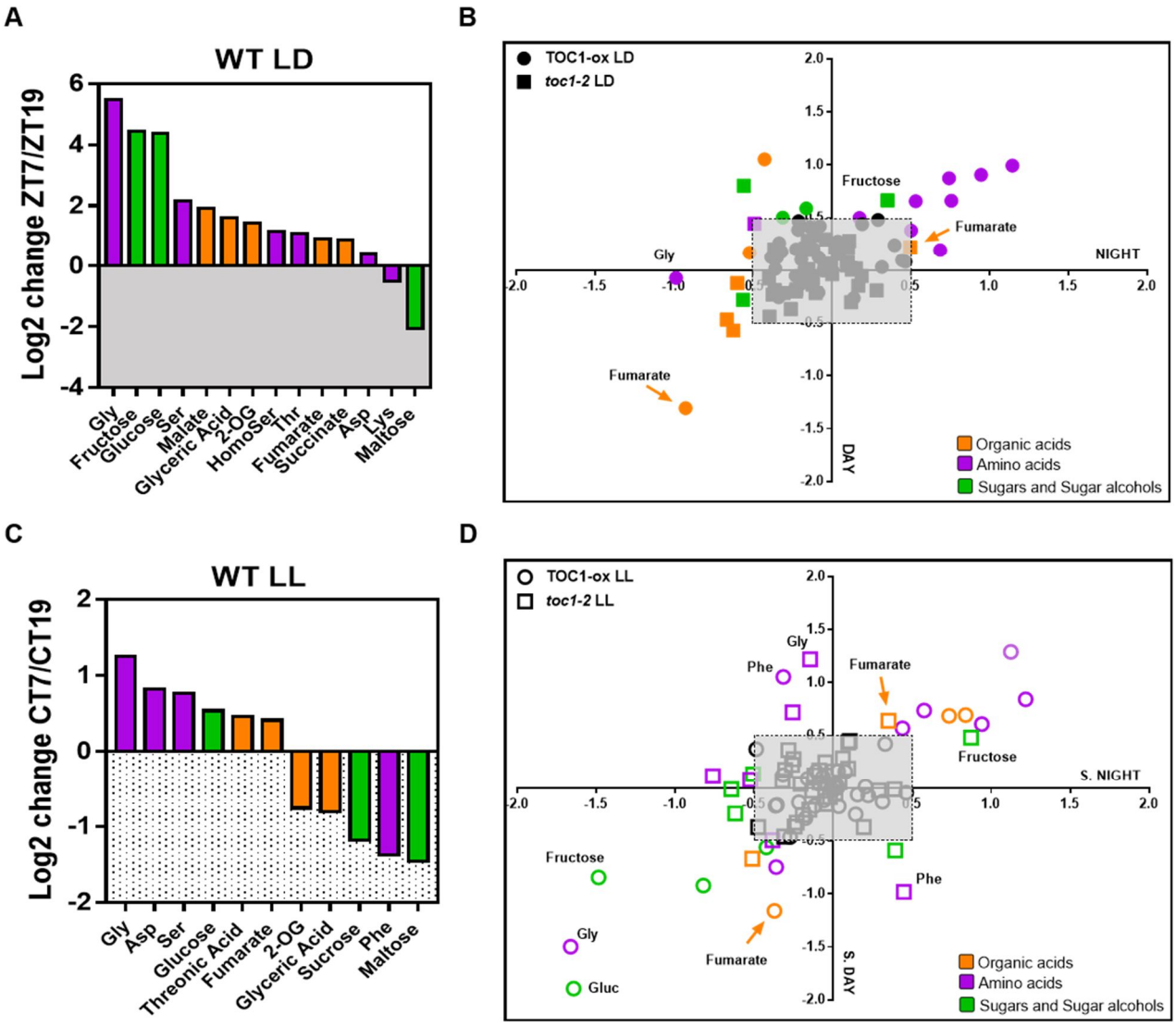

Figure 18. Metabolic profile is disrupted in TOC1 miss-expressing plants. Relative levels of the GC-MS-analyzed metabolites in WT, TOC1-ox and *toc1-2* plants. One set of plants were grown under LD cycles and sampled 14 das and the other entrained under LD cycles for 11 days and then transfer for 2 days to constant light (LL) before sampling at 14 das. Two time points in LD (ZT7, ZT19) and in LL (CT7, CT19) were collected. Metabolites were clustered per class into amino acids (purple), organic acids (orange) and sugars and sugar alcohols (green). (A;C) In the bar graphs, WT relative values of ZT7 to ZT19 or CT7 to CT19 were plotted displaying Log2 metabolite accumulation (A) day/night or (C) subjective day/subjective night. (B;C) In the dispersion plot graph, TOC1-ox (circles) and toc1-2 (squares) metabolite Log2 fold differences relative to WT under (B) LD or (D) LL cycles. X axis represent nigh or subjective night. Y axis represent day or subjective day values. Relative metabolite levels in seedlings of WT, TOC1-ox and *toc1-2* plants under all light conditions were normalized to the mean level of the WT plants under LD or LL conditions and fold-change values were log2 transformed (i.e. the level of all metabolites of Col-0 plants is 0). Values are means ± SE of at least 3 replicates. Log2 fold differences < [0.4] were not considered (gray square). **2-OG** (2-oxoglutarate); **Asp** (aspartate); **Gly** (glycine); **HomoSer** (homoserine); **Lys** (lysine); **Phe** (phenylalanine); **Ser** (serine); **Thr** (threonine); **Gluc** (glucose); **S. NIGHT** (subjective night); **S. DAY** (subjective day).

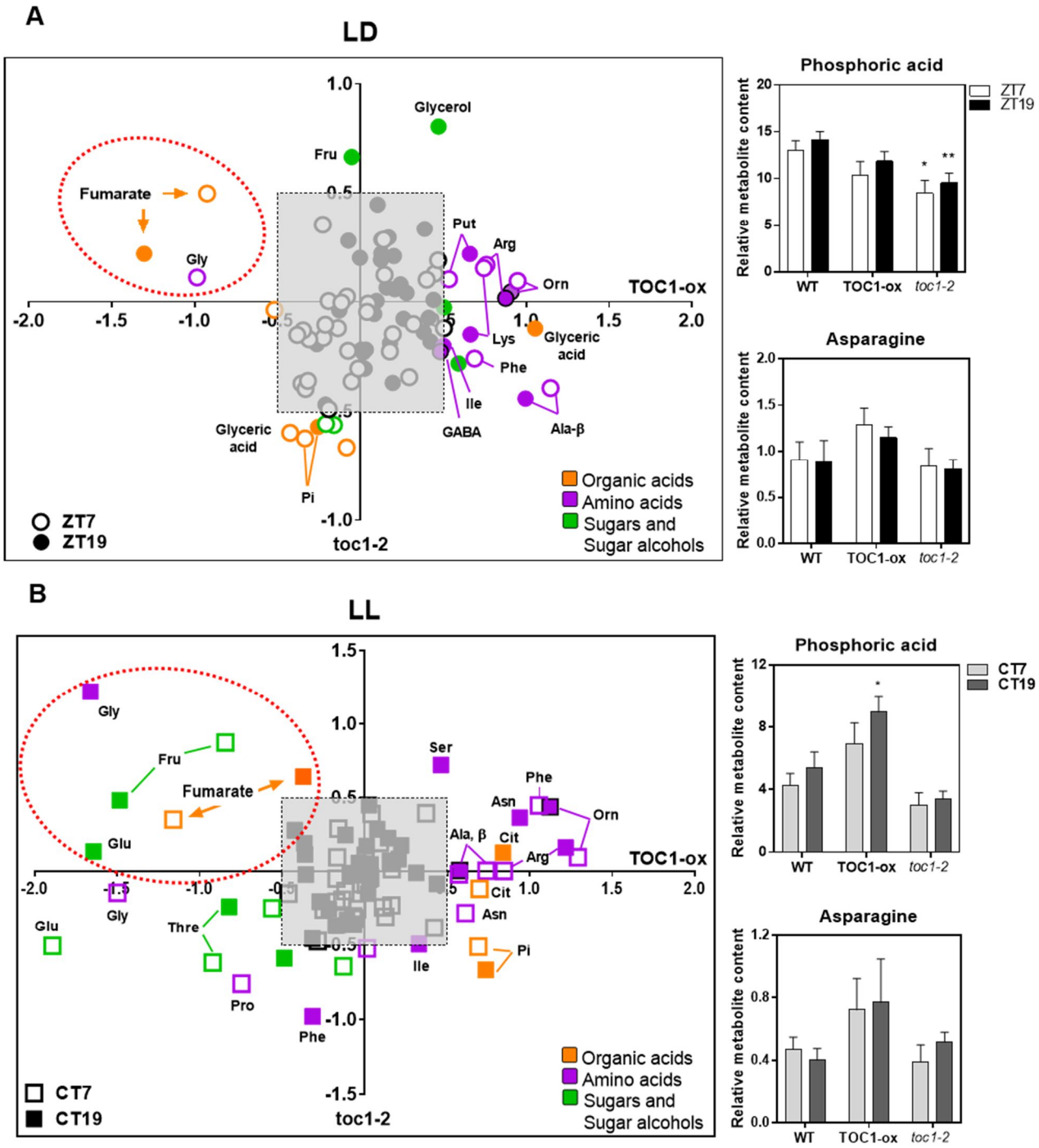

Figure 19. Metabolic diurnal and circadian accumulation is disrupted in TOC1 miss-expressing plants. Sample description same as in Fig. 13. In the dispersion plot graph, X axis represent TOC1-ox values and Y axis represent *toc1-2* values under (A) LD or (B) LL cycles. Solid symbol represents night or subjective night and empty symbols represents day or subjective day. Doted red circle highlights metabolites with increased levels in TOX1-ox and depressed levels in toc1-2 plants. Log2 fold differences < [0.4] were not considered (gray square). In bar graphs, examples of individual metabolite relative content are represented. Values are means + SE of 3-6 replicates. Asterisks denote significant differences (*P < 0.05, **P< 0.01; Student's t-test) to the WT. **Cit** (citrate); **Pi** (phosphoric acid); **Ala-β** (beta-alanine); **Arg** (arginine); **Asn** (asparagine); **GABA** (γ-aminobutyric acid); **Gly** (glycine); **Ile** (isoleucine); **Lys** (lysine); **Orn** (ornithine); **Phe** (phenylalanine); **Pro** (proline); **Put** (putrescine); **Ser** (serine); **Fru** (fructose); **Glu** (glucose); **Thre** (trehalose).

In agreement with previously reported data (Pracharoenwattana et al., 2010), WT plants accumulated more fumarate at day than at night. Fumarate accumulation was significantly lower in TOC1-ox plants and tended to over-accumulate in *toc1-2* plants (**Figure 20A**). The lower and higher fumarate accumulation in TOC1-ox and *toc1-2* plants, respectively was also very evident under LL. Furthermore, diurnal fumarate accumulation was lost in TOC1-ox lines (**Figure 20B**). When the fumarate to malate ratio is represented, the differences relative to WT remained (**Figure 20C**).

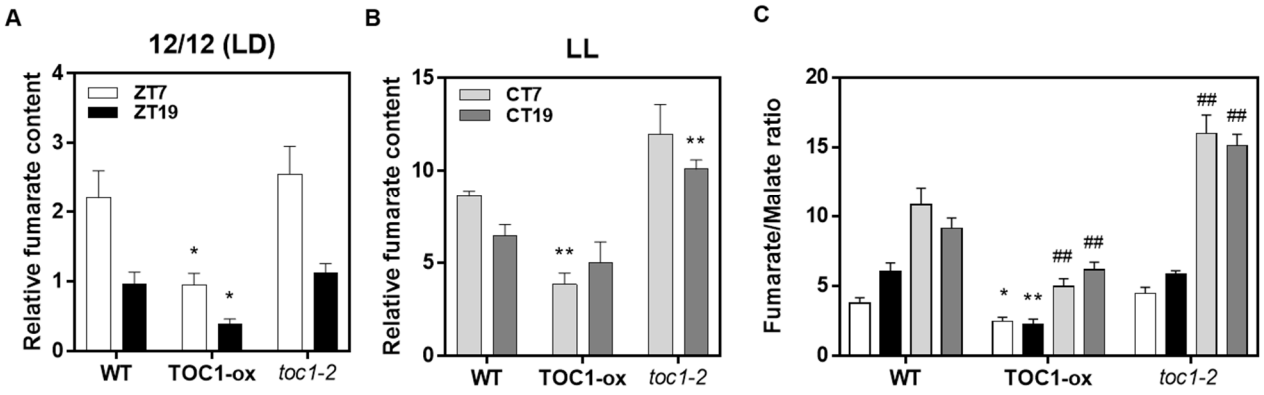

Figure 20. Fumarate accumulation and fumarate/malate ratio s affected in TOC1-ox and *toc1-2* plants. Relative levels of the GC-MS-analyzed fumarate in WT, TOC1-ox and *toc1-2* plants grown under (A) LD cycles and sampled 14 das or (B) under LD cycles for 11 days and then transfer for 2 days to constant light (LL) before sampling at 14 das. Two time points in LD (ZT7, ZT19) and in LL (CT7, CT19) were collected. Values are means + SE of 6 replicates. Asterisks denote significant differences (* P < 0.05, ** P < 0.01; Student's t-test) to the WT. (C) Correlation between fumarate and malate levels. Asterisks or hash signs denote significant differences (***, #** P < 0.05, ****, ##** P < 0.01; Student's t-test) of TOC1-ox or *toc1-2* to the WT respectively.

Specific metabolic changes were clearly observed for amino acid accumulation in TOC1-ox plants. For instance, under LD cycles, Alanine β (Ala-β), Arginine (Arg), Ornithine (Orn), Lysine (Lys) and Putrescine (Put) were accumulated both during the day and night in TOC1-ox compared to WT plants (**Figure 21A-C**). Phenylalanine (Phe) only over-accumulated during the day while GABA and Isoleucine (Ile) were slightly increased at night. Under LL, Arg, Orn and Ala-β as well as Asparagine (Asn) were highly accumulated in TOC1-ox relative to WT plants both during the subjective day and the subjective night while Phe was accumulated only during the subjective day (**Figure 21A-C**). Proline (Pro) and Phe showed reduced levels (just during the subjective day and subjective night, respectively) while Glycine (Gly) was the only amino acid showing an overall reduced accumulation in TOC1-ox plants, which resulted in a disrupted Glycine/Serine ratio (**Figure 21E**).

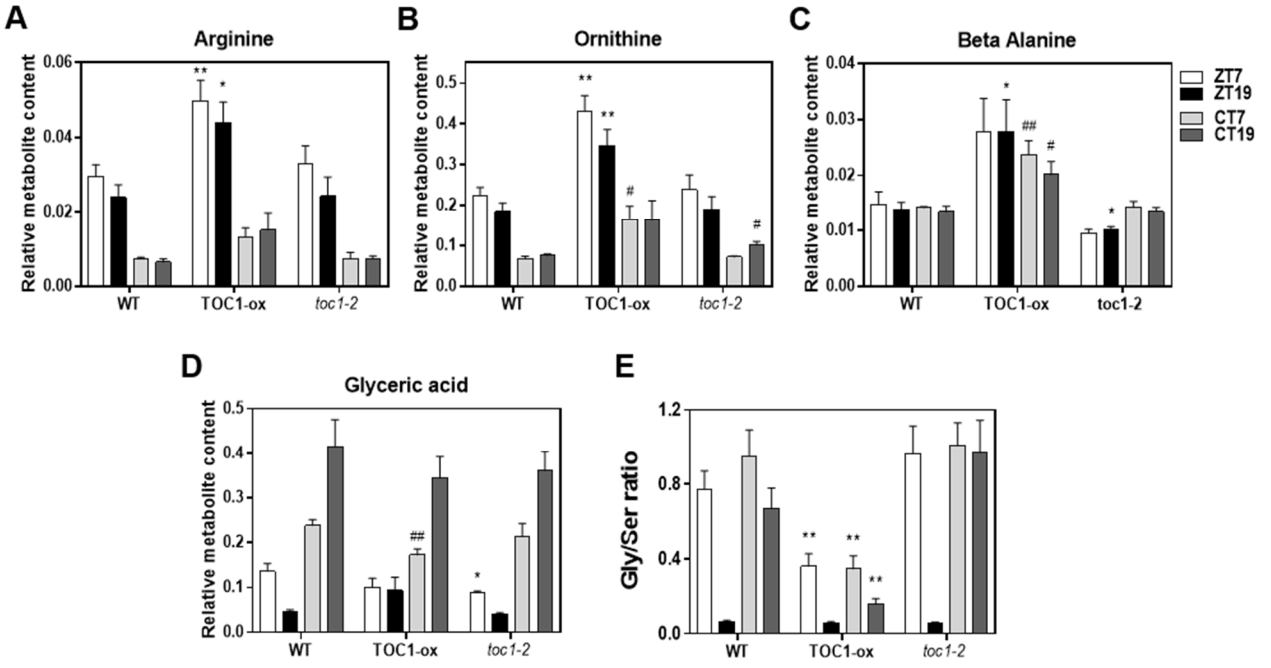

Figure 21. The overall accumulation of amino acids is increased in TOC1-ox while photorespiration-associated metabolites are reduced. Relative levels of the GC-MS-analyzed metabolites in WT, TOC1-ox and *toc1-2* plants grown under LD cycles and sampled 14 das or under LD cycles for 11 days and then transfer for 2 days to constant light (LL) before sampling at 14 das. Two time points in LD (ZT7, ZT19) and in LL (CT7, CT19) were collected. Relative content of amino acids (A) arginine, (B) ornithine, (C) beta-alanine and photorespiration associated metabolite (D) glyceric acid. (E) Correlation between glycine and serine levels. Values are means + SE of 6 replicates. Asterisks denote significant differences (* $P < 0.05$, ** $P < 0.01$; Student's t-test) to the WT. (C) Correlation between glycine and serine. Asterisks or hash signs denote significant differences (***, #** $P < 0.05$, ****, ##** $P < 0.01$; Student's t-test) of TOC1-ox or toc1-2 to the WT respectively

Regarding sugars and sugars alcohols, their accumulation was not highly fluctuating under LD cycles (**Figure 22A-D**) while under LL conditions, sucrose (Suc) during the subjective night (**Figure 22F**) and glucose (Glu), fructose (Fru) and trehalose (Treh) both during the subjective day and subjective night, showed reduced levels in TOC1-ox (**Figure 22E-H**). A putative sugar annotated as maltose was the only sugar over accumulated among all the analyzed sugars (**Figure 22E, J**). The disrupted Glycine/Serine ratio and Glyceric acid levels (**Figure 21D**) are often used as markers of photorespiratory impairment (Novitskaya et al., 2002; Timm et al., 2008). The accumulation of Arg, Orn, (Blume et al., 2019) and the depletion of carbohydrates are also previously reported responses of plants facing energy depletion.

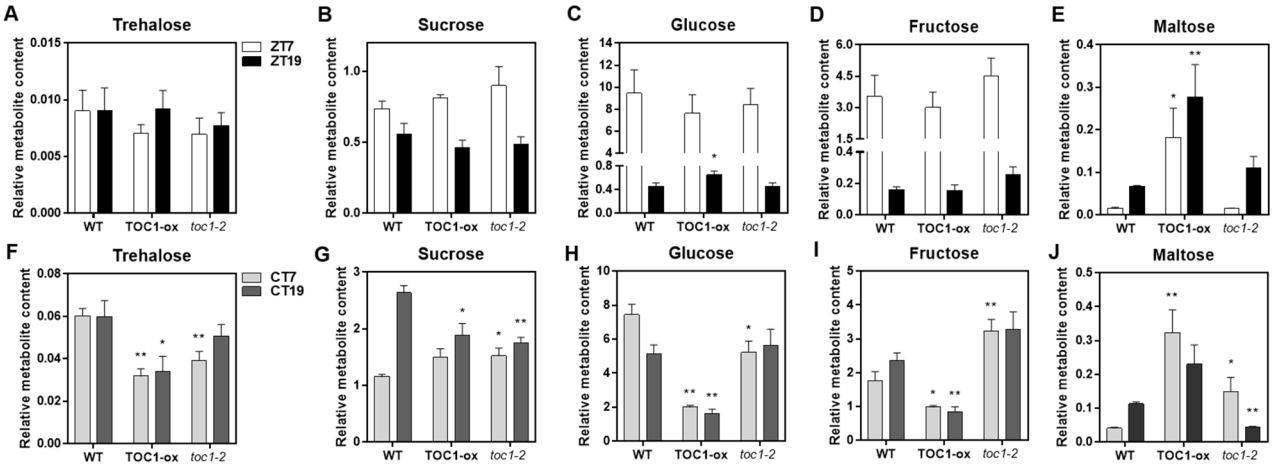

Figure 22. Sugars are generally decreased in TOC1-ox under LL cycles while remained unchanged under LD cycles. Relative levels of the GC-MS-analyzed metabolites in WT, TOC1-ox and *toc1-2* plants grown under LD cycles and sampled 14 das (A-E) or under LD cycles for 11 days and then transfer for 2 days to constant light (LL) before sampling at 14 das (F-J). Two time points in LD (ZT7, ZT19) and in LL (CT7, CT19) were collected. Relative content of sugars (A-F) trehalose, (B-G) sucrose, (C-H) glucose, (D-I) fructose and (E-J) maltose. Values are means + SE of 6 replicates. Asterisks denote significant differences (* $P < 0.05$, ** $P < 0.01$; Student's t-test) to the WT.

7. FUM2 expression is affected in TOC1 miss-expressing plants

Fumaric acid is an intermediary of the TCA cycle synthesized by the activity of two fumarases (FUM1 and FUM2). As the diurnal and circadian oscillation of fumaric acid dampened low in TOC1-ox and high in *toc1-2*, we focused on the possible direct regulation of the *FUM* genes by TOC1. Time course analyses under LD and LL showed that *FUM1* expression did not robustly oscillate and was not evidently altered in TOC1-ox (**Figure 23A-B**). In contrast, *FUM2* expression clearly oscillated with a peak of expression in the middle of the day under different photoperiods and under LL conditions (**Figure 23C-F**). The amplitude of *FUM2* expression was reduced in TOC1-ox and increased in *toc1-2* under entraining conditions while *FUM2* circadian peak was abolished in TOC1-ox (**Figure 23C,E,F**) and its expression was nearly antiphasic in WT and *toc1-2* (**Figure 23D**). These results suggest that the observed phenotypes of fumaric acid content in TOC1-ox and *toc1-2* might be directly correlated with the transcriptional changes of *FUM2* expression.

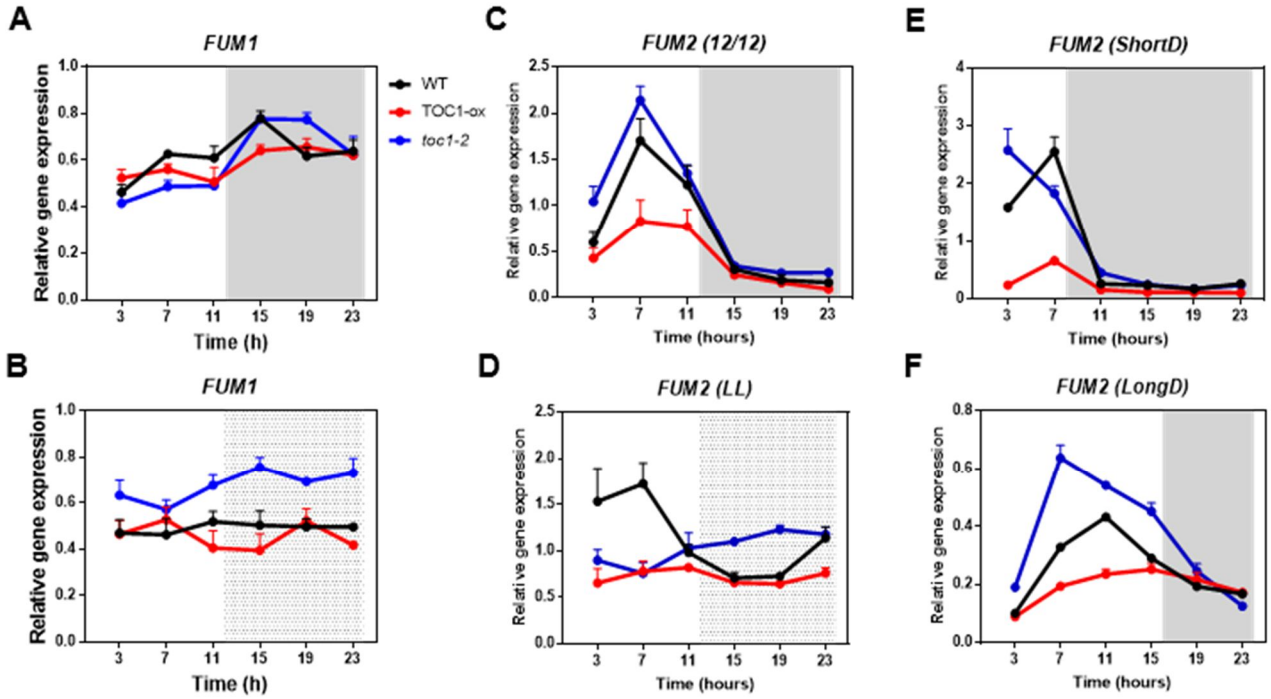

Figure 23. TOC1 regulates the diurnal and circadian expression of *FUM2*. Time course analyses of *FUM1* and *FUM2* expression over a diurnal cycle under LD (A-C) every 4h over a 24h cycle and after 2 days under LL (B-D) every 4h over a 24h cycle. *FUM2* expression over diurnal cycle under short days (E) and long days (F). Relative expression was obtained by Q-PCR analyses. Data are represented as the mean + SEM of technical triplicates. The experiments were repeated at least twice.

ACO1 is the most active of the three described aconitase genes that are involved in a plethora of processes such as amino acid biosynthesis and citrate metabolism (Igamberdiev and Gardeström, 2003). *ACO1* expression was also clearly repressed in TOC1-ox plants (**Figure 24A-D**) although its expression was also reduced in *toc1-2* plants under entraining conditions (**Figure 24A**). The reduced expression of *ACO1* in TOC1-ox correlates with the increased levels of citrate, particularly under LL conditions (**Figure 24E-F**).

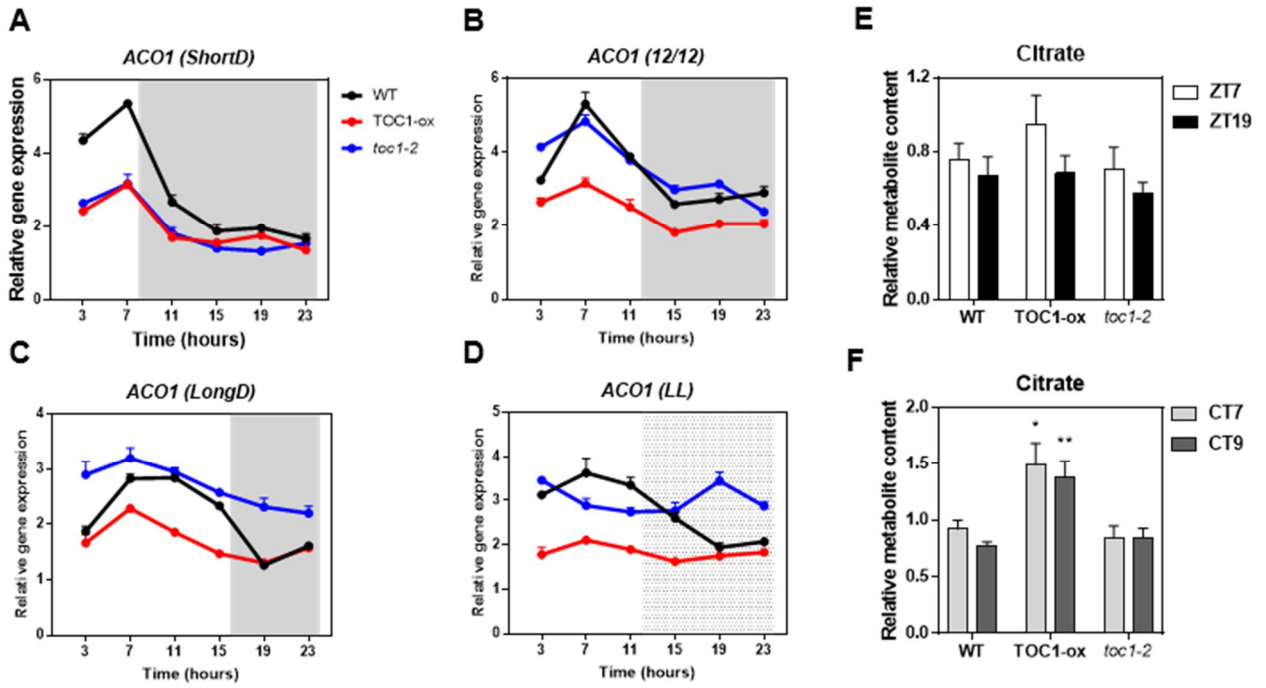

Figure 24 *ACO1* expression is disrupted in TOC1 miss-expressed plants and correlates with citrate levels. Time course analyses of *ACO1* expression over a diurnal cycle under short day (A), LD (B), long day (C) every 4h over a 24h cycle and after 2 days under LL (D) every 4h over a 24h cycle. Relative expression was obtained by Q-PCR analyses. Data are represented as the mean + SEM of technical triplicates. The experiments were repeated at least twice. (E-F) Relative levels of the GC-MS-analyzed citrate in WT, TOC1-ox and *toc1-2* plants grown under (E) LD cycles and sampled 14 das or (F) under LD cycles for 11 days and then transfer for 2 days to constant light (LL) before sampling at 14 das. Two time points in LD (ZT7, ZT19) and in LL (CT7, CT19) were collected. Values are means + SE of 6 replicates. Asterisks denote significant differences (* $P < 0.05$, ** $P < 0.01$; Student's t-test) to the WT.

8. TOC1 directly binds to the FUM2 promoter

As TOC1 acts as a global repressor of gene expression through direct binding to the promoters of its target genes (Huang et al., 2012), we next performed chromatin immunoprecipitation (ChIP) assays followed by Q-PCR analyses of the promoters of selected MRG that could be regulated by TOC1. The ChIP assays were performed with TOC1-ox plants at 10 das (days after stratification) using an anti-MYC antibody to immunoprecipitate the MYC-tagged TOC1 protein. Our results showed specific amplification of the promoter of *FUM2* (**Figure 25**) while no amplification was observed for other promoters including *PDK, ACO1, NDA1, DIC1, TA3 or ACTIN2* or when samples were incubated without antibody (-α). The ChIP enrichment was observed in plants grown under 12h light: 12h dark cycles (**Figure 25A**) or under LL conditions (**Figure 25B**).

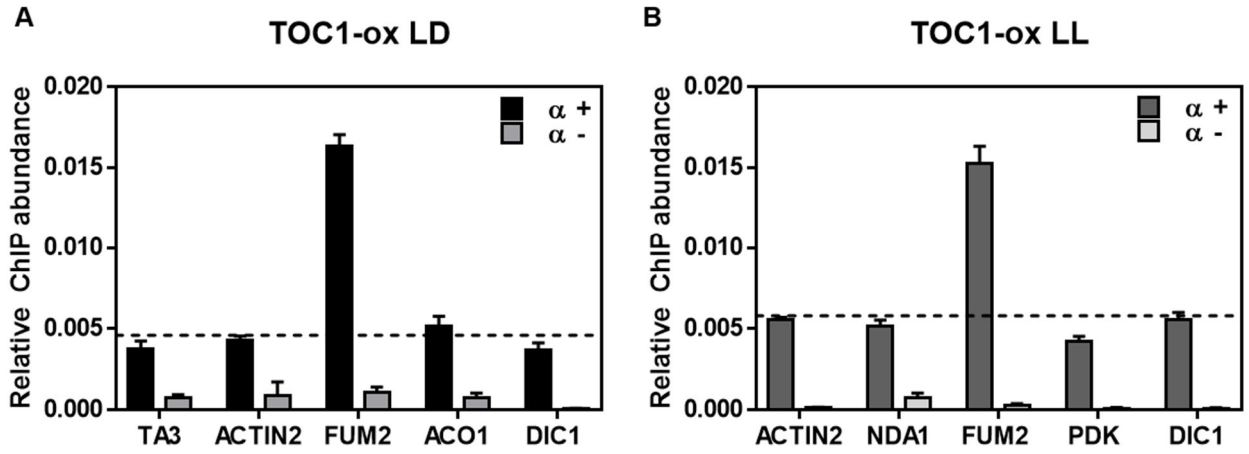

Figure 25. TOC1 binds to the *FUM2* promoter. Chromatin immunoprecipitation (ChIP) assays with TOC1-ox plants examined 14 das and sampled at ZT7 under LD cycles (A) or CT7 after 2 days under continuous light (LL) (B) using an anti-MYC antibody to immunoprecipitate the MYC-tagged TOC1 protein. ChIP enrichment was calculated relative to the input. Samples were incubated with anti-MYC antibody (+α) or without antibody (-α). Values are means + SE of technical triplicates. At least two biological replicates per experiment were performed

The *FUM2* promoter contains previously described TOC1 binding motifs such as two G-box (CACGTG; 1469 and 1360 bp upstream of the TSS) and two Evening Element-like (EEL) (AATATCT; 1304 and 289 upstream of the TSS (Huang et al., 2012) (**Figure 26A**). To further examine TOC1 binding to the *FUM2* promoter and explore the binding site, we performed ChIP assays with TOC1 Minigene (TMG) seedlings, which express the *TOC1* genomic fragment fused to the yellow fluorescent protein in the *toc1-2* mutant background. Fold enrichment analyses following TOC1 immunoprecipitation with the anti-green fluorescent protein (GFP) antibody showed clear amplification of the *FUM2* promoter at the G-box- or EEL-containing regions but not in other *FUM2* promoter regions (e.g. FUM2 -51) or in other loci (*ACO1*, *TA3*) (**Figure 26B**). Time course analyses revealed specific binding that rhythmically oscillated with peak enrichment around ZT15, the peak time of *TOC1* expression (**Figure 26C**). Altogether, the results are consistent with a direct binding of TOC1 to the *FUM2* promoter to regulate its diurnal and circadian transcriptional expression that ultimately correlates with fumaric acid abundance (**Figure 20**).

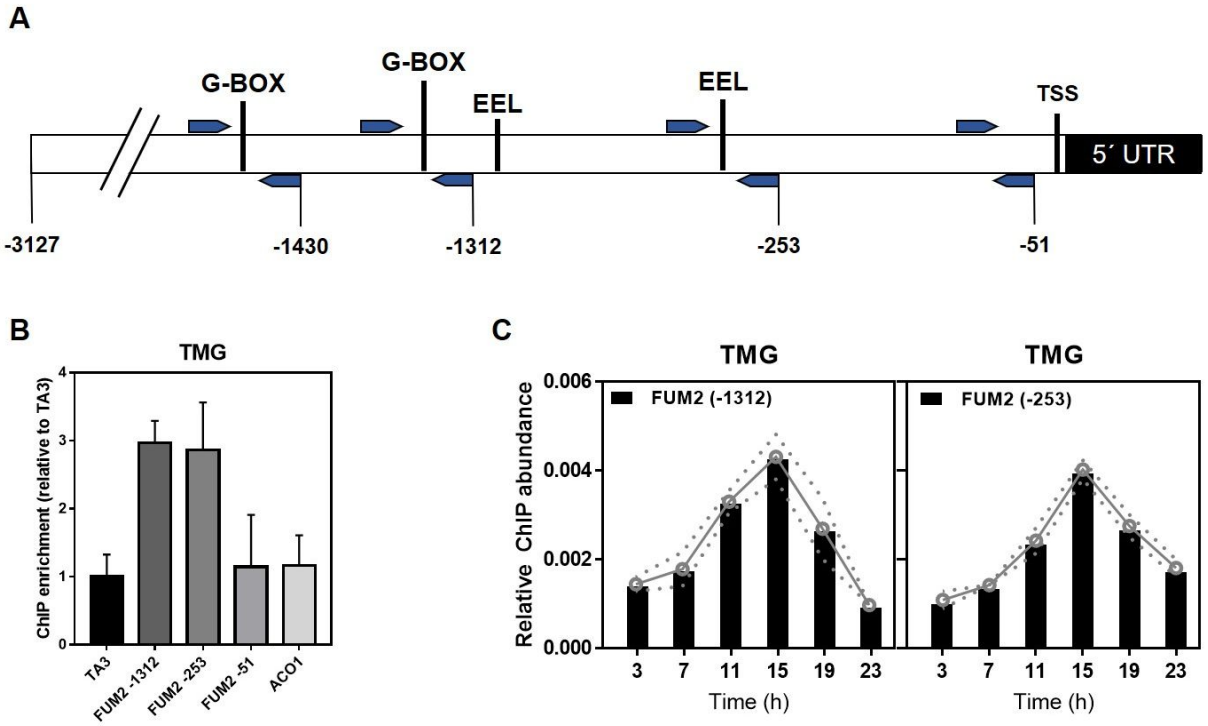

Figure 26. TOC1 binds to the *FUM2* promoter. (A) Schematic representation of *FUM2* promotor highlighting primers binding sites (blue arrows). Numbers shows the position upstream from transcription start site (TSS). G-BOX (CACGTG), EEL (AATATCT). (B) Chromatin immunoprecipitation (ChIP) assays with TMG plants examined 14 das and sampled at ZT7 under LD cycles. Fold enrichment was calculated relative to the TA3 value. (C) ChIP assays with TMG plants grown under LD and collected over a diurnal cycle under LD every 4h over 24h. ChIPs were performed with an anti-GFP antibody to immunoprecipitate the GFP-tagged TOC1 protein. For comparisons of the different time points, fold enrichment was calculated relative to the input and to values without antibody (-α). Values are means + SE of technical triplicates. At least two biological replicates per experiment were performed At least two biological replicates per experiment were performed. Dotted lines denoted the ±SEM.

9. Over-expression of TOC1 mimics a prolonged darkness-like phenotype

The accumulation of amino acids along with the depletion of sugars might be indicative of a starvation phenotype leading to a metabolic rearrangement directed towards protein degradation. Previous studies have shown that under starvation, branched-chain amino acids and Lysine can be used as an alternative respiratory substrates through the electron-transfer flavoprotein:ubiquinone oxidoreductase (ETFQO) and electron-transfer flavoprotein (ETF) (ETF/ETFQ) pathways (Ishizaki et al., 2005b; Liang et al., 2015; Cavalcanti et al., 2017). Consistently, we found that the expression of genes (*BCAT2*, *BCE2*, *ETFQ, MCCA*, *THDP*) encoding BCAA catabolic enzymes is increased in TOC1-ox plants (**Figure 27A-E**). The increased expression might be an indication of a prolonged darkness starvation-like phenotype (Fujiki et al., 2001; Pedrotti et al., 2018).

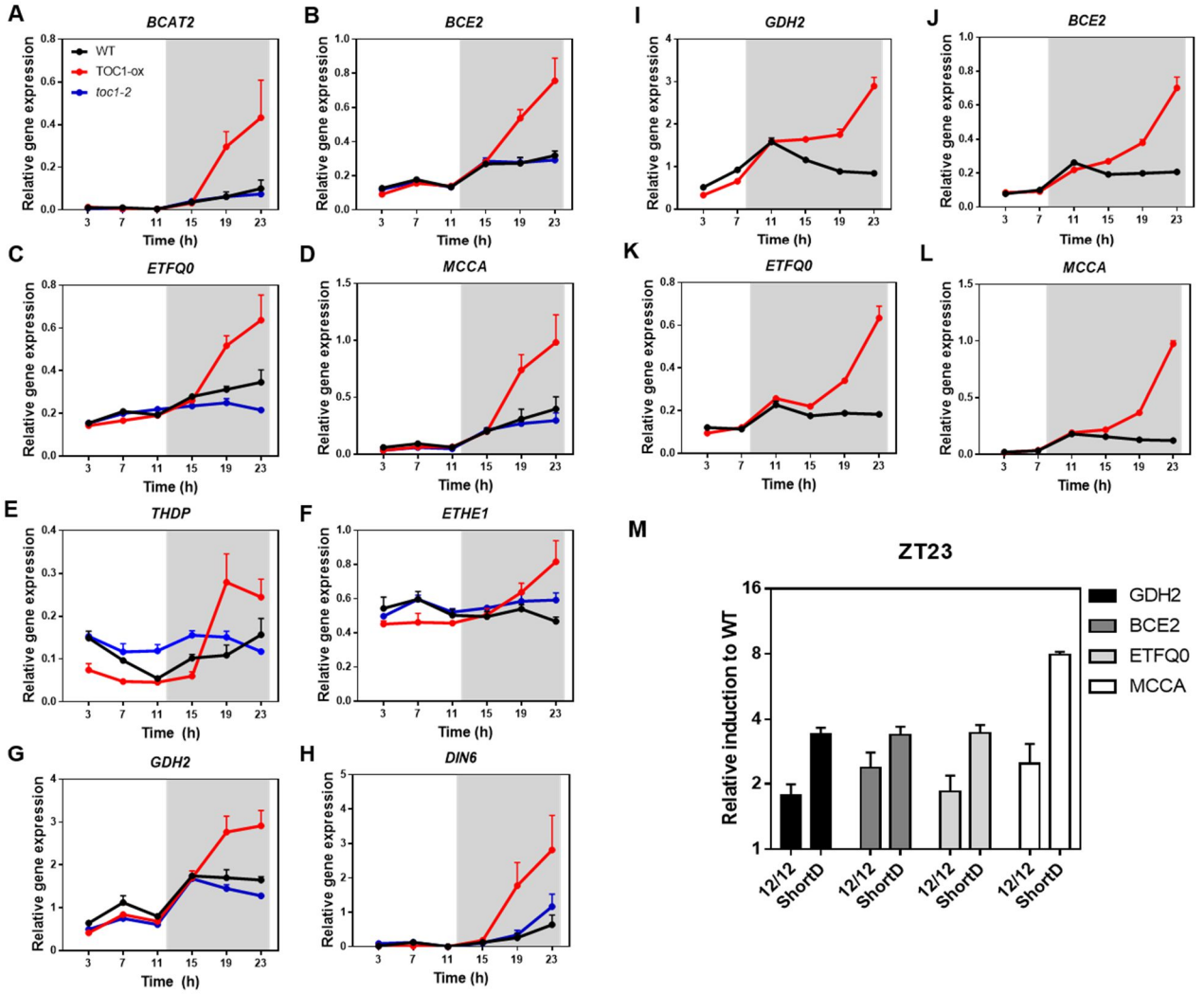

Figure 27. TOC1-ox mimics a prolonged darkness phenotype. Time course analyses of prolonged darkness marker genes over a diurnal cycle under LD (A-H) and short day (I-L) every 4h over a 24h cycle. Expression of (A) ***BCAT2*** (BRANCHED-CHAIN AMINO ACID TRANSFERASE 2), (B;J) ***BCE2*** (DARK INDUCIBLE 3), (C;K) ***ETFQ0*** (ELECTRON-TRANSFER FLAVOPROTEIN:UBIQUINONE OXIDOREDUCTASE), (D;L) ***MCAA*** (METHYLCROTONOYL-COA CARBOXYLASE SUBUNIT ALPHA), (E) ***THDP*** (THIAMIN DIPHOSPHATE-BINDING FOLD (THDP-BINDING) SUPERFAMILY PROTEIN), (F) ***ETHE1*** (GLYOXALASE 2-3), (G;I) ***GDH2*** (GLUTAMATE DEHYDROGENASE 2), (H) ***DIN6*** (GLUTAMINE-DEPENDENT ASPARAGINE SYNTHETASE 1). (M) Fold increase expression of prolonged darkness marker genes in TOC1-ox plants relative to WT. Relative expression was obtained by Q-PCR analyses. Data are represented as the mean + SEM of technical triplicates. The experiments were repeated at least twice.

Other genes encoding amino acid catabolism enzymes such as *ETHE1*, *GDH2* (**Figure 27F-G**) and the sugar starvation marker, *DARK INDUCIBLE 6* (*DIN6*) were also induced in TOC1-ox plants (**Figure 27H**), which is in agreement with a redirected proteolytic metabolism under prolonged darkness (Miyashita and Good, 2008; Krüßel et al., 2014; Baena-González et al., 2007). The induction of these genes in TOC1-ox plants was highly significant under short photoperiods (**Figure 27I-L**) particularly at the end of the night (**Figure 27M**). The results support the notion of an altered

energy status of TOC1-ox and suggest that under normal light:dark cycles, the energy demand is not properly supplied from mitochondria so that alternative pathways for generating energy from non-carbohydrate sources are triggered in TOC1-ox plants.

10. Genetic interaction of FUM2 and TOC1 is essential for proper carbon allocation and biomass accumulation

Our results indicate that proper expression of TOC1 is important for the mitochondrial function, most likely through its direct regulation of *FUM2* expression. To further verify this notion, we performed a genetic interaction study by transforming TOC1-ox plants with a FUM2 over-expressing construct (FUM2-ox) (**Figure 28A-B**). The transcriptional repression of mitochondrial-related genes such as *ACO1* by TOC1 was alleviated by over-expression of FUM2 in the double FUM2/TOC1 over-expressing plants (FUM2/TOC1-ox) under both LL and LD conditions (**Figure 28C-D**).

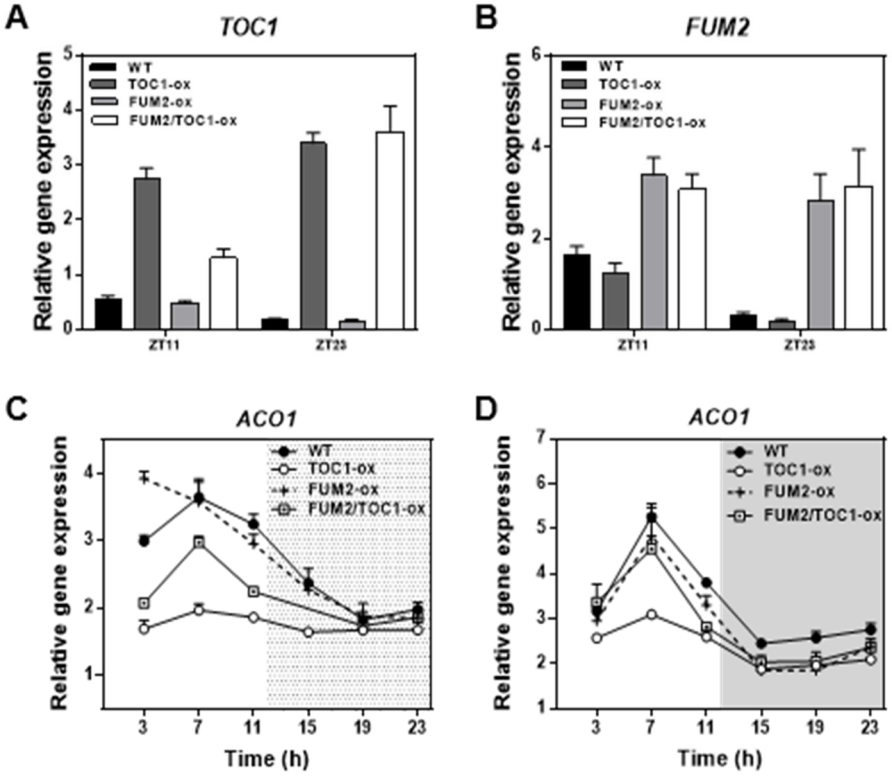

Figure 28. FUM2 over-expression in TOC1-ox releases repression of *ACO1* expression. Expression analyses of (A) *TOC1* and (B) *FUM2* over a diurnal cycle under LD at ZT11 and ZT23. (C-D) Time course analyses of *ACO1* expression over a (D) LD cycle every 4h over a 24h cycle and after 2 days under LL (C) every 4h over a 24h cycle Expression analyses of *ACO1*. Relative expression was obtained by Q-PCR analyses. Data are represented as the mean + SEM of technical triplicates. The experiments were repeated at least twice.

Furthermore, the expression of genes encoding BCAA catabolic enzymes that are induced under prolonged darkness starvation recovered to nearly WT levels in the double FUM2/TOC1 over-expressing plants (**Figure 29A-D**).

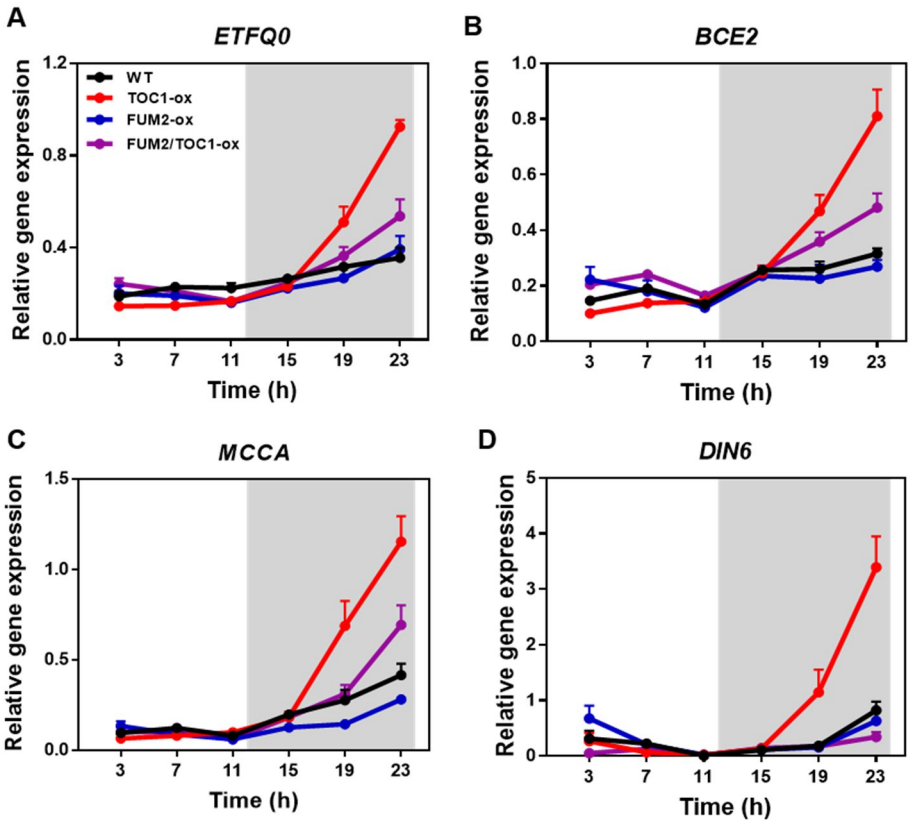

Figure 29. Prolonged darkness marker genes expression in FUM2/TOC1-ox. Time course analyses of prolonged darkness marker genes over a diurnal cycle under LD cycles every 4h over 24h. WT, TOC1-ox, FUM2-ox and FUM2/TOC1-ox plants. Expression of (A) *ETFQ0*, (B) *BCE2*, (C) *MCCA*, (D) *DIN6*. Relative expression was obtained by Q-PCR analyses. Data are represented as the mean + SEM of technical triplicates. The experiments were repeated at least twice.

The reversion of the molecular phenotypes was also apparent when rosette area, perimeter and fresh weight were assessed (Vanhaeren et al., 2015). The severity of the rosette size (area and perimeter) and biomass (fresh weight) phenotypes of TOC1-ox was significantly improved in the double FUM2/TOC1-ox (ox/ox) plants compared to single TOC1-ox (**Figure 30A**). A similar phenotypic recovery was observed in two different double over-expressing lines (**Figure 30B-D**). Size and biomass recovery were not correlated with the rosette shape recovery, which might be dependent of other mechanisms unrelated to fumarase expression (**Figure 30E**).

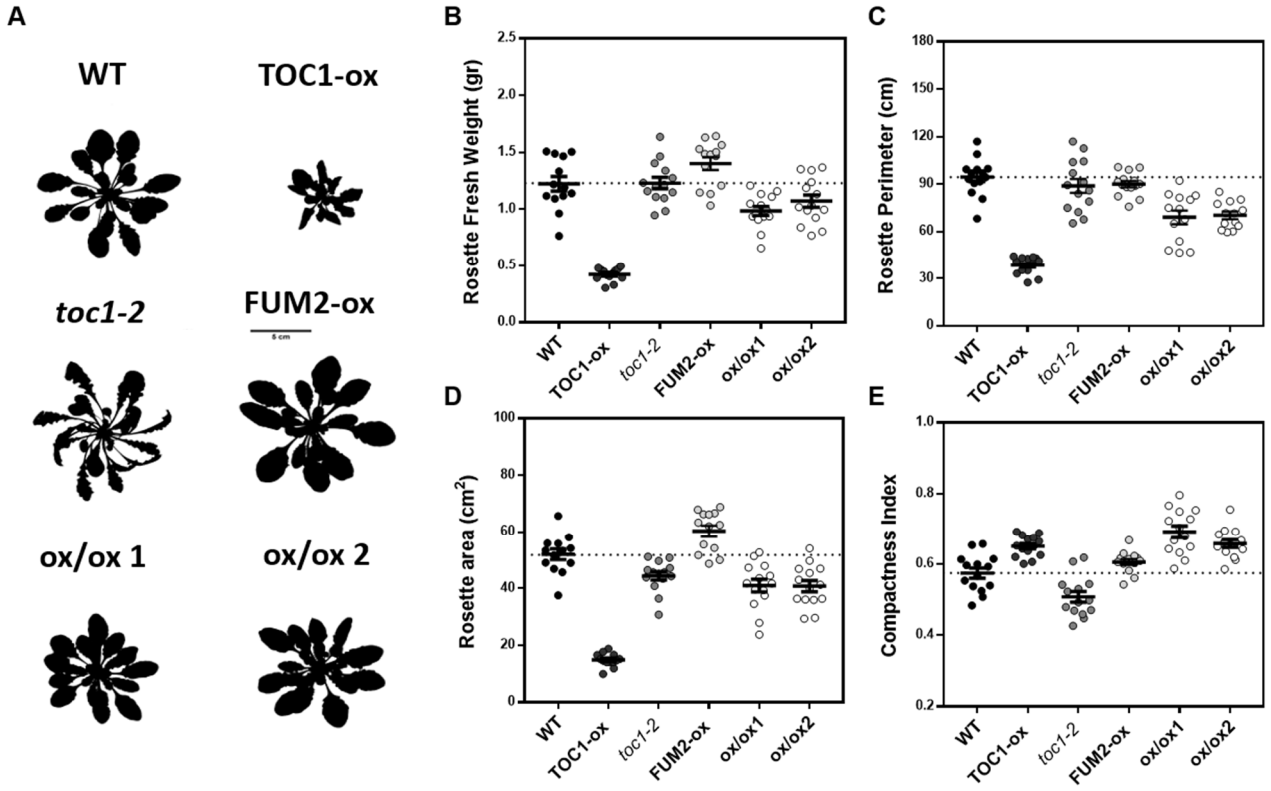

Figure 30 Rosette size and biomass of FUM2/TOC1-ox plants resemble that of WT plants. (A) Rosette 8 bits image of plants grown under long day cycles until flowering. (B) Biomass of rosettes in grams of fresh weight, (C) Perimeter of the rosettes in cm, (D) Area of the rosettes in cm^2, (E) Compactness index, is a mathematical measure of the roundness of the rosette being 1 a perfect circle. Every dot represents a single rosette. Doted lines show the mean of WT. All parameters were obtained with Image J imagine software. Replicates n=20.

Disruption of mitochondria function also affects the photosynthetic apparatus efficiency due to the integrated network between the two energetic organelles in the plant (Blanco et al., 2014; Alber and Vanlerberghe, 2019). Our analysis of chlorophyll fluorescence showed that the quantum yield (φPSII), a parameter considered to be an accurate measure of CO_2 photosynthetic fixation (Baker, 2008) appeared unaltered or very slightly affected (**Figure 31A-B**). Analyses of non-photochemical quenching (NPQ), a process that counteracts the excess energy in PSII by dissipating the excitation energy, is higher in TOC1- ox compared to WT (**Figure 31C-D**). As higher NPQ values are associated with a disrupted electron flow through the mitochondrial ETC (Voon et al., 2018) and with impaired photorespiration (Eisenhut et al., 2017), our results are consistent with the notion that the increased NPQ in TOC1-ox might be attributed to a malfunctioning of the mitochondrial ETC. Notably, analyses of the double FUM2/TOC1 over-expressing plants displaying a decreased NPQ level relative to TOC1-ox in 12-day-old seedlings (**Figure 31D**) while reaching WT levels in older plants (**Figure**

31C). Altogether, our genetic interaction studies show that over-expression of FUM2 reduces the severity of the TOC1-ox phenotypes, suggesting that the reduced expression of *FUM2* in TOC1-ox plants affects the mitochondrial function.

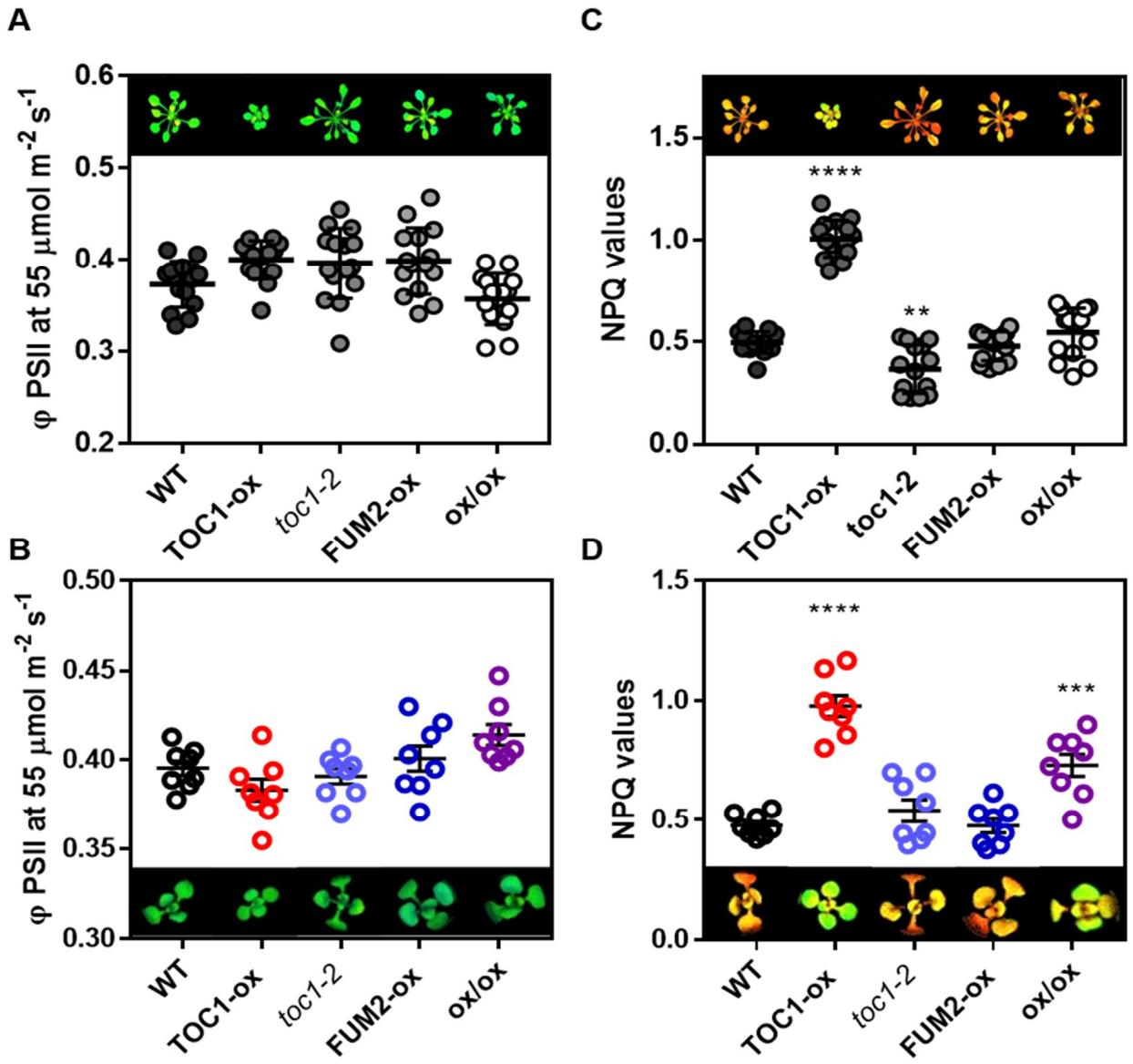

Figure 31. Recovery of non-photochemical quenching values in the FUM2/TOC1-ox plants. Impact of TOC1 miss-expression and FUM2ox overexpression on chlorophyll fluorescence parameters in (A;C) 24-day old plants, (B;D) 10-day old seedlings.). Before the measurement, the treated plants/seedlings were incubated in the dark for 30min. After the maximum and initial fluorescence (Fm-Fo) were determined and a delay of 1min, the plants were illuminated with a light intensity of 55 µmol·m−2·s−1 for 3 min. A saturation pulse was applied at the end of the 3-min illumination to measure the chlorophyll fluorescence parameters (n= 16 plants; mean ± SEM or n = 8 seedlings; mean ± SEM). Groups with significant difference by two-way ANOVA with post hoc Dunnett's multiple comparisons test (**P < 0.001, ***P< 0.0001, ****P<0.00001).

DISCUSSION

This Doctoral Thesis deals with a long-standing question related to how plants are able to compartmentalize their energy in synchronization with the external environmental conditions. We found that the *Arabidopsis thaliana* circadian clock fine-tunes proper mitochondrial activity and metabolic homeostasis through the function of the core clock component TOC1. Miss-expression of *TOC1* results in major changes of mitochondrial-related gene expression that correlate with alterations in metabolite content and physiological outputs. TOC1 regulation of mitochondrial activity relies on the repression of the TCA cycle-related gene *FUM2* through direct binding to its promoter.

The direct implication of the circadian clock controlling a plethora of mitochondrial processes has been extensively reported in mammals [reviewed in (Reinke and Asher, 2019)]. In plants, the circadian function is also important in the regulation of metabolic processes such as starch and sugars utilization (Lu et al., 2005; Pilkington et al., 2015), content of TCA cycle metabolite intermediates (Fukushima et al., 2009), nitrogen assimilation (Gutiérrez et al., 2008), reactive oxygen species accumulation (Lai et al., 2012) and primary metabolism (Annunziata et al., 2018; Flis et al., 2019). Despite the clear involvement of the circadian clock in metabolic homeostasis, the mechanistic insights connecting the plant circadian clock with mitochondrial function remains to be fully elucidated.

A high proportion of mitochondrial- and nuclear-encoded mitochondrial related genes has been previously shown to display a diurnal fluctuation in plants (Welchen et al., 2002; Michalecka et al., 2003; Van Lis and Atteia, 2004; Okada and Brennicke, 2006; Rasmusson and Escobar, 2007). Furthermore, the diurnal changes in protein abundance and activity were also reported (Lee et al., 2010). Previous studies had pointed out a connection between circadian clock and mitochondria through the TCP transcription factor family. TCPs [named after the transcription factors TEOSINTE BRANCHED1, CYCLOIDEA, and PCF (proliferating cell nuclear antigen factor)] bind to site II elements [TGGGCT(C/T)] in the promoter of nuclear genes encoding organellar proteins. TCPs also interact at a protein level with circadian clock components, which provides a molecular link between organellar metabolism and the circadian clock. Nevertheless, these studies just focused in genes that have site II elements [TGGGCT(C/T)] in their promoters, and no direct connection between clock

components and mitochondrial-related genes (MRG) was reported (Giraud et al., 2010). Our bioinformatic analyses have demonstrated a pervasive mRNA oscillatory behavior of MRG under different diurnal and circadian conditions. The fact that most of the genes had peak phases of expression at night or subjective night is consistent with the notion that canonical mitochondrial function occurs mostly at night. During the light period, the main function of the leaf mitochondria is to use Glycine as a respiratory substrate to generate enough ATP to meet the cytosolic energetic demand. Our GO analyses were also fully in agreement with previous diel flux models predicting that protein synthesis occurs during the day (concomitant to glyoxylate consumption) while TCA cycle occurs at night (Maurice Cheung et al., 2014; Shameer et al., 2019).

Our RT-QPCR analysis confirmed the general oscillatory landscape of MRG. Many of the previously published studies have reported the oscillatory patterns of gene expression under diurnal conditions (Staffan Svensson and Rasmusson, 2001; Gibon et al., 2004b; Elhafez et al., 2006; Okada and Brennicke, 2006; Rasmusson and Escobar, 2007; Tronconi et al., 2008; Giraud et al., 2010; Peng et al., 2015). Our results not only validated and extended the previously reported diel oscillatory trends but also unraveled the direct circadian control of MRG expression under constant light conditions. For example, *NDA1*, a type II NADH dehydrogenase located in the internal part of the mitochondria, is well known to oscillate under diurnal conditions but we have observed that its oscillation remains under constant light, which directly involve the circadian clock control. Another example includes the cytochrome c genes (*CYTC-1 and CYTC-2*). These small heme proteins located in the mitochondrial intermembrane are required for the electron transfer between Complex III and IV in the mitochondrial electron transport chain (mETC). Their function is important, among others, for carbohydrate accumulation, gibberellin metabolism and signaling as well as for proper growth and development (Racca et al., 2018). We found a diurnal and circadian mRNA expression of *CYTC-2* but not *CYTC-1*. *CYTCs* had site II elements in their promoters but these elements are not essential for the expression of *CYTC-2* (Welchen and Gonzalez, 2005). Based on the previously described role of the circadian clock on gibberellin metabolism and DELLAs regulation (Arana et al., 2011), our results establish an intricate connection between the circadian clock, gibberellin signaling and cytochrome c expression.

In plants miss-expressing TOC1, we have observed a general disruption of MRG expression in terms of phase and amplitude. In some instances, the alteration of gene expression was similar regardless the environmental condition assayed (LD or LL) while other transcriptomic changes were specific of the condition examined. For instance, *NDA1* displayed a rhythmic mRNA oscillation in WT plants that remained barely unaltered in TOC1 miss-expressed plants under entraining conditions. In contrast, under constant light conditions, *NDA1* expression was highly repressed in TOC1-ox plants and nearly antiphasic in *toc1-2* compared to WT plants. These results suggest that miss-expression of TOC1 is overcome by the light:dark cycles while the circadian regulation of *NDA1* expression fully requires proper expression and function of TOC1. Under constant light conditions, the lack of darkness during the night period might impose a distinct energetic demand, leading to a differential regulation of the mitochondrial activity. Thus, proper clock function might be essential for plants to cope with the energetic requirements under constant light conditions. These results are in agreement with the different metabolic fluxes of mitochondria between illuminated or darkened tissues (Sweetlove et al., 2010; Maurice Cheung et al., 2014).

The transcriptomic changes observed in TOC1 miss-expressed plants led to an alteration in the accumulation of relevant metabolites. The amino acids Arginine (Arg), Ornithine (Orn), Putrescine (Put), γ-aminobutyric acid (GABA), related to one of the major interactive pathways for carbon and nitrogen assimilation and partitioning, were over accumulated in TOC1-ox plants. These results suggest an imbalance in the carbon-nitrogen assimilation (Majumdar et al., 2016). Amino acids are an excellent energy source, therefore protein and amino acid breakdown can compensate for a lack of carbohydrates (Hildebrandt et al., 2015). Moreover, accumulation of Arg and Asparagine (Asn), two amino acids with a high carbon/nitrogen ratio (Lea et al., 2007; Winter et al., 2015) is typically observed during starvation due to prolonged darkness (Gibon et al., 2006; Hildebrandt, 2018).The high levels of Arg, Orn, Put and low levels of Pro might indicate that oxidation of Pro is fueling mitochondria respiration to cope with energy scarcity (Ábrahám et al., 2003; Palmieri et al., 2006). In this context, the plant circadian system has been previously shown to be linked to amino acid metabolism (Annunziata et al., 2018). The core clock component CCA1 is involved in nitrogen assimilation through the direct regulation of Asn metabolism (Gutiérrez et al., 2008). Our results

show that TOC1 might as well be directly involved in the regulation of amino acid metabolic pathways.

There are three aconitate hydratase genes in *Arabidopsis* (*ACO1*, *ACO2*, *ACO3*) (Arnaud et al., 2007) that displayed a clearly disrupted mRNA expression in TOC1-ox plants, especially *ACO1*. Under diurnal cycles, the expression of *ACO1*, and to a lesser extent *ACO2*, was reduced in TOC1-ox while *ACO3* appeared unaltered. Under constant light, the expression of the three genes was disrupted compared to that observed in WT plants. Reduced aconitate hydratase activity has been linked with increased levels of citrate (Carrari et al., 2003). Under diurnal cycles, citrate levels in TOC1-ox plants were slightly increased although the changes were not significant. It is possible that the less affected expression of *ACO2* and *ACO3* might compensate for the reduced ACO1 activity (Hooks et al., 2014). Under constant light conditions, citrate levels in TOC1-ox were significantly increased relative to WT. These results are in agreement with the reduced expression of the three aconitate hydratases under free-running conditions.

In *Arabidopsis thaliana*, fumarate activity is encoded by two genes (*FUM1* and *FUM2*). *FUM2* accounts for the majority of the fumarase activity measured in Arabidopsis leaves (Pracharoenwattana et al., 2010). Fumarases drive the conversion of fumarate (or fumaric acid) to malate, key metabolites of the TCA cycle. Inhibition of *FUM2* mRNA and activity is associated with reduced fumarate accumulation, reduced fumarate/malate ratio and reduced biomass (Dyson et al., 2016; Riewe et al., 2016). Fumarate and malate diurnally oscillate in WT plants. However, when *fum2* mutant plants were transformed with a transgene comprising the 35S promoter fused to *FUM2* cDNA (*35S::FUM2*), fumarate and malate levels were recovered but not their diurnal accumulation patterns. These results point out to the importance of *FUM2* expression regulated by its own promoter. Our results showed that the expression of *FUM2,* but not that of *FUM1,* was severely reduced in TOC1-ox plants. ChIPs assays confirmed that this regulation might occur through direct binding of TOC1 to the *FUM2* promoter. A previous ChIP-Seq study reported the targets of TOC1 and its function as a repressor of oscillator gene expression (Huang et al., 2012). Interestingly, the

FUM2 locus was present in the ChIP-Seq gene list, which is in agreement with our ChIP-QPCR results and the repression of *FUM2* expression in TOC1-ox plants.

Fumaric acid is an intermediate of the TCA cycle (Araújo et al., 2011a) that can be also used as an alternative carbon sink, similar to starch, a much well-studied carbon sink (Chia et al., 2000b; Zell et al., 2010). The circadian clock regulates the starch and maltose mobilization by a mechanism involving sugar signaling (Lu et al., 2005; Graf et al., 2010; Espinoza et al., 2010; Annunziata et al., 2018; Graf and Smith, 2011; Flis et al., 2019). Proper timing of starch mobilization is fundamental to sustain growth at night, avoiding premature exhaustion of starch before the dark period ends (Haydon et al., 2013b; Seki et al., 2017; Frank et al., 2018). Analyses of *fum2* mutant plants showed an increased accumulation of starch (Pracharoenwattana et al., 2010; Dyson et al., 2016). Interestingly, transgenic lines of *fum2* containing the *35S::FUM2* transgene still accumulate more starch, implying that not only *FUM2* expression but also its appropriate timing is needed for proper starch accumulation and usage (Pracharoenwattana et al., 2010). These results are in agreement with our data showing that TOC1-ox plants exhibit a maltose-excess phenotype. Furthermore, a decreased *FUM2* expression, FUM2 activity, and fumarate/malate ratio correlated with growth phenotypes in different accessions of *Arabidopsis thaliana* (Riewe et al., 2016). This is in agreement with the reduced biomass observed in TOC1-ox and the recovery of the phenotype by over-expression of FUM2 in the TOC1-ox lines.

ATP production when energy is scarce can be obtained through alternative pathways such as the electron-transfer flavoprotein/ electron-transfer flavoprotein:ubiquinone oxidoreductase (ETF/ETFQO) protein transport electrons to the ubiquinone pool of the mETC (Pedrotti et al., 2018; Frank et al., 2018). In plants, this pathway is relies on two sources: the catabolism of lysine (Lys) and the branched chain amino acids (BCAA) (Ishizaki et al., 2005a, 2006; Araújo et al., 2011b; Peng et al., 2015). The induced expression observed at the end of the night of the BCAA catabolic related genes along with ETFQ and the Lys accumulation suggest that these alternative ATP production pathways are fully active in TOC1-ox plants. The results suggest that TOC1-ox plants suffer carbon

scarcity at the end of the night. This carbon shortage was partially recovered by over-expression of *FUM2* in TOC1-ox lines, showing WT-like levels of starvation-related genes.

Photosynthetic assimilation becomes impaired when carbon or nitrogen flow through the photorespiratory pathway is restricted. Different cell compartments (chloroplasts, peroxisomes, mitochondria and cytosol) host particular reactions of the photorespiratory process. The conversion of two glycine (Gly) molecules into one serine (Ser) molecule is localized in mitochondria and it is favored in the presence of malate (Bykova et al., 2014). The Gly/Ser ratio is a key marker of the photorespiratory rate (Novitskaya et al., 2002) and alterations in mitochondrial function alters photorespiration and therefore, photosynthetic parameters such as non-photochemical quenching (NPQ) (Cardol et al., 2010; Liang et al., 2015; Voon et al., 2018; Shameer et al., 2019). Our results showed a reduced Gly/Ser ratio and induced NPQ values in TOC1-ox plants, suggesting that the photorespiratory pathway is altered. NADH dehydrogenases are active in glycine oxidation and are involved in photorespiratory pathways (Michalecka et al., 2003). The altered photorespiratory pathway might be a direct consequence of the affected mitochondrial function. It is also possible that the photosynthetic apparatus is affected in TOC1-ox. However, we found unchanged accumulation of soluble sugars under LD conditions and unaltered quantum yield of PSII, which suggest that the observed phenotypes in photorespiration are not mainly due to photosynthetic alterations.

Our genetic interaction studies have shown the direct linked between TOC1 and FUM2, but this regulatory connection could have implications beyond mitochondrial activity. Indeed, a recent study has proposed a link between the hormone abscisic acid (ABA) and *FUM2* expression. Treatment with ABA induced the expression of *FUM2* in WT plants while the induction was significantly reduced in the ABA-insensitive mutants (*srk2d srk2e srk2i* triple mutant and in *aba2-1*) (Yoshida et al., 2019). ABA diurnally oscillates and a number of ABA-related genes are clock controlled (Mizuno and Yamashino, 2008). Notably, TOC1 was proposed as a key factor modulating the plant sensitivity to ABA (Legnaioli et al., 2009). Together, the results open the possibility of an additional novel regulatory node including ABA, TOC1 and FUM2. Furthermore, FUM2 is also important for acclimation to low temperatures by modulating the expression of C-repeat binding factor 3 (*CBF3*)

but not *CBF1* or *CBF2* (Dyson et al., 2016). In turn, the circadian clock has been also connected with cold signaling pathways in part through the direct binding of TOC1 to the *CBF3* promoter (Keily et al., 2013). These results support the idea that FUM2 and TOC1 might be involved in the regulation of plant responses to diverse environmental conditions.

By performing a combination of transcriptomic, metabolic and genetic interaction studies, in this Doctoral Thesis we have identified that the clock component TOC1 is able to fine-tune mitochondrial activity through the regulation of the oscillatory expression of *FUM2* by direct binding to its promoter (Figure **32**)

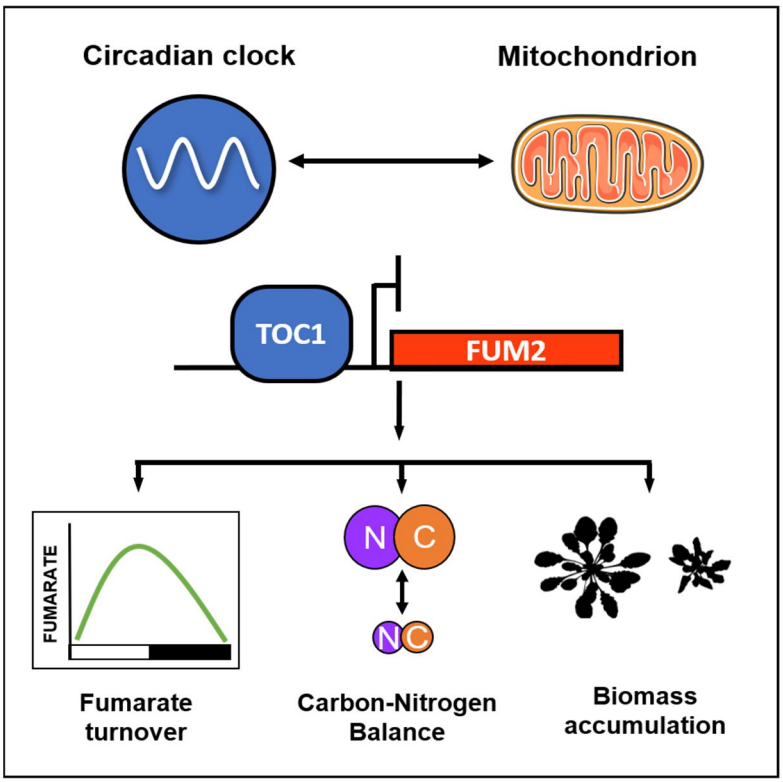

Figure 32. Schematic representation describing the connection between the circadian clock and the mitochondrial function. Circadian clock modulates the mitochondrial activity through the direct binding of TOC1 to the promoter of the TCA cycle related enzyme *FUM2.* TOC1 miss-expressing plants affects the diurnal and circadian mitochondrial gene expression, carbon-nitrogen balance and overall biomass. Ensuring the proper timing of massive fumarate allocation might allow the proper energy balance between different daily energy requirements.

CONCLUSIONS

In this Doctoral Thesis, we have discovered a role for the circadian clock regulating the timing of mitochondrial function in *Arabidopsis thaliana*. The clock component TOC1 regulates the expression of the mitochondrial- related gene *FUMARASE 2* by direct binding to its promoter. We found that the proper timing of *FUMARASE 2* expression and fumarate accumulation affects energy homeostasis. More specifically, the main conclusions of our studies include:

1. **A high proportion of mitochondrial-related genes displays a diurnal and circadian oscillation of mRNA expression**. Bioinformatic and transcriptomic analyses show that the circadian clock pervasively regulates the expression of genes related to the tricarboxylic acid cycle and amino acid catabolism.

2. **Dynamics of cytosolic ATP are controlled by the circadian clock.** The rhythmic changes in gene expression correlate with an oscillatory pattern of cytosolic ATP production.

3. **Proper expression and function of the clock component TOC1 are important for the oscillation of mitochondrial-related gene expression.** Miss-expression of TOC1 by mutation or over-expression affects the oscillatory pattern of mitochondrial-related gene expression.

4. **Proper expression and function of the clock component TOC1 sustain the oscillatory pattern of metabolite content and carbon and nitrogen diurnal allocation.** Miss-expression of TOC1 by mutation or over-expression affects the pattern of tricarboxylic acid intermediates and amino acid accumulation.

5. **Over-expressing of TOC1 leads to low biomass accumulation, reduced size and starvation-like phenotypes.** Physiological responses that require proper energy homeostasis are affected in TOC1 over-expressing plants.

6. **TOC1 regulates the expression of the tricarboxylic acid cycle related gene *FUMARASE 2* by direct binding to its promoter**. Chromatin immunoprecipitation assays using plants over-expressing TOC1 and plants expressing TOC1 under its own promoter showed the rhythmic binding of TOC1 to the *FUMARASE 2* locus.

7. **Genetic interaction studies of TOC1 and FUMARASE 2 confirm that the mitochondrial-related molecular and physiological phenotypes of TOC1 miss-expressing plants are due, at least in part, to TOC1 repression of *FUMARASE 2* expression.** Over-expression of FUMARASE 2 in plants over-expressing TOC1 rescues the alteration of gene expression, biomass accumulation and starvation-like phenotypes observed in TOC1-ox.

.

SUMMARY

Circadian clocks are molecular timekeeping mechanisms that translate environmental cues, mostly light and temperature, into temporal information to generate ~24h rhythms in metabolism and physiology. The temporal coordination by the clock enables organisms to predict and anticipate periodic changes in the environment. Despite its importance for plant fitness and survival, the possible role of the circadian clock directly regulating plant mitochondrial activity and energy homeostasis has remained elusive. In this Doctoral Thesis, we have followed a comprehensive approach to demonstrate the molecular mechanism by which the key clock component TOC1 (TIMING OF CAB EXPRESSION 1) sets the time of mitochondrial activity. To that end, we have followed the in vivo dynamics of cytosolic ATP production using a FRET-based ATP biosensor. We have also performed transcriptomic analyses and examined their correlation with actual changes in metabolite content using plants miss-expressing TOC1. We have identified the molecular mechanism by which TOC1 regulates the mitochondrial activity through direct binding to the promoter of the tricarboxylic acid cycle related gene *FUMARASE 2*. Our genetic interaction studies have validated this mechanism, as over-expression of FUMARASE 2 in TOC1 over-expressing plants alleviates the reduced biomass and the starvation-like phenotypes observed in TOC1 over-expressing plants. Overall, ours studies uncover the role of the circadian clock controlling the cell energetic demands in synchronization with the environment.

RESUMEN

El reloj circadiano es un mecanismo celular endógeno capaz de medir el paso del tiempo y traducir las señales medioambientales, principalmente luz y temperatura, en respuestas temporales que resultan en ritmos metabólicos y fisiológicos de aproximadamente 24 horas. Esta coordinación temporal les permite a los seres vivos predecir y anticipar cambios periódicos en el medioambiente. A pesar de su importancia para la adaptación y supervivencia de las plantas, la posible función regulatoria del reloj circadiano sobre la actividad y homeostasis mitocondrial ha sido difícil de elucidar. En esta Tesis Doctoral, hemos seguido un enfoque integral para demostrar el mecanismo molecular mediante el cual uno de los componentes clave del reloj circadiano, TOC1 (TIMING OF CAB EXPRESSION 1), controla la actividad mitocondrial. Con este fin, hemos estudiado la fluctuación *in vivo* de los niveles del ATP citosólico mediante la utilización de un biosensor de ATP basado en la tecnología FRET. También hemos realizado análisis transcriptómicos correlacionándolos con datos de los cambios en la acumulación de metabolitos observados en plantas sobre-expresantes y mutantes de TOC1. Hemos identificado el mecanismo molecular por el cual TOC1 regula la actividad mitocondrial a través de la unión directa al promotor del gen relacionado con el ciclo del ácido tricarboxílico, *FUMARASE 2*. Nuestros estudios de interacción genética también han validado este mecanismo. Las plantas que sobre-expresan TOC1 acumulan menos biomasa y tienden a presentar un fenotipo similar al de plantas sometidas a inanición. La sobre-expresión del gen *FUMARASE 2* en estas plantas ayuda a la recuperación de la biomasa y alivia el fenotipo de inanición. En general, con este estudio se ha demostrado el papel que ejerce el reloj circadiano en la regulación de la demanda energética celular en sincronización con el medioambiente.

MATERIALS AND METHODS

1. Plant material, sterilization and growing conditions

All *Arabidopsis thaliana* lines used in this study are in Columbia (Col-0) background. WT, TOC1-ox (Huang et al., 2012), TOC1 RNAi (Más et al., 2003a), *toc1-2* (NASC, N2107710) and TMG-YFP/*toc1-2* (Huang et al., 2012) plants were previously described. For sterilization, seeds were placed in 1.5 mL microcentrifuge tubes and surface sterilized by soaking in 70% ethanol (v/v) with 0.1% (v/v) of Triton X-100 for 10 min, followed by 2 washes with 70% ethanol and 1 of 100% ethanol. Seeds were dried on sterile filter paper in a laminar flow cabinet and sown on plates containing Murashige and Skoog (MS) agar medium supplemented or not (as specified for each experiment) with 3% (w/v) sucrose. After 48 hours of stratification at 4ºC in the dark, plates were transferred to environmentally-controlled chambers (Inkoa Sistemas) and plants were grown under different photoperiodic light/dark cycles for 10-14 das (days after sowing) specified for each experiment (ShortD, 8h light:16h dark; LongD, 16h light:8h dark; LD, 12h light:12h dark) with 60-100 µmol $m^{-2}s^{-1}$ of cool white fluorescent light at 22ºC. For experiments under constant light conditions, plants were grown under light/dark cycles and then transferred to constant light for two days before samples were collected.

2. Plasmid construction and plant transformation

Generation of single FUM2-ox and FUM2-ox/TOC1-ox double over-expressing plants (ox/ox) was performed by floral dipping transformation of the FUM2 over-expressing construct using *Agrobacterium tumefaciens* (GV2260)-mediated transfer (Clough and Bent, 1998) of WT and TOC1-ox plants. The construct was generated by PCR-mediated amplification of the *FUM2* coding sequence followed by cloning into the pENTR/D-TOPO vector (Invitrogen). For optimal results, 0.5:1–2:1 molar ratios of PCR products were added to the reaction. The resulting vector containing FUM2 CDS was used to transform chemically competent E. coli (one shot TOP10 cells, Gateway®). The transformed bacteria were spread on selective plates containing 50 µg /ml kanamycin and incubated overnight at 37°C. Approximately 4 resistant colonies were selected for amplification and plasmid purification using the Plant Mini-Prep Kit (Qiagen). The absence of mutations was confirmed by sequencing using the M13 and F13 primers (Gateway®). The FUM2 CDS were introduced in the plant destination vector pGWB514 (35S pro, C-3xHA) (Nakagawa et al., 2007a, 2007b) by

homologous recombination using the LR reaction (Gateway®). For optimal results, 150 ng of entry clone and 150 ng of destination vector were added to the reaction. expression vectors (containing the FUM2 CDS fused to 4X MYC in the C-terminal under the control of the 35S promoter) were used to transform chemically competent E. coli (one shot TOP10, Gateway®). Bacteria were spread on selective plates containing 100 µg /ml spectinomycin and incubated overnight at 37°C. Approximately 4 resistant colonies were selected for amplification and plasmid purification using the Plant Mini-Prep Kit (Quiagen). The expression vectors carrying the FUM2 CDS were introduced by electroporation into the Agrobacterium tumefaciens strain GV2660 as described above. The WT and TOC1-ox plants were transformed with the FUM2-ox construct to generate single FUM2-ox and double FUM2-ox/TOC1-ox plants, respectively. *Agrobacterium tumefaciens* (strain GV2660) transformed with the constructs was used for plant transformation (Logemann et al., 2006). Bacteria were plated in sterile solid YEB medium (5 g/L beef extract, 1 g/L yeast extract, 5 g/L peptone, 5 g/L sucrose, 0.5 g/L MgCl2) for 48 hours at 28ºC. The densely grown bacteria was collected by scraping and resuspended in 30 ml of sterile liquid YEB medium supplemented with antibiotics (ampicillin 100 µg/ml, rifampicin 100 µg/ml and spectinomycin 100 µg/ml) for 3-4 hours (until OD600 was about 2.0). The bacteria solution was added to 5% sucrose solution containing 0.03% of Silwet L-77. Arabidopsis inflorescences were dipped into the Agrobacterium solution for 10-30 seconds under gentle agitation. Plants were placed under a lid cover for 24 hours to ensure high humidity.

3. Real-time quantitative PCR analysis

About 20 seedlings of 12-14 das were sampled every four hours over a diurnal or circadian cycle. RNA was purified using the Maxwell 16 LEV simply RNA Tissue kit (Promega). RNA was incubated with RNase-free TURBO DNase (Ambion) to reduce genomic DNA contamination. Single strand cDNA was synthesized using 1 µg of RNA using iScript™ Reverse Transcription Supermix for RT-Q-PCR (Bio-rad) or AffinityScript Q-PCR cDNA Synthesis Kit (Agilent). For RT-Q-PCR analysis, cDNAs were diluted 5-fold with nuclease-free water and qPCR was performed with 10% of diluted cDNA with Brilliant III Ultra-Fast SYBR Green qPCR Master Mix (Agilent) or iTag Universal SYBR Green Supermix (Bio-Rad) in a 96-well CFX96 Touch Real-Time PCR detection system (Bio-Rad). Three technical replicates were performed for each sample and gene tested. The *IPP2* gene was

used as control (Huang et al., 2012). The amplification data were analyzed using the second derivative maximum method. Resulting Cp values were converted into relative expression values using the comparative Ct method (Livak and Schmittgen, 2001). The list of primers used in this study is shown below in **Table 1**.

4. Chromatin immunoprecipitation

Plants grown under LD and LL conditions 14 days after sowing (das) were sampled at ZT7 and CT7 for TOC1-ox, and every 4 hours (from ZT3 to ZT23) for TMG. ChIP assays were performed essentially as previously described (Perales and Más, 2007). Briefly, approximately 1 g of twelve-day-old seedlings were fixed at the indicated ZT in 30 ml of ice-cold fixation buffer (0.4 M Sucrose, 10 mM Tris-HCl pH 8.0, 1 mM EDTA, 1 mM PMSF, 1% Formaldehyde, 0.05% Triton X-100) for 15 min under vacuum. Fixation was stopped by addition of ice-cold glycine 0.125 M and vacuum incubation for 5 min. Seedlings were then washed 3 times with ice-cold water and dried. The resulting seedlings were grounded in liquid nitrogen and the powder was filtered twice with miracloth. Extraction was performed with extraction buffer I (0.4 M Sucrose, 10 mM Tris-HCl pH 8.0, 5 mM β-mercaptoethanol, 1 mM PMSF, 5 µg/ml Leupeptin, 1 µg/ml Aprotinin, 5 µg/ml Antipain, 1 µg /ml Pepstatin, 5 µg/ml Chymostatin and 50 µm MG132). Nuclei were then purified by centrifugation at 4ºC for 20 minutes at 1000g. Nuclei were washed four times by centrifugation at 4ºC for 20 minutes at 1000g with 2ml of extraction buffer II (0.25 M Sucrose, 10 mM Tris-HCl pH 8.0, 10 mM MgCl2, 1% Triton X-100, 5 mM β-mercaptoethanol, 1 mM PMSF, 5 µg/ml Leupeptin, 1 µg/ml Aprotinin, 5 µg/ml Antipain, 1 µg /ml Pepstatin, 5 µg/ml Chymostatin and 50 µm MG132). Nuclei were resuspended in 1 ml of nuclei lysis buffer (50 mM Tris-HCl pH 8.0, 10 mM EDTA, 1% SDS, 5 µg/ml Leupeptin, 1 µg/ml Aprotinin, 5 µg/ml Antipain, 1 µg /ml Pepstatin, 5 µg/ml Chymostatin and 50 µm MG132). 300 µl of chromatin was sonicated to approximately 500–1000 bp fragments with a sonicator (Bioruptor Next Generation, Diagenode). Following centrifugation at 12.000 x g for 10 minutes at 4ºC, 100 µl of soluble chromatin (the supernatant) was diluted in 400 µl of ChIP dilution buffer (15 mM Tris-HCl pH 8.0, 150 mM NaCl, 1% Triton-X-100, 1 mM EDT , 1 mM PMSF, 5 µg/ml Leupeptin, 1 µg/ml Aprotinin, 5 µg/ml Antipain, 1 µg /ml Pepstatin, 5 µg/ml Chymostatin and 50 µm MG132) and incubated overnight at 4ºC with 50µl of Magnetic beads (Dynabeads protein G, Invitrogen) and with 1:1000 (-)

of Anti-MYC antibody (Sigma-Aldrich) for assays with TOC1-ox plants or Anti-GFP (Invitrogen by Thermo Fisher Scientific) antibody for the assays with TMG plants (Invitrogen). Immunocomplexes were washed twice with 900 µl of low salt buffer (20 mM Tris-HCl pH 8.0, 150 mM NaCl, 1% Triton X-100, 0.1% SDS, 2 mM EDT), twice with 900µl of high salt buffer (20 mM Tris-HCl pH 8.0, 500 mM NaCl, 1% Triton X-100, 0.1% SDS, 2 mM EDTA), twice with 900 µl of LiCl wash buffer (10 mM Tris-HCl pH 8.0, 0.25 M LiCl, 1% NP-40, 1% Sodium Deoxycholate, 1 mM EDT) and twice with 900 µl of TE buffer (10 mM Tris-HCl pH 8.0, 1 mM EDT). Immunocomplexes were eluted 300 µl with 1% SDS and 0.1 M NaHCO3 followed by 1 hour at 65°C to break the bonds between the antibodies and the proteins. Next, 220 mM NaCl were added to precipitate the DNA, following incubation overnight at 65°C for reverse cross-linking. Immunoprecipitated DNA was isolated using the QIAquick kit (Qiagen) following the manufacturer instructions. ChIPs were quantified by QPCR analysis using a 96-well CFX96 Touch Real-Time PCR Detection System (BioRad). Crossing point (Cp) calculation was used for quantification using the Absolute Quantification analysis by the 2nd Derivative Maximum method. ChIP values for each set of primers were normalized to Input values. Table 1 shows the sequences of primers used in this study.

5. GC-MS Based Metabolite Profiling

Metabolite analyses were performed by Takuya Yoshida at Prof. Alisdair Fernie laboratory (institute, country). Whole seedlings were sampled at the indicated time points, immediately frozen in liquid nitrogen, and stored at -80°C until further analysis. Metabolite extraction was performed by rapid grinding in liquid nitrogen and immediate addition of the appropriate extraction buffer. Metabolite profiling was determined by GC-MS (Lisec et al., 2006). Metabolites were identified by comparison with database entries of authentic standards (Kopka et al., 2005; Schauer et al., 2005). Chromatograms and mass spectra were evaluated by using Chroma TOF 1.0 (Leco, http://www.leco.com/) and TAGFINDER 4.0 software (Luedemann et al., 2012). The relative content of metabolites was calculated by normalization of signal intensity to that of ribitol, which was added as an internal standard and then by the dry weight of the material. All data were processed using Xcalibur 2.1 software (Thermo Fisher Scientific, Waltham, MA, USA). Metabolite identification and annotation were performed using metabolite databases (Tohge and Fernie, 2009). Identification and

annotation of detected peaks followed the recommendations for reporting metabolite data (Fernie et al., 2011).

6. Chlorophyll-a Fluorescence Measurements

Fully developed rosettes of about 24 das gown on soil or seedlings of 10-day old grown on MS under 60-100 µmol $m^{-2}s^{-1}$ of cool white fluorescent light at 22ºC were placed in the dark for 30 min prior to determining dark-adapted initial and maximum PSII fluorescence (F_o and F_m). All measurements were performed using an IMAGING-PAM Chlorophyl Fluorometer (Heinz Walz), and the data were collected via the PAM-Data Acquisition System (PDA-100) interfaced with the ImagingWinGigE Software version 2.47 (following the manufacturer's instructions). To induce minimal fluorescence, the weak modulated light source was turned on and data were collected for 1min. Once the signal had stabilized, an 800-ms pulse of 4,000 µmol photons m^{-2} s^{-1} was applied to the plants to close the PSII reaction centers and generate F_m. The plants were then exposed to an actinic light source until a steady-state level of fluorescence was reached (approx. 3min). To estimate the fraction of closed PSII reaction centers at steady state, a saturating flash was applied and maximum PSII fluorescence in the light-adapted state (F_m') was determined. The dark-adapted optimal quantum yield of photosynthesis was calculated as variable PSII fluorescence in the dark-adapted state $(F_v)/F_m$ according to the equation $[F_v/F_m = (F_m - F_o)/F_m]$. The amount of nonphotochemical quenching was estimated using the term NPQ, where NPQ = $(F_m - F_m')/F_m$. (Murchie and Lawson, 2013).

7. ATP determination by fluorometric analysis and confocal imaging

Arabidopsis seedlings (3 per well) were grown on 96-well transparent plates carrying MS agar medium supplemented or not (as specified for each experiment) with 1% or 3% (w/v) sucrose. Plates were kept under different light/dark cycles for 10-14 das specified for each experiment (ShortD, 8h light:16h dark; LongD, 16h light:8h dark; LD, 12h light:12h dark) with 60-100 µmol $m^{-2}s^{-1}$ of cool white fluorescent light at 22ºC. After 6 das the plate carrying ATeam1.03-nD/nA or WT plants was place for measurement. Plants were excited with monochromatic light at a wavelength of 435 ± 10 nm in a SpectraMax® M3 Multi-Mode Microplate Reader (Molecular Devices LLC). Emission was

recorded at 483 ± 9 nm (CFP) and 539 ± 6.5 nm (Venus).By using the SoftMax software the number of readings per well was set to 14 and PMT (photomultiplier tube) sensitivity set to MEDIUM with an automatic emission cutoff. Automated measurements were recorded over a cycle of several days under light/dark or continuous light conditions every 1 to 4 hours. During the day time point plate was kept under light. The internal temperature was kept at 22°C. Along with the ATeam1.03-nD/nA plants the WT plants were also recorded and values were used as negative control. For inhibitor treatment, 50 µl of Antimycin A (100 µM), KCN (100 µM) or mock were added to the well. Confocal imaging was performed at 20°C using a LEICA TCS SP5 microscope and a ×20 lens (HCX PL APO CS 20.0x0.70 DRY UV., water immersion). ATeam1.03-nD/nA was excited with an Argon Laser at 458 nm and fluorescence of CFP and Venus were measured at 465–500 nm and 526–561 nm, respectively, with the pinhole set to one airy unit.

8. Whole rosette phenotyping

Whole rosettes of 35-day old seedling growing on soil pots were detached and immediately weigh in a precision balance (OHAUS Pioneer PA114C Analytical Balance) to calculate fresh weight. Immediately after, detached rosettes were placed on top a transilluminator to reduced shadowed edges and photographed (NIKON D7000) for further analysis. Rosette images were processed with ImageJ software (Schneider et al., 2012). Firstly, images were split by RGB color tool and blue color channel images were then converted to 8 bit black/white images. After same scale was set, rosettes were defined by the wand tracing tool and area and perimeter was obtained. Compactness is a mathematical measure of the roundness of the rosette and is calculated as followed (Vanhaeren et al., 2015): $Compactness = 4\frac{\pi\, x\, area}{perimeter^2}$.

Table 1. List of primers used in dis study. (Exp =expression)

Name	Sequence (5'-->3')	Use
CYTC1_FW	CGGTCACAAACAAGGACCCAATC	Exp
CYTC1_RV	CAGCAGAGTAAGAGTAACCAGCAG	Exp
CYCT2_FW	TGCCGGTCACAAACAAGGAC	Exp
CYCT2_RV	GTCTTCTCCTCCCAATTCACAGC	Exp
ATP3_FW	GGCAGCCATTTACTGCACTTC	Exp
ATP3_RV	TCCACCACAGAGACCCTTGT	Exp
ATPQ_FW	TGGCTAAGGTCCTTGTCACAGATG	Exp
ATPQ_RV	ACCTCATCGAAAGCACGACGAAG	Exp
QRC7-2_FW	GATGCTCGGAACCAGCGTCTTATG	Exp
QRC7-2_RV	GAATGGAGTCTGCACTGCCTGAAG	Exp
CI51_FW	ACCTTGTTAACCAGAGGGAGTTTG	Exp
CI51_RV	CCTTCTGAAGTAGCTTTGCATCCC	Exp
NDUFA1_FW	TCATGGCCGTCCTAAGCACATC	Exp
NDUFA1_RV	TCGCGTCTTTCCATAGCAACATCC	Exp
SDH1-1_FW	CTGGTGGTGCTGGTCTTAGG	Exp
SDH1-1_RV	GTGACCTTGTGGGGAAAAGC	Exp
SDH2-1_FW	GCGTCTGGTTTGATCGGAAG	Exp
SDH2-1_RV	TCTCGCCGGAATTAACCTCG	Exp
SDH2-2_FW	AGCTATTGGTGGAACCCTGAGTC	Exp
SDH2-2_RV	CGGCTATCACTTATCCACCTGTTG	Exp
COX10_FW	CGGTTTCATCGCCTATGACTGG	Exp
COX10_RV	ATGGTCCGGTCTCGGTAGAATG	Exp
COX5b-2 FW	ACTGCTGTGAAGAAGCGTGT	Exp
COX5b-2 RV	CCAGCTTCCTCCCCTCCAAT	Exp
COB_FW	GGTTCGGTCCGTTAGCTGG	Exp
COB_RV	ACGCTGTTGAAAGCTAAATCCAC	Exp
CAL2c_FW	CTGGTGAACTATGGGGAGGC	Exp
CAL2c_RV	ATGGCAACAGCAAGTTTCGG	Exp
ME2_FW	TTCTGAATGCCTTGCGTCCT	Exp
ME2_RV	GCCCCGACTTCAGCTGTTAT	Exp
PDK_FW	ACGGTTCTGCACCGGAAATAAAC	Exp
PDK_RV	ATGCAAATGCGTTGGAACATACGG	Exp
ME1_FW	GGGTTGCTATCGCTGGTCTT	Exp
ME1_RV	CGCCAGCAACAACGATCTTC	Exp
CYS4_FW	AGTTAATTCCGGAACAGCAGGAC	Exp
CYS4_RV	TGTTTCCCAGTTGGACCTTCCC	Exp
ACO1_FW	TAACGGGTCAGGAGCTTTACACC	Exp
ACO1_RV	CGAAATAAGCCAACTCCACCTCTG	Exp
IDH1_FW	TCCGCAAGTTTCATGATGTTAGCC	Exp
IDH1_RV	CAGTGGCCTTGAACATCAGGTTG	Exp
IDH6_FW	TCGCTGAATCTGTCAAGCAGGTG	Exp
IDH6_RV	ACCAACAAACTGTTCGTCCCAATC	Exp
mMDH1_FW	GGTGTACCAAGGAAGCCTGG	Exp
mMDH1_RV	AGTACTTGGCGATGGCAGTG	Exp
FUM2_FW	GCATGTACTCTACCCCGCAT	Exp
FUM2_RV	AACTTGTTTTCTGCGGTGACG	Exp
PDH1b_FW	TGGAGCTCAACATTCTCAGTGC	Exp
PDH1b_RV	CAGCTGAATACGGAGCAAGGAC	Exp
ACO3_FW	TGAGTATGGAAGTGGTAGCTCACG	Exp
ACO3_RV	AATCACCGCTTTAACACCCTGTAG	Exp
ACO2_FW	GCTAGGAATTCCACTCCGGTTATG	Exp
ACO2_RV	CCTTGTAGGAATGCTCAGAAGCC	Exp
ODC1-1_FW	TGGTACTTTGCTCCGGAAAGGTC	Exp
ODC1-1_RV	AACATCTGTTGCGCCAACCTTC	Exp
mtLDH2_FW	CGCTCTCGGTGGTACTTGTC	Exp
mtLDH2_RV	AACGTGCTTTGCTTCATGGT	Exp
mtLDH1_FW	GCTCTCGGTGGTACTTGTCTCAAC	Exp
mtLDH1_RV	TGTGAAGAGTGAAGCAGAGCCTTG	Exp
SuccoAla-1_FW	AAGGCAAGTGGTACTGAGAAGCC	Exp
SuccoAla-1_RV	TGTCCTGAGCCGTACCTTTACC	Exp
SuccoAla-2_FW	CATGCGGGAGCCATTGTTTC	Exp
SuccoAla-2_RV	TCCTGCGTCTCTTAGGCTCT	Exp
mMDH2_FW	TCACAAAGCGTACCCAGGAC	Exp
mMDH2_RV	AAAGAGTGCTCCCGCATAGG	Exp

Name	Sequence (5'-->3')	Use
PDH2-1_FW	GAGTTTCAAGGAGGGACATTCAGC	Exp
PDH2-1_RV	GATTGCGCAGAAATTATCCACAGG	Exp
PDH1a_FW	CCAATGCCAGAGCCTTCTGA	Exp
PDH1a_RV	TGTCAGGTCCAAATGACTCGG	Exp
ODC1-2_FW	GGGCATAACGAGATAGACGAACCG	Exp
ODC1-2_RV	AGGGATGACTGCGTATCACCTTG	Exp
IDH2_FW	ATATGCAGGTCTTGAACATGAAGT	Exp
IDH2_RV	CTGAACAGAACTTTGTAATCACCTT	Exp
IDH5_FW	CAGTGGCCTTGAACATCAGGTTG	Exp
IDH5_RV	TCAAACTCGCCTGACGGGTAATG	Exp
FUM1_FW	GCGTTATGCCACCTCTCTGA	Exp
FUM1_RV	AACTTGAATCGGCCCGAAGG	Exp
IAR4_FW	CAGGAAGCACTTACCGTACTCGTG	Exp
IAR4_RV	TCAATTGGATCACGCACCTGTC	Exp
NDA1_FW	GTATCCAACCGGCGATTTCACG	Exp
NDA1_RV	AGTTACAGTCTCACAATGCACCTC	Exp
NDB2_FW	AGGAGAAGGTCGTCACCGTT	Exp
NDB2_RV	TGGTCCAATGCACATGACTCAG	Exp
AOX1a_FW	GAATCGCGAGCTATTGGGGT	Exp
AOX1a_RV	ACGTTTCCCATGGCCTGAAA	Exp
NDA2_FW	CTGGTGTTGGTCCTTCTCCTTTCG	Exp
NDA2_RV	CCATTCGTCAATGCCAATCCTTCC	Exp
TOC1_FW	TCTTCGCAGAATCCCTGTGAT	Exp
TOC1_RV	GCTGCACCTAGCTTCAAGCA	Exp
BCAT2_FW	TCACAAATTATGCGCCAGTT	Exp
BCAT2-_RV	CGAGATAAAGAACGTCTGAAAACC	Exp
BCE2_FW	ATTCAGCCGAGCAATGGTCA	Exp
BCE2_RV	CTCCACAAGTGAGTCGCAGT	Exp
ETFQ_FW	CAGAGTCACGTTACTGCCCA	Exp
ETFQ_RV	AGCGTTGATCTGCAGTTTTGG	Exp
MCCA_FW	AAAGTTCCGCGCAAACTTAGG	Exp
MCCA_RV	AAATTCCACCGTCCCAGCAT	Exp
THDP_FW	CTCCGTCATGAGTCTACGGC	Exp
THDP_RV	GGAAATCCAGTTCCTGGGCA	Exp
ETH1_FW	GTTCGTGCTACACCTGGACA	Exp
ETH1_RV	TGAGTACAGCATCCCCGGTA	Exp
GDH2_FW	AGTGGTTGCAGTAAGCGACA	Exp
GDH2_RV	TGAGACTTCCAGTTGCGTCC	Exp
DIN6_FW	AACTTGTCGCAAGATCAAGG	Exp
DIN6_RV	GGAACACGTGCCTCTAGTCC	Exp
ACT2-FW-CHIP	CGTTTCGCTTTCCTTAGTGTTAGCT	ChIP
ACT2-RV-CHIP	AGCGAACGGATCTAGAGACTCACCTTG	ChIP
TA3-FW-CHIP	CTGCGTGGAAGTCTGTCAAA	ChIP
TA3-RV-CHIP	CTATGCCACAGGGCAGTTTT	ChIP
FUM2_ChIP_FW	ATGAATGTGTAGAGCCACCTG	ChIP
FUM2_ChIP_RV	CAGGTGGCTCTACACATTCA	ChIP
NDA1_ChIP_FW	GACCCCTTCCATATCATGACCA	ChIP
NDA1_ChIP_RV	TTTGGGTTTATGGCCCACGA	ChIP
DIC1_ChIP_FW	ATTCGTACCGGATTGACAGTG	ChIP
DIC1_ChIP_RV	CCATGTGGTGGGGTGGAAAATA	ChIP
ACO1_ChIP_FW	TATACACTGACCACGTTCAGG	ChIP
ACO1_ChIP_RV	CTCTTAGGAACACTTCAAGTCTC	ChIP
PDK_ChIP_FW	GTAGATTGTAGAGGAGTCGCAA	ChIP
PDK_ChIP_RV	CGCTTCAGAAAAAGCAAGCCAT	ChIP
FUM2_-1316_FW	CATTGGTTGGCAAGCATTTTGT	ChIP
FUM2_-1316_RV	ACCAACCATAATAGGCCACGTC	ChIP
FUM2_-253_FW	GACATTTCAATCAGTTCACAC	ChIP
FUM2_-253_RV	GTGGAACTGATTGTACTCTC	ChIP
FUM2_-51_FW	CAGGTGGCTCTACACATTCA	ChIP
FUM2_-51_RV	GAAACTGAAGAGACAAGTTTCA	ChIP
FUM2_CDS_FW	CACCATGGCCGCTTTGACAATGCAGTTT	cloning
FUM2_CDS_RV	AATCCAAAATAGAACAACAAATATATTG	cloning

.

REFERENCES

Ábrahám, E., Rigó, G., Székely, G., Nagy, R., Koncz, C., and Szabados, L. (2003). Light-dependent induction of proline biosynthesis by abscisic acid and salt stress is inhibited by brassinosteroid in Arabidopsis. Plant Mol. Biol. **51**: 363–372.

Adams, S., Manfield, I., Stockley, P., and Carré, I.A. (2015). Revised Morning Loops of the Arabidopsis Circadian Clock Based on Analyses of Direct Regulatory Interactions. PLoS One **10**: e0143943.

Ahmad, P., Jaleel, C.A., Salem, M.A., Nabi, G., and Sharma, S. (2010). Roles of enzymatic and nonenzymatic antioxidants in plants during abiotic stress. Crit. Rev. Biotechnol. **30**: 161–175.

Van Aken, O. and Van Breusegem, F. (2015). Licensed to Kill: Mitochondria, Chloroplasts, and Cell Death. Trends Plant Sci. **20**: 754–766.

Alabadí, D., Oyama, T., Yanovsky, M.J., Harmon, F.G., Más, P., and Kay, S.A. (2001). Reciprocal regulation between TOC1 and LHY/CCA1 within the Arabidopsis circadian clock. Science (80-.). **293**: 880–883.

Alber, N.A. and Vanlerberghe, G.C. (2019). Signaling interactions between mitochondria and chloroplasts in Nicotiana tabacum leaf. Physiol. Plant.

Amirsadeghi, S., Robson, C.A., and Vanlerberghe, G.C. (2007). The role of the mitochondrion in plant responses to biotic stress. Physiol. Plant. **129**: 253–266.

Amthor, J.S. (2000). The McCree-de Wit-Penning de Vries-Thornley respiration paradigms: 30 Years later. Ann. Bot. **86**: 1–20.

Andrés, F. and Coupland, G. (2012). The genetic basis of flowering responses to seasonal cues. Nat. Rev. Genet. **13**: 627–639.

Andrews, J.L. et al. (2010). CLOCK and BMAL1 regulate MyoD and are necessary for maintenance of skeletal muscle phenotype and function. Proc. Natl. Acad. Sci. U. S. A. **107**: 19090–19095.

Annunziata, M.G., Apelt, F., Carillo, P., Krause, U., Feil, R., Koehl, K., Lunn, J.E., and Stitt, M. (2018). Response of Arabidopsis primary metabolism and circadian clock to low night temperature in a natural light environment. J. Exp. Bot. **69**: 4881–4895.

Aon, M.A. and Camara, A.K.S. (2015). Mitochondria: Hubs of cellular signaling, energetics and redox balance. A rich, vibrant, and diverse landscape of mitochondrial research. Front. Physiol. **6**.

Arana, M.V., Marín-De La Rosa, N., Maloof, J.N., Blázqueza, M.A., and Alabadí, D. (2011). Circadian oscillation of gibberellin signaling in Arabidopsis. Proc. Natl. Acad. Sci. U. S. A. **108**: 9292–9297.

Araújo, W.L., Ishizaki, K., Nunes-Nesi, A., Larson, T.R., Tohge, T., Krahnert, I., Witt, S., Obata, T., Schauer, N., Graham, I.A., Leaver, C.J., and Fernie, A.R. (2010). Identification of the 2-hydroxyglutarate and isovaleryl-CoA dehydrogenases as alternative electron donors linking lysine catabolism to the electron transport chain of Arabidopsis mitochondria. Plant Cell **22**: 1549–1563.

Araújo, W.L., Nunes-Nesi, A., and Fernie, A.R. (2011a). Fumarate: Multiple functions of a simple metabolite. Phytochemistry **72**: 838–843.

Araújo, W.L., Tohge, T., Ishizaki, K., Leaver, C.J., and Fernie, A.R. (2011b). Protein degradation - an alternative respiratory substrate for stressed plants. Trends Plant Sci. **16**: 489–498.

Arnaud, N., Ravet, K., Borlotti, A., Touraine, B., Boucherez, J., Fizames, C., Briat, J.F., Cellier, F., and Gaymard, F. (2007). The iron-responsive element (IRE)/iron-regulatory protein 1 (IRP1)-cytosolic aconitase iron-regulatory switch does not operate in plants. Biochem. J. **405**: 523–531.

Aschoff, J. (1979). Circadian Rhythms: Influences of Internal and External Factors on the Period Measured in Constant Conditions. Z. Tierpsychol. **49**: 225–249.

Asher, G. and Sassone-Corsi, P. (2015). Time for food: The intimate interplay between nutrition, metabolism, and the circadian clock. Cell **161**: 84–92.

Atkins, K.A. and Dodd, A.N. (2014). Circadian regulation of chloroplasts. Curr. Opin. Plant Biol. **21**: 43–50.

Baena-González, E., Rolland, F., Thevelein, J.M., and Sheen, J. (2007). A central integrator of transcription networks in plant stress and energy signalling. Nature **448**: 938–942.

Baker, N.R. (2008). Chlorophyll Fluorescence: A Probe of Photosynthesis In Vivo. Annu. Rev. Plant Biol. **59**: 89–113.

Baldwin, J.E. and Krebs, H. (1981). The evolution of metabolic cycles. Nature **291**: 381–382.

Bancos, S., Szatmári, A.M., Castle, J., Kozma-Bognár, L., Shibata, K., Yokota, T., Bishop, G.J., Nagy, F., and Szekeres, M. (2006). Diurnal regulation of the brassinosteroid-biosynthetic CPD gene in Arabidopsis. Plant Physiol. **141**: 299–309.

Bartoli, C.G., Pastori, G.M., and Foyer, C.H. (2000). Ascorbate biosynthesis in mitochondria is linked to the electron transport chain between complexes III and IV. Plant Physiol. **123**: 335–343.

Bass, J. (2012). Circadian topology of metabolism. Nature **491**: 348–356.

Bell-Pedersen, D., Cassone, V.M., Earnest, D.J., Golden, S.S., Hardin, P.E., Thomas, T.L., and Zoran, M.J. (2005). Circadian rhythms from multiple oscillators: Lessons from diverse organisms. Nat. Rev. Genet. **6**: 544–556.

Blanco, N.E., Guinea-Díaz, M., Whelan, J., and Strand, Å. (2014). Interaction between plastid and mitochondrial retrograde signalling pathways during changes to plastid redox status. Philos. Trans. R. Soc. B Biol. Sci. **369**: 20130231.

Bläsing, O.E., Gibon, Y., Günther, M., Höhne, M., Morcuende, R., Osuna, D., Thimm, O., Usadel, B., Scheible, W.R., and Stitt, M. (2005). Sugars and circadian regulation make major contributions to the global regulation of diurnal gene expression in Arabidopsis. Plant Cell **17**: 3257–3281.

Blume, C., Ost, J., Mühlenbruch, M., Peterhänsel, C., and Laxa, M. (2019). Low CO 2 induces urea cycle intermediate accumulation in Arabidopsis thaliana. PLoS One **14**: e0210342.

Braun, H.P. and Schmitz, U.K. (1999). The protein-import apparatus of plant mitochondria. Planta **209**: 267–274.

Braymer, J.J. and Lill, R. (2017). Iron–sulfur cluster biogenesis and trafficking in mitochondria. J. Biol. Chem. **292**: 12754–12763.

Brotman, Y., Riewe, D., Lisec, J., Meyer, R.C., Willmitzer, L., and Altmann, T. (2011). Identification of enzymatic and regulatory genes of plant metabolism through QTL analysis in Arabidopsis. J. Plant Physiol. **168**: 1387–1394.

Bykova, N. V., Møller, I.M., Gardeström, P., and Igamberdiev, A.U. (2014). The function of glycine decarboxylase complex is optimized to maintain high photorespiratory flux via buffering of its reaction products. Mitochondrion **19**: 357–364.

Cabassa-Hourton, Ć. et al. (2016). Proteomic and functional analysis of proline dehydrogenase 1 link proline catabolism to mitochondrial electron transport in Arabidopsis thaliana. Biochem. J. **473**: 2623–2634.

Calvo, S.E. and Mootha, V.K. (2010). The Mitochondrial Proteome and Human Disease. Annu. Rev. Genomics Hum. Genet. **11**: 25–44.

Cardol, P., De Paepe, R., Franck, F., Forti, G., and Finazzi, G. (2010). The onset of NPQ and ΔμH+ upon illumination of tobacco plants studied through the influence of mitochondrial electron transport. Biochim. Biophys. Acta - Bioenerg. **1797**: 177–188.

Carlsson, J., Leino, M., Sohlberg, J., Sundström, J.F., and Glimelius, K. (2008). Mitochondrial regulation of flower development. Mitochondrion **8**: 74–86.

Carrari, F., Nunes-Nesi, A., Gibon, Y., Lytovchenko, A., Loureiro, M.E., and Fernie, A.R. (2003). Reduced Expression of Aconitase Results in an Enhanced Rate of Photosynthesis and Marked Shifts in Carbon Partitioning in Illuminated Leaves of Wild Species Tomato. Plant Physiol. **133**: 1322–1335.

Cashmore, A.R., Jarillo, J.A., Wu, Y.J., and Liu, D. (1999). Cryptochromes: Blue light receptors for plants and animals. Science (80-.). **284**: 760–765.

Cavalcanti, J.H.F., Quinhones, C.G.S., Schertl, P., Brito, D.S., Eubel, H., Hildebrandt, T., Nunes-Nesi, A., Braun, H.P., and Araújo, W.L. (2017). Differential impact of amino acids on OXPHOS system activity following carbohydrate starvation in Arabidopsis cell suspensions. Physiol. Plant. **161**: 451–467.

Cecchini, G. (2003). Function and Structure of Complex II of the Respiratory Chain. Annu. Rev. Biochem. **72**: 77–109.

Cela, O. et al. (2016). Clock genes-dependent

acetylation of complex I sets rhythmic activity of mitochondrial OxPhos. Biochim. Biophys. Acta - Mol. Cell Res. **1863**: 596–606.

Chew, O., Whelan, J., and Millar, A.H. (2003). Molecular Definition of the Ascorbate-Glutathione Cycle in Arabidopsis Mitochondria Reveals Dual Targeting of Antioxidant Defenses in Plants. J. Biol. Chem. **278**: 46869–46877.

Chia, D.W., Yoder, T.J., Reiter, W.D., and Gibson, S.I. (2000a). Fumaric acid: An overlooked form of fixed carbon in Arabidopsis and other plant species. Planta **211**: 743–751.

Chia, D.W., Yoder, T.J., Reiter, W.D., and Gibson, S.I. (2000b). Fumaric acid: An overlooked form of fixed carbon in Arabidopsis and other plant species. Planta **211**: 743–751.

Chow, B.Y., Helfer, A., Nusinow, D.A., and Kay, S.A. (2012). ELF3 recruitment to the PRR9 promoter requires other Evening Complex members in the Arabidopsis circadian clock. Plant Signal. Behav. **7**: 170–173.

Chow, B.Y., Sanchez, S.E., Breton, G., Pruneda-Paz, J.L., Krogan, N.T., and Kay, S.A. (2014). Transcriptional regulation of LUX by CBF1 mediates cold input to the circadian clock in Arabidopsis. Curr. Biol. **24**: 1518–1524.

Chrobok, D. et al. (2016). Dissecting the metabolic role of mitochondria during developmental leaf senescence. Plant Physiol. **172**: 2132–2153.

Clough, S.J. and Bent, A.F. (1998). Floral dip: A simplified method for Agrobacterium-mediated transformation of Arabidopsis thaliana. Plant J. **16**: 735–743.

De Col, V. et al. (2017). ATP sensing in living plant cells reveals tissue gradients and stress dynamics of energy physiology. Elife **6**.

Coruzzi, G.M. (2003). Primary N-assimilation into Amino Acids in Arabidopsis. Arab. B. **2**: e0010.

Covington, M.F. and Harmer, S.L. (2007). The circadian clock regulates auxin signaling and responses in Arabidopsis. PLoS Biol. **5**: 1773–1784.

Covington, M.F., Maloof, J.N., Straume, M., Kay, S.A., and Harmer, S.L. (2008). Global transcriptome analysis reveals circadian regulation of key pathways in plant growth and development. Genome Biol. **9**: R130.

Dalchau, N., Baek, S.J., Briggs, H.M., Robertson, F.C., Dodd, A.N., Gardner, M.J., Stancombe, M.A., Haydon, M.J., Stan, G.B., Gonçalves, J.M., and Webb, A.A.R. (2011). The circadian oscillator gene GIGANTEA mediates a long-term response of the Arabidopsis thaliana circadian clock to sucrose. Proc. Natl. Acad. Sci. U. S. A. **108**: 5104–5109.

Devlin, P.F. and Kay, S.A. (2000). Cryptochromes are required for phytochrome signaling to the circadian clock but not for rhythmicity. Plant Cell **12**: 2499–2509.

Dibner, C., Schibler, U., and Albrecht, U. (2010). The Mammalian Circadian Timing System: Organization and Coordination of Central and Peripheral Clocks. Annu. Rev. Physiol. **72**: 517–549.

Dinakar, C., Raghavendra, A.S., and Padmasree, K. (2010). Importance of AOX pathway in optimizing photosynthesis under high light stress: Role of pyruvate and malate in activating AOX. Physiol. Plant. **139**: 13–26.

Dixon, L.E., Knox, K., Kozma-Bognar, L., Southern, M.M., Pokhilko, A., and Millar, A.J. (2011). Temporal repression of core circadian genes is mediated through EARLY FLOWERING 3 in Arabidopsis. Curr. Biol. **21**: 120–125.

Dodd, A.N., Gardner, M.J., Hotta, C.T., Hubbard, K.E., Dalchau, N., Love, J., Assie, J.M., Robertson, F.C., Jakobsen, M.K., Gonçalves, J., Sanders, D., and Webb, A.A.R. (2007). The Arabidopsis circadian clock incorporates a cADPR-based feedback loop. Science (80-.). **318**: 1789–1792.

Dodd, A.N., Salathia, N., Hall, A., Kévei, E., Tóth, R., Nagy, F., Hibberd, J.M., Millar, A.J., and Webb, A.A.R. (2005). Cell biology: Plant circadian clocks increase photosynthesis, growth, survival, and competitive advantage. Science (80-.). **309**: 630–633.

van Dongen, J.T., Gupta, K.J., Ramírez-Aguilar, S.J., Araújo, W.L., Nunes-Nesi, A., and Fernie, A.R. (2011). Regulation of respiration in plants: A role for alternative metabolic pathways. J. Plant Physiol. **168**: 1434–1443.

Doyle, M.R., Davis, S.J., Bastow, R.M., McWatters, H.G., Kozma-Bognár, L., Nagy, F., and Millar, A.J. (2002). The ELF4 gene controls circadian rhythms and flowering time

in Arabidopsis thaliana. Nature **419**: 74–77.

Dyson, B.C., Miller, M.A.E., Feil, R., Rattray, N., Bowsher, C.G., Goodacre, R., Lunn, J.E., and Johnson, G.N. (2016). FUM2, a cytosolic fumarase, is essential for acclimation to low temperature in arabidopsis thaliana. Plant Physiol. **172**: 118–127.

Eisenhut, M., Bräutigam, A., Timm, S., Florian, A., Tohge, T., Fernie, A.R., Bauwe, H., and Weber, A.P.M. (2017). Photorespiration Is Crucial for Dynamic Response of Photosynthetic Metabolism and Stomatal Movement to Altered CO2 Availability. Mol. Plant **10**: 47–61.

Elhafez, D., Murcha, M.W., Clifton, R., Soole, K.L., Day, D.A., and Whelan, J. (2006). Characterization of mitochondrial alternative NAD(P)H dehydrogenases in arabidopsis: Intraorganelle location and expression. Plant Cell Physiol. **47**: 43–54.

Endo, M., Shimizu, H., Nohales, M.A., Araki, T., and Kay, S.A. (2014). Tissue-specific clocks in Arabidopsis show asymmetric coupling. Nature **515**: 419–422.

Engel, N., Van Den Daele, K., Kolukisaoglu, Ü., Morgenthal, K., Weckwerth, W., Pärnik, T., Keerberg, O., and Bauwe, H. (2007). Deletion of glycine decarboxylase in arabidopsis is lethal under nonphotorespiratory conditions. Plant Physiol. **144**: 1328–1335.

Espinoza, C., Degenkolbe, T., Caldana, C., Zuther, E., Leisse, A., Willmitzer, L., Hincha, D.K., and Hannah, M.A. (2010). Interaction with diurnal and circadian regulation results in dynamic metabolic and transcriptional changes during cold acclimation in arabidopsis. PLoS One **5**: e14101.

Ezer, D. et al. (2017). The evening complex coordinates environmental and endogenous signals in Arabidopsis. Nat. Plants **3**: 17087.

Farinas, B. and Mas, P. (2011). Functional implication of the MYB transcription factor RVE8/LCL5 in the circadian control of histone acetylation. Plant J. **66**: 318–329.

Farré, E.M., Harmer, S.L., Harmon, F.G., Yanovsky, M.J., and Kay, S.A. (2005). Overlapping and distinct roles of PRR7 and PRR9 in the Arabidopsis circadian clock. Curr. Biol. **15**: 47–54.

Fernie, A.R., Aharoni, A., Willmitzer, L., Stitt, M., Tohge, T., Kopka, J., Carroll, A.J., Saito, K., Fraser, P.D., and de Luca, V. (2011). Recommendations for reporting metabolite data. Plant Cell **23**: 2477–2482.

Feugier, F.G. and Satake, A. (2013). Dynamical feedback between circadian clock and sucrose availability explains adaptive response of starch metabolism to various photoperiods. Front. Plant Sci. **3**: 305.

Figueroa, C.M. et al. (2016). Trehalose 6-phosphate coordinates organic and amino acid metabolism with carbon availability. Plant J. **85**: 410–423.

Flis, A. et al. (2019). Multiple circadian clock outputs regulate diel turnover of carbon and nitrogen reserves. Plant Cell Environ. **42**: 549–573.

Fontaine, J.X., Tercé-Laforgue, T., Armengaud, P., Clément, G., Renou, J.P., Pelletier, S., Catterou, M., Azzopardi, M., Gibon, Y., Lea, P.J., Hirel, B., and Dubois, F. (2012). Characterization of a NADH-dependent glutamate dehydrogenase mutant of arabidopsis demonstrates the key role of this enzyme in root carbon and nitrogen metabolism. Plant Cell **24**: 4044–4065.

Frank, A. et al. (2018). Circadian Entrainment in Arabidopsis by the Sugar-Responsive Transcription Factor bZIP63. Curr. Biol. **28**: 2597-2606.e6.

Friedberg, D., Peleg, Y., Monsonego, A., Maissi, S., Battat, E., Rokem, J.S., and Goldberg, I. (1995). The fumR gene encoding fumarase in the filamentous fungus Rhizopus oryzae: cloning, structure and expression. Gene **163**: 139–144.

Fritz, C., Mueller, C., Matt, P., Feil, R., and Stitt, M. (2006). Impact of the C-N status on the amino acid profile in tobacco source leaves. Plant, Cell Environ. **29**: 2055–2076.

Fromm, S., Braun, H.P., and Peterhansel, C. (2016). Mitochondrial gamma carbonic anhydrases are required for complex I assembly and plant reproductive development. New Phytol. **211**: 194–207.

Fujiki, Y., Ito, M., Nishida, I., and Watanabe, A. (2001). Leucine and its keto acid enhance the coordinated expression of genes for branched-chain amino acid catabolism in Arabidopsis under sugar starvation. FEBS Lett. **499**: 161–165.

Fujiwara, S., Wang, L., Han, L., Suh, S.S.,

Salomé, P.A., McClung, C.R., and Somers, D.E. (2008). Post-translational regulation of the Arabidopsis circadian clock through selective proteolysis and phosphorylation of pseudo-response regulator proteins. J. Biol. Chem. **283**: 23073–23083.

Fukushima, A., Kusano, M., Nakamichi, N., Kobayashi, M., Hayashi, N., Sakakibara, H., Mizuno, T., and Saito, K. (2009). Impact of clock-associated Arabidopsis pseudoresponse regulators in metabolic coordination. Proc. Natl. Acad. Sci. U. S. A. **106**: 7251–7256.

Fung-Uceda, J., Lee, K., Seo, P.J., Polyn, S., De Veylder, L., and Mas, P. (2018). The Circadian Clock Sets the Time of DNA Replication Licensing to Regulate Growth in Arabidopsis. Dev. Cell **45**: 101-113.e4.

Gardeström, P. and Igamberdiev, A.U. (2016). The origin of cytosolic ATP in photosynthetic cells. Physiol. Plant. **157**: 367–379.

Gauthier, P.P.G., Bligny, R., Gout, E., Mahé, A., Nogués, S., Hodges, M., and Tcherkez, G.G.B. (2010). In folio isotopic tracing demonstrates that nitrogen assimilation into glutamate is mostly independent from current CO2 assimilation in illuminated leaves of Brassica napus. New Phytol. **185**: 988–999.

Gendron, J.M., Pruneda-Paz, J.L., Doherty, C.J., Gross, A.M., Kang, S.E., and Kay, S.A. (2012). Arabidopsis circadian clock protein, TOC1,is a DNA-binding transcription factor. Proc. Natl. Acad. Sci. U. S. A. **109**: 3167–3172.

Gibon, Y., Blaesing, O.E., Hannemann, J., Carillo, P., Höhne, M., Hendriks, J.H.M., Palacios, N., Cross, J., Selbig, J., and Stitt, M. (2004a). A robot-based platform to measure multiple enzyme activities in Arabidopsis using a set of cycling assays: Comparison of changes of enzyme activities and transcript levels during diurnal cycles and in prolonged darkness. Plant Cell **16**: 3304–3325.

Gibon, Y., Blaesing, O.E., Hannemann, J., Carillo, P., Höhne, M., Hendriks, J.H.M., Palacios, N., Cross, J., Selbig, J., and Stitt, M. (2004b). A robot-based platform to measure multiple enzyme activities in Arabidopsis using a set of cycling assays: Comparison of changes of enzyme activities and transcript levels during diurnal cycles and in prolonged darkness. Plant Cell **16**: 3304–3325.

Gibon, Y., Bläsing, O.E., Palacios-Rojas, N., Pankovic, D., Hendriks, J.H.M., Fisahn, J., Höhne, M., Günther, M., and Stitt, M. (2004c). Adjustment of diurnal starch turnover to short days: Depletion of sugar during the night leads to a temporary inhibition of carbohydrate utilization, accumulation of sugars and post-translational activation of ADP-glucose pyrophosphorylase in the followin. Plant J. **39**: 847–862.

Gibon, Y., Pyl, E.T., Sulpice, R., Lunn, J.E., HÖhne, M., GÜnther, M., and Stitt, M. (2009). Adjustment of growth, starch turnover, protein content and central metabolism to a decrease of the carbon supply when Arabidopsis is grown in very short photoperiods. Plant, Cell Environ. **32**: 859–874.

Gibon, Y., Usadel, B., Blaesing, O.E., Kamlage, B., Hoehne, M., Trethewey, R., and Stitt, M. (2006). Integration of metabolite with transcript and enzyme activity profiling during diurnal cycles in Arabidopsis rosettes. Genome Biol. **7**: R76.

Giraud, E., Ng, S., Carrie, C., Duncan, O., Low, J., Lee, C.P., van Aken, O., Harvey Millar, A., Murcha, M., and Whelan, J. (2010). TCP transcription factors link the regulation of genes encoding mitochondrial proteins with the circadian clock in Arabidopsis Thaliana. Plant Cell **22**: 3921–3934.

Glen Uhrig, R., Labandera, A.M., Tang, L.Y., Sieben, N.A., Goudreault, M., Yeung, E., Gingras, A.C., Samuel, M.A., and Moorhead, G.B.G. (2017). Activation of mitochondrial protein phosphatase SLP2 by MIA40 regulates seed germination. Plant Physiol. **173**: 956–969.

Gould, P.D., Locke, J.C.W., Larue, C., Southern, M.M., Davis, S.J., Hanano, S., Moyle, R., Milich, R., Putterill, J., Millar, A.J., and Hall, A. (2006). The molecular basis of temperature compensation in the Arabidopsis circadian clock. Plant Cell **18**: 1177–1187.

Graf, A., Schlereth, A., Stitt, M., and Smith, A.M. (2010). Circadian control of carbohydrate availability for growth in Arabidopsis plants at night. Proc. Natl. Acad. Sci. U. S. A. **107**: 9458–9463.

Graf, A. and Smith, A.M. (2011). Starch and the clock: The dark side of plant productivity. Trends Plant Sci. **16**: 169–175.

Gray, J.A., Shalit-Kaneh, A., Chu, D.N., Hsu, P.Y., and Harmer, S.L. (2017). The REVEILLE clock genes inhibit growth of

juvenile and adult plants by control of cell size. Plant Physiol. **173**: 2308–2322.

Greenham, K. and McClung, C.R. (2015). Integrating circadian dynamics with physiological processes in plants. Nat. Rev. Genet. **16**: 598–610.

Grimaldi, B., Bellet, M.M., Katada, S., Astarita, G., Hirayama, J., Amin, R.H., Granneman, J.G., Piomelli, D., Leff, T., and Sassone-Corsi, P. (2010). PER2 controls lipid metabolism by direct regulation of PPARγ. Cell Metab. **12**: 509–520.

Gueguen, V., Macherel, D., Jaquinod, M., Douce, R., and Bourguignon, J. (2000). Fatty acid and lipoic acid biosynthesis in higher plant mitochondria. J. Biol. Chem. **275**: 5016–5025.

Guo, R., Zong, S., Wu, M., Gu, J., and Yang, M. (2017). Architecture of Human Mitochondrial Respiratory Megacomplex I2III2IV2. Cell **170**: 1247-1257.e12.

Gupta, K.J., Shah, J.K., Brotman, Y., Jahnke, K., Willmitzer, L., Kaiser, W.M., Bauwe, H., and Igamberdiev, A.U. (2012). Inhibition of aconitase by nitric oxide leads to induction of the alternative oxidase and to a shift of metabolism towards biosynthesis of amino acids. J. Exp. Bot. **63**: 1773–1784.

Gutiérrez, R.A., Stokes, T.L., Thum, K., Xu, X., Obertello, M., Katari, M.S., Tanurdzic, M., Dean, A., Nero, D.C., McClung, C.R., and Coruzzi, G.M. (2008). Systems approach identifies an organic nitrogen-responsive gene network that is regulated by the master clock control gene CCA1. Proc. Natl. Acad. Sci. U. S. A. **105**: 4939–4944.

Harmer, S.L. (2009). The Circadian System in Higher Plants. Annu. Rev. Plant Biol. **60**: 357–377.

Hassidim, M., Dakhiya, Y., Turjeman, A., Hussien, D., Shor, E., Anidjar, A., Goldberg, K., and Green, R.M. (2017). CIRCADIAN CLOCK ASSOCIATED1 (CCA1) and the circadian control of stomatal aperture. Plant Physiol. **175**: 1864–1877.

Haydon, M.J., Hearn, T.J., Bell, L.J., Hannah, M.A., and Webb, A.A.R. (2013a). Metabolic regulation of circadian clocks. Semin. Cell Dev. Biol. **24**: 414–421.

Haydon, M.J., Mielczarek, O., Frank, A., Román, Á., and Webb, A.A.R. (2017). Sucrose and ethylene signaling interact to modulate the circadian clock. Plant Physiol. **175**: 947–958.

Haydon, M.J., Mielczarek, O., Robertson, F.C., Hubbard, K.E., and Webb, A.A.R. (2013b). Photosynthetic entrainment of the Arabidopsis thaliana circadian clock. Nature **502**: 689–692.

Hazen, S.P., Schultz, T.F., Pruneda-Paz, J.L., Borevitz, J.O., Ecker, J.R., and Kay, S.A. (2005). LUX ARRHYTHMO encodes a Myb domain protein essential for circadian rhythms. Proc. Natl. Acad. Sci. U. S. A. **102**: 10387–10392.

Heazlewood, J.L. and Millar, A.H. (2005). AMPDB: The Arabidopsis Mitochondrial Protein Database. Nucleic Acids Res. **33**: D605–D610.

Hemmes, H., Henriques, R., Jang, I.C., Kim, S., and Chua, N.H. (2012). Circadian clock regulates dynamic chromatin modifications associated with arabidopsis CCA1/LHY and TOC1 transcriptional rhythms. Plant Cell Physiol. **53**: 2016–2029.

Hicks, K.A., Albertson, T.M., and Wagner, D.R. (2001). EARLY FLOWERING3 encodes a novel protein that regulates circadian clock function and flowering in arabidopsis. Plant Cell **13**: 1281–1292.

Hildebrandt, T.M. (2018). Synthesis versus degradation: directions of amino acid metabolism during Arabidopsis abiotic stress response. Plant Mol. Biol. **98**: 121–135.

Hildebrandt, T.M., Nunes Nesi, A., Araújo, W.L., and Braun, H.P. (2015). Amino Acid Catabolism in Plants. Mol. Plant **8**: 1563–1579.

Hirano, A., Fu, Y.H., and Ptáek, L.J. (2016). The intricate dance of post-translational modifications in the rhythm of life. Nat. Struct. Mol. Biol. **23**: 1053–1060.

Hooks, M.A., Allwood, J.W., Harrison, J.K.D., Kopka, J., Erban, A., Goodacre, R., and Balk, J. (2014). Selective induction and subcellular distribution of ACONITASE 3 reveal the importance of cytosolic citrate metabolism during lipid mobilization in Arabidopsis. Biochem. J. **463**: 309–317.

Hsu, P.Y., Devisetty, U.K., and Harmer, S.L. (2013). Accurate timekeeping is controlled by a cycling activator in Arabidopsis. Elife **2013**.

Huang, H., Alvarez, S., Bindbeutel, R., Shen, Z., Naldrett, M.J., Evans, B.S., Briggs, S.P.,

Hicks, L.M., Kay, S.A., and Nusinow, D.A. (2016a). Identification of evening complex associated proteins in arabidopsis by affinity purification and mass spectrometry. Mol. Cell. Proteomics **15**: 201–217.

Huang, S., Van Aken, O., Schwarzländer, M., Belt, K., and Millar, A.H. (2016b). The roles of mitochondrial reactive oxygen species in cellular signaling and stress response in plants. Plant Physiol. **171**: 1551–1559.

Huang, S. and Millar, A.H. (2013). Succinate dehydrogenase: The complex roles of a simple enzyme. Curr. Opin. Plant Biol. **16**: 344–349.

Huang, S., Taylor, N.L., Ströher, E., Fenske, R., and Millar, A.H. (2013). Succinate dehydrogenase assembly factor 2 is needed for assembly and activity of mitochondrial complex II and for normal root elongation in Arabidopsis. Plant J. **73**: 429–441.

Huang, W., Pérez-García, P., Pokhilko, A., Millar, A.J., Antoshechkin, I., Riechmann, J.L., and Mas, P. (2012). Mapping the core of the Arabidopsis circadian clock defines the network structure of the oscillator. Science (80-.). **335**: 75–79.

Igamberdiev, A.U. and Gardeström, P. (2003). Regulation of NAD- and NADP-dependent isocitrate dehydrogenases by reduction levels of pyridine nucleotides in mitochondria and cytosol of pea leaves. Biochim. Biophys. Acta - Bioenerg. **1606**: 117–125.

Imamura, H., Huynh Nhat, K.P., Togawa, H., Saito, K., Iino, R., Kato-Yamada, Y., Nagai, T., and Noji, H. (2009). Visualization of ATP levels inside single living cells with fluorescence resonance energy transfer-based genetically encoded indicators. Proc. Natl. Acad. Sci. U. S. A. **106**: 15651–15656.

Ishida, K., Yamashino, T., and Mizuno, T. (2008). Expression of the cytokinin-induced type-A response regulator gene ARR9 is regulated by the circadian clock in Arabidopsis thaliana. Biosci. Biotechnol. Biochem. **72**: 3025–3029.

Ishihara, H., Moraes, T.A., Pyl, E.T., Schulze, W.X., Obata, T., Scheffel, A., Fernie, A.R., Sulpice, R., and Stitt, M. (2017). Growth rate correlates negatively with protein turnover in Arabidopsis accessions. Plant J. **91**: 416–429.

Ishihara, H., Obata, T., Sulpice, R., Fernie, A.R., and Stitt, M. (2015). Quantifying protein synthesis and degradation in arabidopsis by dynamic ^{13} CO<inf>2</inf> labeling and analysis of enrichment in individual amino acids in their free pools and in protein. Plant Physiol. **168**: 74–93.

Ishizaki, K., Larson, T.R., Schauer, N., Fernie, A.R., Graham, I.A., and Leaver, C.J. (2005a). The critical role of Arabidopsis electron-transfer flavoprotein:ubiquinone oxidoreductase during dark-induced starvation. Plant Cell **17**: 2587–2600.

Ishizaki, K., Larson, T.R., Schauer, N., Fernie, A.R., Graham, I.A., and Leaver, C.J. (2005b). The critical role of Arabidopsis electron-transfer flavoprotein:ubiquinone oxidoreductase during dark-induced starvation. Plant Cell **17**: 2587–2600.

Ishizaki, K., Schauer, N., Larson, T.R., Graham, I.A., Fernie, A.R., and Leaver, C.J. (2006). The mitochondrial electron transfer flavoprotein complex is essential for survival of Arabidopsis in extended darkness. Plant J. **47**: 751–760.

Jacobi, D. et al. (2015). Hepatic Bmal1 regulates rhythmic mitochondrial dynamics and promotes metabolic fitness. Cell Metab. **22**: 709–720.

James, A.B., Syed, N.H., Bordage, S., Marshall, J., Nimmo, G.A., Jenkins, G.I., Herzyk, P., Brown, J.W.S., and Nimmo, H.G. (2012). Alternative splicing mediates responses of the Arabidopsis circadian clock to temperature changes. Plant Cell **24**: 961–981.

Jarillo, J.A., Capel, J., Tang, R.H., Yang, H.Q., Alonso, J.M., Ecker, J.R., and Cashmore, A.R. (2001). An Arabidopsis circadian clock component interacts with both CRY1 and phyB. Nature **410**: 487–490.

Jones, A.R., Forero-Vargas, M., Withers, S.P., Smith, R.S., Traas, J., Dewitte, W., and Murray, J.A.H. (2017). Cell-size dependent progression of the cell cycle creates homeostasis and flexibility of plant cell size. Nat. Commun. **8**: 15060.

Kamioka, M., Takao, S., Suzuki, T., Taki, K., Higashiyam, T., Kinoshita, T., and Nakamichi, N. (2016). Direct repression of evening genes by CIRCADIAN CLOCK-ASSOCIATED1 in the Arabidopsis circadian clock. Plant Cell **28**: 696–711.

Keily, J., MacGregor, D.R., Smith, R.W., Millar, A.J., Halliday, K.J., and Penfield, S. (2013). Model selection reveals control of cold

signalling by evening-phased components of the plant circadian clock. Plant J. **76**: 247–257.

Kidokoro, S., Maruyama, K., Nakashima, K., Imura, Y., Narusaka, Y., Shinwari, Z.K., Osakabe, Y., Fujita, Y., Mizoi, J., Shinozaki, K., and Yamaguchi-Shinozaki, K. (2009). The phytochrome-interacting factor PIF7 negatively regulates dreb1 expression under circadian control in Arabidopsis. Plant Physiol. **151**: 2046–2057.

Kim, H., Kim, H.J., Vu, Q.T., Jung, S., Robertson McClung, C., Hong, S., and Nam, H.G. (2018). Circadian control of ORE1 by PRR9 positively regulates leaf senescence in Arabidopsis. Proc. Natl. Acad. Sci. U. S. A. **115**: 8448–8453.

Kim, W.Y., Fujiwara, S., Suh, S.S., Kim, J., Kim, Y., Han, L., David, K., Putterill, J., Nam, H.G., and Somers, D.E. (2007). ZEITLUPE is a circadian photoreceptor stabilized by GIGANTEA in blue light. Nature **449**: 356–360.

Klodmann, J., Sunderhaus, S., Nimtz, M., Jänsch, L., and Braun, H.P. (2010). Internal architecture of mitochondrial complex I from Arabidopsis thaliana. Plant Cell **22**: 797–810.

Knight, H., Thomson, A.J.W., and McWatters, H.G. (2008). Sensitive to freezing6 integrates cellular and environmental inputs to the plant circadian clock. Plant Physiol. **148**: 293–303.

Kohsaka, A., Das, P., Hashimoto, I., Nakao, T., Deguchi, Y., Gouraud, S.S., Waki, H., Muragaki, Y., and Maeda, M. (2014). The circadian clock maintains cardiac function by regulating mitochondrial metabolism in mice. PLoS One **9**: e112811.

Kopka, J. et al. (2005). GMD@CSB.DB: The Golm metabolome database. Bioinformatics **21**: 1635–1638.

Korneli, C., Danisman, S., and Staiger, D. (2014). Differential control of pre-invasive and post-invasive antibacterial defense by the Arabidopsis circadian clock. Plant Cell Physiol. **55**: 1613–1622.

Kriebs, A. et al. (2017). Circadian repressors CRY1 and CRY2 broadly interact with nuclear receptors and modulate transcriptional activity. Proc. Natl. Acad. Sci. U. S. A. **114**: 8776–8781.

Krüßel, L., Junemann, J., Wirtz, M., Birke, H., Thornton, J.D., Browning, L.W., Poschet, G., Hell, R., Balk, J., Braun, H.P., and Hildebrandt, T.M. (2014). The mitochondrial sulfur dioxygenase ETHYLMALONIC ENCEPHALOPATHY PROTEIN1 is required for amino acid catabolism during carbohydrate starvation and embryo development in Arabidopsis. Plant Physiol. **165**: 92–104.

Kühn, K., Obata, T., Feher, K., Bock, R., Fernie, A.R., and Meyer, E.H. (2015). Complete mitochondrial complex I deficiency induces an up-regulation of respiratory fluxes that is abolished by traces of functional complex I. Plant Physiol. **168**: 1537–1549.

Kühn, K., Richter, U., Meyer, E.H., Delannoy, E., De Longevialle, A.F., Otoole, N., Börner, T., Millar, A.H., Small, I.D., and Whelan, J. (2009). Phage-type RNA polymerase RPOTmp performs gene-specific transcription in mitochondria of arabidopsis thaliana. Plant Cell **21**: 2762–2779.

Kumar, V. and Sharma, A. (2018). Common features of circadian timekeeping in diverse organisms. Curr. Opin. Physiol. **5**: 58–67.

Kwon, Y.J., Park, M.J., Kim, S.G., Baldwin, I.T., and Park, C.M. (2014). Alternative splicing and nonsense-mediated decay of circadian clock genes under environmental stress conditions in Arabidopsis. BMC Plant Biol. **14**: 136.

Lai, A.G., Doherty, C.J., Mueller-Roeber, B., Kay, S.A., Schippers, J.H.M., and Dijkwel, P.P. (2012). Circadian Clock-Associated 1 regulates ROS homeostasis and oxidative stress responses. Proc. Natl. Acad. Sci. U. S. A. **109**: 17129–17134.

Launay, A. et al. (2019). Proline oxidation fuels mitochondrial respiration during dark-induced leaf senescence in Arabidopsis thaliana. J. Exp. Bot.

Lea, P.J., Sodek, L., Parry, M.A.J., Shewry, P.R., and Halford, N.G. (2007). Asparagine in plants. Ann. Appl. Biol. **150**: 1–26.

Lee, C.P., Eubel, H., and Millar, A.H. (2010). Diurnal changes in mitochondrial function reveal daily optimization of light and dark respiratory metabolism in Arabidopsis. Mol. Cell. Proteomics **9**: 2125–2139.

Lee, H.G., Mas, P., and Seo, P.J. (2016). MYB96 shapes the circadian gating of ABA signaling in Arabidopsis. Sci. Rep. **6**: 17754.

Legnaioli, T., Cuevas, J., and Mas, P. (2009).

TOC1 functions as a molecular switch connecting the circadian clock with plant responses to drought. EMBO J. **28**: 3745–3757.

Leivar, P. and Quail, P.H. (2011). PIFs: Pivotal components in a cellular signaling hub. Trends Plant Sci. **16**: 19–28.

León, G., Holuigue, L., and Jordana, X. (2007). Mitochondrial complex II is essential for gametophyte development in Arabidopsis. Plant Physiol. **143**: 1534–1546.

Li, G. et al. (2011). Coordinated transcriptional regulation underlying the circadian clock in Arabidopsis. Nat. Cell Biol. **13**: 616–622.

Liang, C., Zhang, Y., Cheng, S., Osorio, S., Sun, Y., Fernie, A.R., Cheung, C.Y.M., and Lim, B.L. (2015). Impacts of high ATP supply from chloroplasts and mitochondria on the leaf metabolism of arabidopsis thaliana. Front. Plant Sci. **6**: 922.

Van Lis, R. and Atteia, A. (2004). Control of mitochondrial function via photosynthetic redox signals. Photosynth. Res. **79**: 133–148.

Lisec, J., Schauer, N., Kopka, J., Willmitzer, L., and Fernie, A.R. (2006). Gas chromatography mass spectrometry–based metabolite profiling in plants. Nat. Protoc. **1**: 387–396.

Litthauer, S., Chan, K.X., and Jones, M.A. (2018). 3'-Phosphoadenosine 5'-Phosphate Accumulation Delays the Circadian System. Plant Physiol. **176**: 3120–3135.

Liu, C., Li, S., Liu, T., Borjigin, J., and Lin, J.D. (2007). Transcriptional coactivator PGC-1α integrates the mammalian clock and energy metabolism. Nature **447**: 477–481.

Livak, K.J. and Schmittgen, T.D. (2001). Analysis of relative gene expression data using real-time quantitative PCR and the 2-ΔΔCT method. Methods **25**: 402–408.

Logemann, E., Birkenbihl, R.P., Ülker, B., and Somssich, I.E. (2006). An improved method for preparing Agrobacterium cells that simplifies the Arabidopsis transformation protocol. Plant Methods **2**: 16.

Loizides-Mangold, U. et al. (2017). Lipidomics reveals diurnal lipid oscillations in human skeletal muscle persisting in cellular myotubes cultured in vitro. Proc. Natl. Acad. Sci. U. S. A. **114**: E8565–E8574.

Lu, D., Wang, T., Persson, S., Mueller-Roeber, B., and Schippers, J.H.M. (2014). Transcriptional control of ROS homeostasis by KUODA1 regulates cell expansion during leaf development. Nat. Commun. **5**: 3767.

Lu, S.X., Knowles, S.M., Andronis, C., Ong, M.S., and Tobin, E.M. (2009). Circadian clock associated1 and late elongated hypocotyl function synergistically in the circadian clock of arabidopsis. Plant Physiol. **150**: 834–843.

Lu, S.X., Webb, C.J., Knowles, S.M., Kim, S.H.J., Wang, Z., and Tobin, E.M. (2012). CCA1 and ELF3 interact in the control of hypocotyl length and flowering time in arabidopsis. Plant Physiol. **158**: 1079–1088.

Lu, Y., Gehan, J.P., and Sharkey, T.D. (2005). Daylength and circadian effects on starch degradation and maltose metabolism. Plant Physiol. **138**: 2280–2291.

Luedemann, A., Von Malotky, L., Erban, A., and Kopka, J. (2012). TagFinder: Preprocessing software for the fingerprinting and the profiling of gas chromatography-mass spectrometry based metabolome analyses. In Methods in Molecular Biology (Humana Press), pp. 255–286.

Ma, Y., Gil, S., Grasser, K.D., and Mas, P. (2018). Targeted recruitment of the basal transcriptional machinery by LNK clock components controls the circadian rhythms of nascent RNAs in arabidopsis. Plant Cell **30**: 907–924.

Magnone, M.C., Langmesser, S., Bezdek, A.C., Tallone, T., Rusconi, S., and Albrecht, U. (2015). The mammalian circadian clock gene Per2 modulates cell death in response to oxidative stress. Front. Neurol. **6**: 289.

Majumdar, R., Barchi, B., Turlapati, S.A., Gagne, M., Minocha, R., Long, S., and Minocha, S.C. (2016). Glutamate, ornithine, arginine, proline, and polyamine metabolic interactions: The pathway is regulated at the post-transcriptional level. Front. Plant Sci. **7**: 78.

Makino, S., Kiba, T., Imamura, A., Hanaki, N., Nakamura, A., Suzuki, T., Taniguchi, M., Ueguchi, C., Sugiyama, T., and Mizuno, T. (2000). Genes encoding pseudo-response regulators: Insight into His-to-Asp phosphorelay and circadian rhythm in Arabidopsis thaliana. Plant Cell Physiol. **41**: 791–803.

Malapeira, J., Khaitova, L.C., and Mas, P. (2012). Ordered changes in histone modifications at the core of the Arabidopsis circadian clock. Proc. Natl. Acad. Sci. U. S. A. **109**: 21540–21545.

Marshall, C.M., Tartaglio, V., Duarte, M., and Harmon, F.G. (2016). The arabidopsis sickle mutant exhibits altered circadian clock responses to cool temperatures and temperature-dependent alternative splicing. Plant Cell **28**: 2560–2575.

Martin-Tryon, E.L., Kreps, J.A., and Harmer, S.L. (2007). GIGANTEA acts in blue light signaling and has biochemically separable roles in circadian clock and flowering time regulation. Plant Physiol. **143**: 473–486.

Martín, G. et al. (2018). Circadian Waves of Transcriptional Repression Shape PIF-Regulated Photoperiod-Responsive Growth in Arabidopsis. Curr. Biol. **28**: 311-318.e5.

Más, P., Alabadí, D., Yanovsky, M.J., Oyama, T., and Kay, S.A. (2003a). Dual role of TOC1 in the control of circadian and photomorphogenic responses in Arabidopsis. Plant Cell **15**: 223–236.

Más, P., Kim, W.Y., Somers, D.E., and Kay, S.A. (2003b). Targeted degradation of TOC1 by ZTL modulates circadian function in Arabidopsis thaliana. Nature **426**: 567–570.

Masri, S., Patel, V.R., Eckel-Mahan, K.L., Peleg, S., Forne, I., Ladurner, A.G., Baldi, P., Imhof, A., and Sassone-Corsi, P. (2013). Circadian acetylome reveals regulation of mitochondrial metabolic pathways. Proc. Natl. Acad. Sci. U. S. A. **110**: 3339–3344.

Masri, S. and Sassone-Corsi, P. (2010). Plasticity and specificity of the circadian epigenome. Nat. Neurosci. **13**: 1324–1329.

Matsushika, A., Makino, S., Kojima, M., and Mizuno, T. (2000). Circadian waves of expression of the APRR1/TOC1 family of pseudo-response regulators in Arabidopsis thaliana: Insight into the plant circadian clock. Plant Cell Physiol. **41**: 1002–1012.

Maurice Cheung, C.Y., Poolman, M.G., Fell, D.A., George Ratcliffe, R., and Sweetlove, L.J. (2014). A diel flux balance model captures interactions between light and dark metabolism during day-night cycles in C3 and crassulacean acid metabolism leaves. Plant Physiol. **165**: 917–929.

Mauvoisin, D., Wang, J., Jouffe, C., Martin, E., Atger, F., Waridel, P., Quadroni, M., Gachon, F., and Naef, F. (2014). Circadian clock-dependent and -independent rhythmic proteomes implement distinct diurnal functions in mouse liver. Proc. Natl. Acad. Sci. U. S. A. **111**: 167–172.

McClung, C.R. (2006). Plant circadian rhythms. Plant Cell **18**: 792–803.

Mengin, V., Pyl, E.T., Moraes, T.A., Sulpice, R., Krohn, N., Encke, B., and Stitt, M. (2017). Photosynthate partitioning to starch in arabidopsis thaliana is insensitive to light intensity but sensitive to photoperiod due to a restriction on growth in the light in short photoperiods. Plant Cell Environ. **40**: 2608–2627.

Meyer, E.H., Tomaz, T., Carroll, A.J., Estavillo, G., Delannoy, E., Tanz, S.K., Small, I.D., Pogson, B.J., and Millar, A.H. (2009). Remodeled respiration in ndufs4 with Low phosphorylation efficiency suppresses Arabidopsis germination and growth and alters control of metabolism at night. Plant Physiol. **151**: 603–619.

Mi, H., Muruganujan, A., Huang, X., Ebert, D., Mills, C., Guo, X., and Thomas, P.D. (2019). Protocol Update for large-scale genome and gene function analysis with the PANTHER classification system (v.14.0). Nat. Protoc. **14**: 703–721.

Michaeli, S., Fait, A., Lagor, K., Nunes-Nesi, A., Grillich, N., Yellin, A., Bar, D., Khan, M., Fernie, A.R., Turano, F.J., and Fromm, H. (2011). A mitochondrial GABA permease connects the GABA shunt and the TCA cycle, and is essential for normal carbon metabolism. Plant J. **67**: 485–498.

Michalecka, A.M., Svensson, Å.S., Johansson, F.I., Agius, S.C., Johanson, U., Brennicke, A., Binder, S., and Rasmusson, A.G. (2003). Arabidopsis Genes Encoding Mitochondrial Type II NAD(P)H Dehydrogenases Have Different Evolutionary Origin and Show Distinct Responses to Light. Plant Physiol. **133**: 642–652.

Millar, A.H., Eubel, H., Jänsch, L., Kruft, V., Heazlewood, J.L., and Braun, H.P. (2004). Mitochondrial cytochrome c oxidase and succinate dehydrogenase complexes contain plant specific subunits. Plant Mol. Biol. **56**: 77–90.

Millar, A.H., Whelan, J., Soole, K.L., and Day, D.A. (2011). Organization and Regulation of Mitochondrial Respiration in Plants. Annu. Rev. Plant Biol. **62**: 79–104.

Millar, A.J. (2016). The Intracellular Dynamics of Circadian Clocks Reach for the Light of Ecology and Evolution. Annu. Rev. Plant Biol. **67**: 595–618.

Millar, A.J., Carré, I.A., Strayer, C.A., Chua, N.H., and Kay, S.A. (1995). Circadian clock mutants in Arabidopsis identified by luciferase imaging. Science (80-.). **267**: 1161–1163.

Mitchell, P. (1961). Coupling of phosphorylation to electron and hydrogen transfer by a chemi-osmotic type of mechanism. Nature **191**: 144–148.

Miyashita, Y. and Good, A.G. (2008). NAD(H)-dependent glutamate dehydrogenase is essential for the survival of Arabidopsis thaliana during dark-induced carbon starvation. J. Exp. Bot. **59**: 667–680.

Mizuno, T., Nomoto, Y., Oka, H., Kitayama, M., Takeuchi, A., Tsubouchi, M., and Yamashino, T. (2014). Ambient temperature signal feeds into the circadian clock transcriptional circuitry through the EC night-time repressor in arabidopsis thaliana. Plant Cell Physiol. **55**: 958–976.

Mizuno, T. and Yamashino, T. (2008). Comparative transcriptome of diurnally oscillating genes and hormone-responsive genes in Arabidopsis thaliana: Insight into circadian clock-controlled daily responses to common ambient stresses in plants. Plant Cell Physiol. **49**: 481–487.

Mockler, T.C., Michael, T.P., Priest, H.D., Shen, R., Sullivan, C.M., Givan, S.A., Mcentee, C., Kay, S.A., and Chory, J. (2007). The diurnal project: Diurnal and circadian expression profiling, model-based pattern matching, and promoter analysis. Cold Spring Harb. Symp. Quant. Biol. **72**: 353–363.

Mohawk, J.A., Green, C.B., and Takahashi, J.S. (2012). Central and Peripheral Circadian Clocks in Mammals. Annu. Rev. Neurosci. **35**: 445–462.

Moraes, T.A., Mengin, V., Annunziata, M.G., Encke, B., Krohn, N., Höhne, M., and Stitt, M. (2019). Response of the circadian clock and diel starch turnover to one day of low light or low co2. Plant Physiol. **179**: 1457–1478.

Murchie, E.H. and Lawson, T. (2013). Chlorophyll fluorescence analysis: A guide to good practice and understanding some new applications. J. Exp. Bot. **64**: 3983–3998.

Nagel, D.H. and Kay, S.A. (2012). Complexity in the wiring and regulation of plant circadian networks. Curr. Biol. **22**: R648–R657.

Nakagawa, T. et al. (2007a). Improved gateway binary vectors: High-performance vectors for creation of fusion constructs in transgenic analysis of plants. Biosci. Biotechnol. Biochem. **71**: 2095–2100.

Nakagawa, T., Kurose, T., Hino, T., Tanaka, K., Kawamukai, M., Niwa, Y., Toyooka, K., Matsuoka, K., Jinbo, T., and Kimura, T. (2007b). Development of series of gateway binary vectors, pGWBs, for realizing efficient construction of fusion genes for plant transformation. J. Biosci. Bioeng. **104**: 34–41.

Nakamichi, N., Ito, S., Oyama, T., Yamashino, T., Kondo, T., and Mizuno, T. (2004). Characterization of Plant Circadian Rhythms by Employing Arabidopsis Cultured Cells with Bioluminescence Reporters. Plant Cell Physiol. **45**: 57–67.

Nakamichi, N., Kiba, T., Henriques, R., Mizuno, T., Chua, N.H., and Sakakibara, H. (2010). PSEUDO-RESPONSE ReGULATORS 9, 7, and 5 are transcriptional repressors in the Arabidopsis circadian clock. Plant Cell **22**: 594–605.

Nakamichi, N., Kiba, T., Kamioka, M., Suzukie, T., Yamashino, T., Higashiyama, T., Sakakibara, H., and Mizuno, T. (2012). Transcriptional repressor PRR5 directly regulates clock-output pathways. Proc. Natl. Acad. Sci. U. S. A. **109**: 17123–17128.

Nakamichi, N., Kita, M., Ito, S., Yamashino, T., and Mizuno, T. (2005). PSEUDO-RESPONSE REGULATORS, PRR9, PRR7 and PRR5, Together play essential roles close to the circadian clock of Arabidopsis thaliana. Plant Cell Physiol. **46**: 686–698.

Neufeld-Cohen, A., Robles, M.S., Aviram, R., Manella, G., Adamovich, Y., Ladeuix, B., Nir, D., Rousso-Noori, L., Kuperman, Y., Golik, M., Mann, M., and Asher, G. (2016). Circadian control of oscillations in mitochondrial rate-limiting enzymes and nutrient utilization by PERIOD proteins. Proc. Natl. Acad. Sci. U. S. A. **113**: E1673–E1682.

Ni, P., Fan, H.R., and Ding, J.Y. (2014). Progress in fluid inclusions. Bull. Mineral. Petrol. Geochemistry **33**: 1–5.

Nohales, M.A. and Kay, S.A. (2016). Molecular mechanisms at the core of the plant circadian oscillator. Nat. Struct. Mol. Biol. **23**: 1061–

1069.

Noordally, Z.B., Ishii, K., Atkins, K.A., Wetherill, S.J., Kusakina, J., Walton, E.J., Kato, M., Azuma, M., Tanaka, K., Hanaoka, M., and Dodd, A.N. (2013). Circadian control of chloroplast transcription by a nuclear-encoded timing signal. Science (80-.). **339**: 1316–1319.

Novitskaya, L., Trevanion, S.J., Driscoll, S., Foyer, C.H., and Noctor, G. (2002). How does photorespiration modulate leaf amino acid contents? A dual approach through modelling and metabolite analysis. Plant, Cell Environ. **25**: 821–835.

Nozue, K., Covington, M.F., Duek, P.D., Lorrain, S., Fankhauser, C., Harmer, S.L., and Maloof, J.N. (2007). Rhythmic growth explained by coincidence between internal and external cues. Nature **448**: 358–361.

Nunes-Nesi, A., Fernie, A.R., and Stitt, M. (2010). Metabolic and signaling aspects underpinning the regulation of plant carbon nitrogen interactions. Mol. Plant **3**: 973–996.

Nunnari, J. and Suomalainen, A. (2012). Mitochondria: In sickness and in health. Cell **148**: 1145–1159.

Nusinow, D.A., Helfer, A., Hamilton, E.E., King, J.J., Imaizumi, T., Schultz, T.F., Farré, E.M., and Kay, S.A. (2011). The ELF4-ELF3-"LUX complex links the circadian clock to diurnal control of hypocotyl growth. Nature **475**: 398–404.

Oakenfull, R.J. and Davis, S.J. (2017). Shining a light on the Arabidopsis circadian clock. Plant. Cell Environ. **40**: 2571–2585.

Okada, S. and Brennicke, A. (2006). Transcript levels in plant mitochondria show a tight homeostasis during day and night. Mol. Genet. Genomics **276**: 71–78.

Osellame, L.D., Blacker, T.S., and Duchen, M.R. (2012). Cellular and molecular mechanisms of mitochondrial function. Best Pract. Res. Clin. Endocrinol. Metab. **26**: 711–723.

Pal, S.K. et al. (2013). Diurnal changes of polysome loading track sucrose content in the rosette of wild-type arabidopsis and the starchless pgm mutant. Plant Physiol. **162**: 1246–1265.

Palmieri, L., Todd, C.D., Arrigoni, R., Hoyos, M.E., Santoro, A., Polacco, J.C., and Palmieri, F. (2006). Arabidopsis mitochondria have two basic amino acid transporters with partially overlapping specificities and differential expression in seedling development. Biochim. Biophys. Acta - Bioenerg. **1757**: 1277–1283.

Para, A., Farré, E.M., Imaizumi, T., Pruneda-Paz, J.L., Harmon, F.G., and Kay, S.A. (2007). PRR3 is a vascular regulator of TOC1 stability in the Arabidopsis circadian clock. Plant Cell **19**: 3462–3473.

Park, D.H., Somers, D.E., Kim, Y.S., Choy, Y.H., Lim, H.K., Soh, M.S., Kim, H.J., Kay, S.A., and Nam, H.G. (1999). Control of circadian rhythms and photoperiodic flowering by the Arabidopsis GIGANTEA gene. Science (80-.). **285**: 1579–1582.

Pedrotti, L., Weiste, C., Nägele, T., Wolf, E., Lorenzin, F., Dietrich, K., Mair, A., Weckwerth, W., Teige, M., Baena-González, E., and Dröge-Laser, W. (2018). Snf1-RELATED KINASE1-controlled C/S1-bZIP signaling activates alternative mitochondrial metabolic pathways to ensure plant survival in extended darkness. Plant Cell **30**: 495–509.

Peek, C.B. et al. (2013). Circadian clock NAD+ cycle drives mitochondrial oxidative metabolism in mice. Science (80-.). **342**: 1243417.

Peng, C., Uygun, S., Shiu, S.H., and Last, R.L. (2015). The impact of the branched-chain ketoacid dehydrogenase complex on amino acid homeostasis in Arabidopsis. Plant Physiol. **169**: 1807–1820.

Perales, M. and Más, P. (2007). A functional link between rhythmic changes in chromatin structure and the Arabidopsis biological clock. Plant Cell **19**: 2111–2123.

Pérez-García, P., Ma, Y., Yanovsky, M.J., and Mas, P. (2015). Time-dependent sequestration of RVE8 by LNK proteins shapes the diurnal oscillation of anthocyanin biosynthesis. Proc. Natl. Acad. Sci. U. S. A. **112**: 5249–5253.

Philippou, K., Ronald, J., Sánchez-Villarreal, A., Davis, A.M., and Davis, S.J. (2019). Physiological and Genetic Dissection of Sucrose Inputs to the Arabidopsis thaliana Circadian System. Genes (Basel). **10**: 334.

Pilgrim, M.L., Caspar, T., Quail, P.H., and McClung, C.R. (1993). Circadian and light-regulated expression of nitrate reductase in Arabidopsis. Plant Mol. Biol. **23**: 349–364.

Pilkington, S.M., Encke, B., Krohn, N., Höhne, M., Stitt, M., and Pyl, E.T. (2015). Relationship between starch degradation and carbon demand for maintenance and growth in Arabidopsis thaliana in different irradiance and temperature regimes. Plant, Cell Environ. **38**: 157–171.

Pokhilko, A., Fernández, A.P., Edwards, K.D., Southern, M.M., Halliday, K.J., and Millar, A.J. (2012). The clock gene circuit in Arabidopsis includes a repressilator with additional feedback loops. Mol. Syst. Biol. **8**: 574.

Pokhilko, A., Flis, A., Sulpice, R., Stitt, M., and Ebenhöh, O. (2014). Adjustment of carbon fluxes to light conditions regulates the daily turnover of starch in plants: A computational model. Mol. Biosyst. **10**: 613–627.

Polidoros, A.N., Mylona, P. V., and Arnholdt-Schmitt, B. (2009). Aox gene structure, transcript variation and expression in plants. Physiol. Plant. **137**: 342–353.

Portolés, S. and Más, P. (2010). The functional interplay between protein kinase CK2 and cca1 transcriptional activity is essential for clock temperature compensation in Arabidopsis. PLoS Genet. **6**: e1001201.

Pracharoenwattana, I., Zhou, W., Keech, O., Francisco, P.B., Udomchalothorn, T., Tschoep, H., Stitt, M., Gibon, Y., and Smith, S.M. (2010). Arabidopsis has a cytosolic fumarase required for the massive allocation of photosynthate into fumaric acid and for rapid plant growth on high nitrogen. Plant J. **62**: 785–795.

Pruneda-Paz, J.L., Breton, G., Para, A., and Kay, S.A. (2009). A functional genomics approach reveals CHE as a component of the Arabidopsis circadian clock. Science (80-.). **323**: 1481–1485.

Pyl, E.T., Piques, M., Ivakov, A., Schulze, W., Ishihara, H., Stitt, M., and Sulpice, R. (2012). Metabolism and growth in Arabidopsis depend on the daytime temperature but are temperature-compensated against cool nights. Plant Cell **24**: 2443–2469.

Quail, P.H. (1996). Phytochromes: Photosensory perception and signal transduction. Biochem. Soc. Trans. **24**: 675–680.

Racca, S., Welchen, E., Gras, D.E., Tarkowská, D., Turečková, V., Maurino, V.G., and Gonzalez, D.H. (2018). Interplay between cytochrome c and gibberellins during Arabidopsis vegetative development. Plant J. **94**: 105–121.

Radelfahr, F. and Klopstock, T. (2019). Mitochondrial diseases. Nervenarzt **90**: 121–130.

Rasmusson, A.G. and Escobar, M.A. (2007). Light and diurnal regulation of plant respiratory gene expression. Physiol. Plant. **129**: 57–67.

Ratajczak, E., Małecka, A., Ciereszko, I., and Staszak, A.M. (2019). Mitochondria are important determinants of the aging of seeds. Int. J. Mol. Sci. **20**.

Rawat, R., Takahashi, N., Hsu, P.Y., Jones, M.A., Schwartz, J., Salemi, M.R., Phinney, B.S., and Harmer, S.L. (2011). REVEILLE8 and PSEUDO-REPONSE REGULATOR5 form a negative feedback loop within the arabidopsis circadian clock. PLoS Genet. **7**: e1001350.

Reinke, H. and Asher, G. (2019). Crosstalk between metabolism and circadian clocks. Nat. Rev. Mol. Cell Biol. **20**: 227–241.

Rhoads, D.M., Umbach, A.L., Subbaiah, C.C., and Siedow, J.N. (2006). Mitochondrial reactive oxygen species. Contribution to oxidative stress and interorganellar signaling. Plant Physiol. **141**: 357–366.

Riewe, D., Jeon, H.J., Lisec, J., Heuermann, M.C., Schmeichel, J., Seyfarth, M., Meyer, R.C., Willmitzer, L., and Altmann, T. (2016). A naturally occurring promoter polymorphism of the Arabidopsis FUM2 gene causes expression variation, and is associated with metabolic and growth traits. Plant J. **88**: 826–838.

Rizzini, L., Favory, J.J., Cloix, C., Faggionato, D., O'Hara, A., Kaiserli, E., Baumeister, R., Schäfer, E., Nagy, F., Jenkins, G.I., and Ulm, R. (2011). Perception of UV-B by the arabidopsis UVR8 protein. Science (80-.). **332**: 103–106.

Robison, M.M., Ling, X., Smid, M.P.L., Zarei, A., and Wolyn, D.J. (2009). Antisense expression of mitochondrial ATP synthase subunits OSCP (ATP5) and γ (ATP3) alters leaf morphology, metabolism and gene expression in arabidopsis. Plant Cell Physiol. **50**: 1840–1850.

Rugnone, M.L., Soverna, A.F., Sanchez, S.E., Schlaen, R.G., Hernando, C.E., Seymour, D.K., Mancini, E., Chernomoretz, A.,

Weigel, D., Mas, P., and Yanovsky, M.J. (2013). LNK genes integrate light and clock signaling networks at the core of the Arabidopsis oscillator. Proc. Natl. Acad. Sci. U. S. A. **110**: 12120–12125.

Ruts, T., Matsubara, S., Wiese-Klinkenberg, A., and Walter, A. (2012). Aberrant temporal growth pattern and morphology of root and shoot caused by a defective circadian clock in Arabidopsis thaliana. Plant J. **72**: 154–161.

Sahar, S. and Sassone-Corsi, P. (2009). Metabolism and cancer: The circadian clock connection. Nat. Rev. Cancer **9**: 886–896.

Salomé, P.A. and McClung, C.R. (2005). Pseudo-response Regulator 7 and 9 are partially redundant genes essential for the temperature responsiveness of the Arabidopsis circadian clock. Plant Cell **17**: 791–803.

Salomé, P.A., Weigel, D., and McClunga, C.R. (2010). The role of the Arabidopsis morning loop components CCA1, LHY, PRR7, and PRR9 in temperature compensation. Plant Cell **22**: 3650–3661.

Schaffer, R., Ramsay, N., Samach, A., Corden, S., Putterill, J., Carré, I.A., and Coupland, G. (1998). The late elongated hypocotyl mutation of Arabidopsis disrupts circadian rhythms and the photoperiodic control of flowering. Cell **93**: 1219–1229.

Schauer, N., Steinhauser, D., Strelkov, S., Schomburg, D., Allison, G., Moritz, T., Lundgren, K., Roessner-Tunali, U., Forbes, M.G., Willmitzer, L., Fernie, A.R., and Kopka, J. (2005). GC-MS libraries for the rapid identification of metabolites in complex biological samples. FEBS Lett. **579**: 1332–1337.

Schertl, P. and Braun, H.P. (2014). Respiratory electron transfer pathways in plant mitochondria. Front. Plant Sci. **5**: 163.

Schertl, P., Cabassa, C., Saadallah, K., Bordenave, M., Savouré, A., and Braun, H.P. (2014). Biochemical characterization of proline dehydrogenase in Arabidopsis mitochondria. FEBS J. **281**: 2794–2804.

Schlaen, R.G., Mancini, E., Sanchez, S.E., Perez-Santángelo, S., Rugnone, M.L., Simpson, C.G., Brown, J.W.S., Zhang, X., Chernomoretz, A., and Yanovsky, M.J. (2015). The spliceosome assembly factor GEMIN2 attenuates the effects of temperature on alternative splicing and circadian rhythms. Proc. Natl. Acad. Sci. U. S. A. **112**: 9382–9387.

Schmidt, O., Pfanner, N., and Meisinger, C. (2010). Mitochondrial protein import: From proteomics to functional mechanisms. Nat. Rev. Mol. Cell Biol. **11**: 655–667.

Schmitt, K. et al. (2018). Circadian Control of DRP1 Activity Regulates Mitochondrial Dynamics and Bioenergetics. Cell Metab. **27**: 657-666.e5.

Schneider, C.A., Rasband, W.S., and Eliceiri, K.W. (2012). NIH Image to ImageJ: 25 years of image analysis. Nat. Methods **9**: 671–675.

Schwarzländer, M. and Finkemeier, I. (2013). Mitochondrial energy and redox signaling in plants. Antioxidants Redox Signal. **18**: 2122–2144.

Scialdone, A., Mugford, S.T., Feike, D., Skeffngton, A., Borrill, P., Graf, A., Smith, A.M., and Howard, M. (2013). Arabidopsis plants perform arithmetic division to prevent starvation at night. Elife **2013**: e00669.

Scott, I.M., Ward, J.L., Miller, S.J., and Beale, M.H. (2014). Opposite variations in fumarate and malate dominate metabolic phenotypes of Arabidopsis salicylate mutants with abnormal biomass under chilling. Physiol. Plant. **152**: 660–674.

Seki, M., Ohara, T., Hearn, T.J., Frank, A., Da Silva, V.C.H., Caldana, C., Webb, A.A.R., and Satake, A. (2017). Adjustment of the Arabidopsis circadian oscillator by sugar signalling dictates the regulation of starch metabolism. Sci. Rep. **7**: 8305.

Seo, P.J., Park, M.J., Lim, M.H., Kim, S.G., Lee, M., Baldwin, I.T., and Park, C.M. (2012). A self-regulatory circuit of CIRCADIAN CLOCK-ASSOCIATED1 underlies the circadian clock regulation of temperature responses in Arabidopsis. Plant Cell **24**: 2427–2442.

Seung, D., Risopatron, J.P.M., Jones, B.J., and Marc, J. (2012). Circadian clock-dependent gating in ABA signalling networks. Protoplasma **249**: 445–457.

Shameer, S., Ratcliffe, R.G., and Sweetlove, L.J. (2019). Leaf Energy Balance Requires Mitochondrial Respiration and Export of Chloroplast NADPH in the Light. Plant Physiol. **180**: 1947–1961.

Shim, J.S., Kubota, A., and Imaizumi, T. (2017). Circadian clock and photoperiodic flowering

in arabidopsis: CONSTANS is a Hub for Signal integration. Plant Physiol. **173**: 5–15.

Shin, J., Sánchez-Villarreal, A., Davis, A.M., Du, S.X., Berendzen, K.W., Koncz, C., Ding, Z., Li, C., and Davis, S.J. (2017). The metabolic sensor AKIN10 modulates the Arabidopsis circadian clock in a light-dependent manner. Plant Cell Environ. **40**: 997–1008.

Shinde, S., Villamor, J.G., Lin, W., Sharma, S., and Verslues, P.E. (2016). Proline coordination with fatty acid synthesis and redox metabolism of chloroplast and mitochondria. Plant Physiol. **172**: 1074–1088.

Singh, M. and Mas, P. (2018). A functional connection between the circadian clock and hormonal timing in arabidopsis. Genes (Basel). **9**.

Smith, A.M. and Stitt, M. (2007). Coordination of carbon supply and plant growth. Plant, Cell Environ. **30**: 1126–1149.

Smith, S.M., Fulton, D.C., Chia, T., Thorneycroft, D., Chapple, A., Dunstan, H., Hylton, C., Zeeman, S.C., and Smith, A.M. (2004). Diurnal changes in the transcriptome encoding enzymes of starch metabolism provide evidence for both transcriptional and posttranscriptional regulation of starch metabolism in arabidopsis leaves. Plant Physiol. **136**: 2687–2699.

Somers, D.E., Devlin, P.F., and Kay, S.A. (1998a). Phytochromes and cryptochromes in the entrainment of the Arabidopsis circadian clock. Science (80-.). **282**: 1488–1490.

Somers, D.E., Webb, A.A.R., Pearson, M., and Kay, S.A. (1998b). The short-period mutant, toc1-1, alters circadian clock regulation of multiple outputs throughout development in Arabidopsis thaliana. Development **125**: 485–494.

Soy, J., Leivar, P., González-Schain, N., Martín, G., Diaz, C., Sentandreu, M., Al-Sady, B., Quail, P.H., and Monte, E. (2016). Molecular convergence of clock and photosensory pathways through PIF3-TOC1 interaction and co-occupancy of target promoters. Proc. Natl. Acad. Sci. U. S. A. **113**: 4870–4875.

Spinelli, J.B. and Haigis, M.C. (2018). The multifaceted contributions of mitochondria to cellular metabolism. Nat. Cell Biol. **20**: 745–754.

Staffan Svensson, Å. and Rasmusson, A.G. (2001). Light-dependent gene expression for proteins in the respiratory chain of potato leaves. Plant J. **28**: 73–82.

Stock, D., Leslie, A.G.W., and Walker, J.E. (1999). Molecular architecture of the rotary motor in ATP synthase. Science (80-.). **286**: 1700–1705.

Strayer, C., Oyama, T., Schultz, T.F., Raman, R., Somers, D.E., Mas, P., Panda, S., Kreps, J.A., and Kay, S.A. (2000). Cloning of the Arabidopsis clock gene TOC1, an autoregulatory response regulator homolog. Science (80-.). **289**: 768–771.

Sulpice, R., Flis, A., Ivakov, A.A., Apelt, F., Krohn, N., Encke, B., Abel, C., Feil, R., Lunn, J.E., and Stitt, M. (2014). Arabidopsis coordinates the diurnal regulation of carbon allocation and growth across a wide range of Photoperiods. Mol. Plant **7**: 137–155.

Sweetlove, L.J., Beard, K.F.M., Nunes-Nesi, A., Fernie, A.R., and Ratcliffe, R.G. (2010). Not just a circle: Flux modes in the plant TCA cycle. Trends Plant Sci. **15**: 462–470.

Szal, B. and Podgórska, A. (2012). The role of mitochondria in leaf nitrogen metabolism. Plant, Cell Environ. **35**: 1756–1768.

Szarka, A., Bánhegyi, G., and Asard, H. (2013). The inter-relationship of ascorbate transport, metabolism and mitochondrial, plastidic respiration. Antioxidants Redox Signal. **19**: 1036–1044.

Takahashi, N., Hirata, Y., Aihara, K., and Mas, P. (2015). A Hierarchical Multi-oscillator Network Orchestrates the Arabidopsis Circadian System. Cell **163**: 148–159.

Tcherkez, G., Boex-Fontvieille, E., Mahé, A., and Hodges, M. (2012). Respiratory carbon fluxes in leaves. Curr. Opin. Plant Biol. **15**: 308–314.

Teng, Y., Cui, H., Wang, M., and Liu, X. (2017). Nitrate reductase is regulated by CIRCADIAN CLOCK-ASSOCIATED1 in Arabidopsis thaliana. Plant Soil **416**: 477–485.

Thain, S.C., Vandenbussche, F., Laarhoven, L.J.J., Dowson-Day, M.J., Wang, Z.Y., Tobin, E.M., Harren, F.J.M., Millar, A.J., and Van Der Straeten, D. (2004). Circadian rhythms of ethylene emission in Arabidopsis. Plant Physiol. **136**: 3751–3761.

Thines, B. and Harmon, F.G. (2010). Ambient temperature response establishes ELF3 as a

required component of the core Arabidopsis circadian clock. Proc. Natl. Acad. Sci. U. S. A. **107**: 3257–3262.

Timm, S., Nunes-Nesi, A., Pärnik, T., Morgenthal, K., Wienkoop, S., Keerberg, O., Weckwerth, W., Kleczkowski, L.A., Fernie, A.R., and Bauwe, H. (2008). A cytosolic pathway for the conversion of hydroxypyruvate to glycerate during photorespiration in Arabidopsis. Plant Cell **20**: 2848–2859.

Tohge, T. and Fernie, A.R. (2009). Web-based resources for mass-spectrometry-based metabolomics: A user's guide. Phytochemistry **70**: 450–456.

Tomaz, T., Bagard, M., Pracharoenwattana, I., Lindén, P., Lee, C.P., Carroll, A.J., Ströher, E., Smith, S.M., Gardeström, P., and Millar, A.H. (2010). Mitochondrial malate dehydrogenase lowers leaf respiration and alters photorespiration and plant growth in Arabidopsis. Plant Physiol. **154**: 1143–1157.

Tronconi, M.A., Fahnenstich, H., Gerrard Weehler, M.C., Andreo, C.S., Flügge, U.I., Drincovich, M.F., and Maurino, V.G. (2008). Arabidopsis NAD-malic enzyme functions as a homodimer and heterodimer and has a major impact on nocturnal metabolism. Plant Physiol. **146**: 1540–1552.

Tronconi, M.A., Gerrard Wheeler, M.C., Drincovich, M.F., and Andreo, C.S. (2012). Differential fumarate binding to Arabidopsis NAD +-malic enzymes 1 and -2 produces an opposite activity modulation. Biochimie **94**: 1421–1430.

Tronconi, M.A., Gerrard Wheeler, M.C., Martinatto, A., Zubimendi, J.P., Andreo, C.S., and Drincovich, M.F. (2015). Allosteric substrate inhibition of Arabidopsis NAD-dependent malic enzyme 1 is released by fumarate. Phytochemistry **111**: 37–47.

Tschoep, H., Gibon, Y., Carillo, P., Armengaud, P., Szecowka, M., Nunes-Nesi, A., Fernie, A.R., Koehl, K., and Stitt, M. (2009). Adjustment of growth and central metabolism to a mild but sustained nitrogen-limitation in Arabidopsis. Plant, Cell Environ. **32**: 300–318.

Urbanczyk-Wochniak, E., Baxter, C., Kolbe, A., Kopka, J., Sweetlove, L.J., and Fernie, A.R. (2005). Profiling of diurnal patterns of metabolite and transcript abundance in potato (Solanum tuberosum) leaves. Planta **221**: 891–903.

Vanhaeren, H., Gonzalez, N., and Inzé, D. (2015). A Journey Through a Leaf: Phenomics Analysis of Leaf Growth in Arabidopsis thaliana . Arab. B. **13**: e0181.

Villena, J.A. (2015). New insights into PGC-1 coactivators: Redefining their role in the regulation of mitochondrial function and beyond. FEBS J. **282**: 647–672.

Voon, C.P., Guan, X., Sun, Y., Sahu, A., Chan, M.N., Gardeström, P., Wagner, S., Fuchs, P., Nietzel, T., Versaw, W.K., Schwarzländer, M., and Lim, B.L. (2018). ATP compartmentation in plastids and cytosol of Arabidopsis thaliana revealed by fluorescent protein sensing. Proc. Natl. Acad. Sci. U. S. A. **115**: E10778–E10787.

Wang, L., Fujiwara, S., and Somers, D.E. (2010). PRR5 regulates phosphorylation, nuclear import and subnuclear localization of TOC1 in the Arabidopsis circadian clock. EMBO J. **29**: 1903–1915.

Wang, T.A., Yu, Y. V., Govindaiah, G., Ye, X., Artinian, L., Coleman, T.P., Sweedler, J. V., Cox, C.L., and Gillette, M.U. (2012a). Circadian rhythm of redox state regulates excitability in suprachiasmatic nucleus neurons. Science (80-.). **337**: 839–842.

Wang, W., Barnaby, J.Y., Tada, Y., Li, H., Tör, M., Caldelari, D., Lee, D.U., Fu, X.D., and Dong, X. (2011a). Timing of plant immune responses by a central circadian regulator. Nature **470**: 110–115.

Wang, X. et al. (2012b). SKIP is a component of the spliceosome linking alternative splicing and the circadian clock in Arabidopsis. Plant Cell **24**: 3278–3295.

Wang, Y., Wu, J.F., Nakamichi, N., Sakakibara, H., Nam, H.G., and Wu, S.H. (2011b). LIGHT-REGULATED WD1 and PSEUDO-RESPONSE REGULATOR9 Form a positive feedback regulatory loop in the Arabidopsis circadian clock. Plant Cell **23**: 486–498.

Wang, Z.Y. and Tobin, E.M. (1998). Constitutive expression of the CIRCADIAN CLOCK ASSOCIATED 1 (CCA1) gene disrupts circadian rhythms and suppresses its own expression. Cell **93**: 1207–1217.

Webb, A.A.R., Seki, M., Satake, A., and Caldana, C. (2019). Continuous dynamic adjustment of the plant circadian oscillator. Nat. Commun. **10**: 550.

Welchen, E., Chan, R.L., and Gonzalez, D.H.

(2002). Metabolic regulation of genes encoding cytochrome c and cytochrome c oxidase subunit Vb in Arabidopsis. Plant, Cell Environ. **25**: 1605–1615.

Welchen, E. and Gonzalez, D.H. (2005). Differential expression of the Arabidopsis cytochrome c genes Cytc-1 and Cytc-2. Evidence for the involvement of TCP-domain protein-binding elements in anther- and meristem-specific expression of the Cytc-1 gene. Plant Physiol. **139**: 88–100.

Welchen, E. and Gonzalez, D.H. (2006). Overrepresentation of elements recognized by TCP-domain transcription factors in the upstream regions of nuclear genes encoding components of the mitochondrial oxidative phosphorylation machinery. Plant Physiol. **141**: 540–545.

Winter, G., Todd, C.D., Trovato, M., Forlani, G., and Funck, D. (2015). Physiological implications of arginine metabolism in plants. Front. Plant Sci. **6**: 534.

Wu, J.F., Tsai, H.L., Joanito, I., Wu, Y.C., Chang, C.W., Li, Y.H., Wang, Y., Hong, J.C., Chu, J.W., Hsu, C.P., and Wu, S.H. (2016). LWD-TCP complex activates the morning gene CCA1 in Arabidopsis. Nat. Commun. **7**: 13181.

Wu, J.F., Wang, Y., and Wu, S.H. (2008). Two new clock proteins, LWD1 and LWD2, regulate arabidopsis photoperiodic flowering. Plant Physiol. **148**: 948–959.

Xie, Q. et al. (2014). LNK1 and LNK2 are transcriptional coactivators in the Arabidopsis circadian oscillator. Plant Cell **26**: 2843–2857.

Xing Liang Liu, Covington, M.F., Fankhauser, C., Chory, J., and Wagner, D.R. (2001). ELF3 encodes a circadian clock-regulated nuclear protein that functions in an Arabidopsis PHYB signal transduction pathway. Plant Cell **13**: 1293–1304.

Yakir, E., Hassidim, M., Melamed-Book, N., Hilman, D., Kron, I., and Green, R.M. (2011). Cell autonomous and cell-type specific circadian rhythms in Arabidopsis. Plant J. **68**: 520–531.

Yamamoto, Y., Sato, E., Shimizu, T., Nakamich, N., Sato, S., Kato, T., Tabata, S., Nagatani, A., Yamashino, T., and Mizuno, T. (2003). Comparative Genetic Studies on the APRR5 and APRR7 Genes Belonging to the APRR1/TOC1 Quintet Implicated in Circadian Rhythm, Control of Flowering Time, and Early Photomorphogenesis. Plant Cell Physiol. **44**: 1119–1130.

Yanovsky, M.J., Mazzella, M.A., and Casal, J.J. (2000). A quadruple photoreceptor mutant still keeps track of time. Curr. Biol. **10**: 1013–1015.

Yazdanbakhsh, N., Sulpice, R., Graf, A., Stitt, M., and Fisahn, J. (2011). Circadian control of root elongation and C partitioning in Arabidopsis thaliana. Plant, Cell Environ. **34**: 877–894.

Yeom, M., Kim, H., Lim, J., Shin, A.Y., Hong, S., Kim, J. Il, and Nam, H.G. (2014). How do phytochromes transmit the light quality information to the circadian clock in arabidopsis? Mol. Plant **7**: 1701–1704.

Yogev, O., Naamati, A., and Pines, O. (2011). Fumarase: A paradigm of dual targeting and dual localized functions. FEBS J. **278**: 4230–4242.

Yoshida, K. and Noguchi, K. (2009). Differential gene expression profiles of the mitochondrial respiratory components in illuminated arabidopsis leaves. Plant Cell Physiol. **50**: 1449–1462.

Yoshida, K., Watanabe, C.K., Terashima, I., and Noguchi, K. (2011). Physiological impact of mitochondrial alternative oxidase on photosynthesis and growth in Arabidopsis thaliana. Plant, Cell Environ. **34**: 1890–1899.

Yoshida, T., Obata, T., Feil, R., Lunn, J.E., Fujita, Y., Yamaguchi-Shinozaki, K., and Fernie, A.R. (2019). The role of abscisic acid signaling in maintaining the metabolic balance required for arabidopsis growth under nonstress conditions. Plant Cell **31**: 84–105.

Zell, M.B., Fahnenstich, H., Maier, A., Saigo, M., Voznesenskaya, E. V., Edwards, G.E., Andreo, C., Schleifenbaum, F., Zell, C., Drincovich, M.F., and Maurino, V.G. (2010). Analysis of Arabidopsis with highly reduced levels of malate and fumarate sheds light on the role of these organic acids as storage carbon molecules. Plant Physiol. **152**: 1251–1262.

Zhang, C., Xie, Q., Anderson, R.G., Ng, G., Seitz, N.C., Peterson, T., McClung, C.R., McDowell, J.M., Kong, D., Kwak, J.M., and Lu, H. (2013). Crosstalk between the Circadian Clock and Innate Immunity in Arabidopsis. PLoS Pathog. **9**: e1003370.

Zhang, S., Li, C., Wang, R., Chen, Y., Shu, S., Huang, R., Zhang, D., Li, J., Xiao, S., Yao, N., and Yang, C. (2017). The arabidopsis mitochondrial protease FtSH4 is involved in leaf senescence via regulation of WRKY-dependent salicylic acid accumulation and signaling. Plant Physiol. **173**: 2294–2307.

Zhang, Y., Wang, Y., Wei, H., Li, N., Tian, W., Chong, K., and Wang, L. (2018). Circadian Evening Complex Represses Jasmonate-Induced Leaf Senescence in Arabidopsis. Mol. Plant **11**: 326–337.

Zhou, M., Wang, W., Karapetyan, S., Mwimba, M., Marqués, J., Buchler, N.E., and Dong, X. (2015). Redox rhythm reinforces the circadian clock to gate immune response. Nature **523**: 472–476.

Zhu, J.Y., Oh, E., Wang, T., and Wang, Z.Y. (2016). TOC1-PIF4 interaction mediates the circadian gating of thermoresponsive growth in Arabidopsis. Nat. Commun. **7**: 13692.

Zubimendi, J.P., Martinatto, A., Valacco, M.P., Moreno, S., Andreo, C.S., Drincovich, M.F., and Tronconi, M.A. (2018). The complex allosteric and redox regulation of the fumarate hydratase and malate dehydratase reactions of Arabidopsis thaliana Fumarase 1 and 2 gives clues for understanding the massive accumulation of fumarate. FEBS J. **285**: 2205–2224.